BSIM6.0 MOSFET Compact Model

Technical Manual

Authors:
Yogesh Singh Chauhan, Mohammed A. Karim,
Sriramkumar Venugopalan, Harshit Agarwal, Pankaj Thakur,
Navid Paydavosi, Ali Niknejad, and Chenming Hu

Project Director:
Prof. Ali Niknejad and Prof. Chenming Hu

Department of Electrical Engineering and Computer Sciences
University of California, Berkeley, CA 94720

Nondisclosure Statement

The content of BSIM6 model (including source code, manual, technical note, and equation list) is currently distributed by BSIM Group, a research group at EECS Department, University of California at Berkeley, to designated Receiving Parties only.

The content of BSIM6 model can not be distributed by Receiving Party to any third party without written agreement by BSIM Group.

BSIM6 Web Page

http://www-device.eecs.berkeley.edu/bsim/?page=BSIM6

Contents

1 BSIM6.0 Model Equations

1.1 Physical constants

Physical quantities are in M.K.S units unless specified otherwise.

$$q = 1.6 \times 10^{-19} C \tag{1.1}$$

$$\epsilon_0 = 8.8542 \times 10^{-12} \quad \frac{F}{m} \tag{1.2}$$

$$\epsilon_{sub} = EPSRSUB \cdot \epsilon_0 \quad \frac{F}{m} \tag{1.3}$$

$$\epsilon_{ox} = EPSROX \cdot \epsilon_0 \quad \frac{F}{m} \tag{1.4}$$

$$C_{ox} = \frac{3.9 \cdot \epsilon_0}{TOX} \quad \frac{F}{m^2} \tag{1.5}$$

$$\epsilon_{ratio} = \frac{EPSRSUB}{3.9} \tag{1.6}$$

$$\tag{1.7}$$

1.2 Effective Channel Length & Width

$$\Delta L = LINT \tag{1.8}$$

$$\Delta W = WINT \tag{1.9}$$

$$\Delta L_{CV} = DLC \tag{1.10}$$

$$\Delta W_{CV} = DWC \tag{1.11}$$

$$L_{eff} = L + XL - 2\Delta L \tag{1.12}$$

$$W_{eff} = W + XW - 2\Delta W \tag{1.13}$$

$$L_{eff,CV} = L + XL - 2\Delta L_{CV} \tag{1.14}$$

$$W_{eff,CV} = W + XW - 2\Delta W_{CV} \tag{1.15}$$

1.3 Binning Calculations

For a given L and W, each model parameter $PARAM_i$ is calculated as a function of PARAM, and length dependent term, LPARAM, width dependent term, WPARAM, area dependent term, PPARAM:

$$PARAM_i = PARAM + \frac{LPARAM}{L_{eff}} + \frac{WPARAM}{W_{eff}} + \frac{PPARAM}{L_{eff} \cdot W_{eff}} \tag{1.16}$$

For the list of binable parameters, please refer to the complete parameter list at the end of this technical note.

1.4 Global geomertical scaling

Following scaling formulation is used in global scaling -

$$\begin{aligned} PARAM[L] = PARAM \cdot \Bigg[& 1 + PARAML \cdot \left(\frac{1}{L_{eff}^{PARAMLEXP}} - \frac{1}{LLONG^{PARAMLEXP}} \right) \\ & + PARAMW \cdot \left(\frac{1}{W_{eff}^{PARAMWEXP}} - \frac{1}{WWIDE^{PARAMWEXP}} \right) \\ & + PARAMWL \cdot \left(\frac{1}{(L_{eff} \cdot W_{eff})^{PARAMWLEXP}} \right) \Bigg] \end{aligned} \tag{1.17}$$

LLONG is the length of extracted long channel device and WWIDE is the width for extracted wide device. They are used to ensure that scaling parameters do not affect long-wide fitting. We will not mention LLONG and WWIDE part again but all of the following scaling equation use above kind of formulation.

$$\begin{aligned} NDEP[L] = NDEP \cdot \Bigg[& 1 + NDEPL1 \cdot \frac{1}{L_{eff}^{NDEPLEXP1}} + NDEPL2 \cdot \frac{1}{L_{eff}^{NDEPLEXP2}} \\ & + NDEPW \cdot \frac{1}{W_{eff}^{NDEPWEXP}} + NDEPWL \cdot \frac{1}{(L_{eff} \cdot W_{eff})^{NDEPWLEXP}} \Bigg] \end{aligned} \tag{1.18}$$

$$NFACTOR[L] = NFACTOR \cdot \left[1 + NFACTORL \cdot \frac{1}{L_{eff}^{NFACTORLEXP}} + NFACTORW \cdot \frac{1}{W_{eff}^{NFACTORWEXP}} + NFACTORWL \cdot \frac{1}{(L_{eff} \cdot W_{eff})^{NFACTORWLEXP}}\right] \tag{1.19}$$

$$CDSCD[L] = CDSCD \cdot \left[1 + CDSCDL \cdot \frac{1}{L_{eff}^{CDSCDLEXP}}\right] \tag{1.20}$$

$$CDSCB[L] = CDSCB \cdot \left[1 + CDSCBL \cdot \frac{1}{L_{eff}^{CDSCBLEXP}}\right] \tag{1.21}$$

$$U0[L] = \begin{cases} U0 \cdot \left[1 - U0L \cdot \frac{1}{L_{eff}^{U0LEXP}}\right] & U0LEXP > 0 \\ U0 \cdot [1 - U0L] & \text{Otherwise} \end{cases} \tag{1.22}$$

$$UA[L] = UA \cdot \left[1 + UAL \cdot \frac{1}{L_{eff}^{UALEXP}} + UAW \cdot \frac{1}{W_{eff}^{UAWEXP}} + UAWL \cdot \frac{1}{(L_{eff} \cdot W_{eff})^{UAWLEXP}}\right] \tag{1.23}$$

$$EU[L] = EU \cdot \left[1 + EUL \cdot \frac{1}{L_{eff}^{EULEXP}} + EUW \cdot \frac{1}{W_{eff}^{EUWEXP}} + EUWL \cdot \frac{1}{(L_{eff} \cdot W_{eff})^{EUWLEXP}}\right] \tag{1.24}$$

$$UD[L] = UD \cdot \left[1 + UDL \cdot \frac{1}{L_{eff}^{UDLEXP}}\right] \tag{1.25}$$

$$UC[L] = UC \cdot \left[1 + UCL \cdot \frac{1}{L_{eff}^{UCLEXP}} + UCW \cdot \frac{1}{W_{eff}^{UCWEXP}} + UCWL \cdot \frac{1}{(L_{eff} \cdot W_{eff})^{UCWLEXP}}\right] \tag{1.26}$$

$$ETA0[L] = ETA0 \cdot \left[\frac{1}{L_{eff}^{DSUB}}\right] \tag{1.27}$$

$$ETAB[L] = ETAB \cdot \left[\frac{1}{L_{eff}^{ETABLEXP}}\right] \tag{1.28}$$

$$PDIBLC[L] = PDIBLC \cdot \left[1 + PDIBLCL \cdot \frac{1}{L_{eff}^{PDIBLCLEXP}}\right] \tag{1.29}$$

$$DELTA[L] = DELTA \cdot \left[1 + DELTAL \cdot \frac{1}{L_{eff}^{DELTALEXP}}\right] \tag{1.30}$$

$$FPROUT[L] = FPROUT \cdot \left[1 + FPROUTL \cdot \frac{1}{L_{eff}^{FPROUTLEXP}}\right] \tag{1.31}$$

$$PCLM[L] = PCLM \cdot \left[1 + PCLML \cdot \frac{1}{L_{eff}^{PCLMLEXP}}\right] \tag{1.32}$$

$$\begin{aligned} VSAT[L] = VSAT \cdot \Bigg[1 &+ VSATL \cdot \frac{1}{L_{eff}^{VSATLEXP}} + VSATW \cdot \frac{1}{W_{eff}^{VSATWEXP}} \\ &+ VSATWL \cdot \frac{1}{(L_{eff} \cdot W_{eff})^{VSATWLEXP}}\Bigg] \end{aligned} \tag{1.33}$$

$$PSAT[L] = PSAT \cdot \left[1 + PSATL \cdot \frac{1}{L_{eff}^{PSATLEXP}}\right] \tag{1.34}$$

$$PTWG[L] = PTWG \cdot \left[1 + PTWGL \cdot \frac{1}{L_{eff}^{PTWGLEXP}}\right] \tag{1.35}$$

$$ALPHA0[L] = ALPHA0 \cdot \left[1 + ALPHA0L \cdot \frac{1}{L_{eff}^{ALPHA0LEXP}}\right] \tag{1.36}$$

$$AGIDL[L] = AGIDL \cdot \left[1 + AGIDLL \cdot \frac{1}{L_{eff}} + AGIDLW \cdot \frac{1}{W_{eff}}\right] \tag{1.37}$$

$$AGISL[L] = AGISL \cdot \left[1 + AGISLL \cdot \frac{1}{L_{eff}} + AGISLW \cdot \frac{1}{W_{eff}}\right] \tag{1.38}$$

$$AIGC[L] = AIGC \cdot \left[1 + AIGCL \cdot \frac{1}{L_{eff}} + AIGCW \cdot \frac{1}{W_{eff}}\right] \tag{1.39}$$

$$AIGS[L] = AIGS \cdot \left[1 + AIGSL \cdot \frac{1}{L_{eff}} + AIGSW \cdot \frac{1}{W_{eff}}\right] \tag{1.40}$$

$$AIGD[L] = AIGD \cdot \left[1 + AIGDL \cdot \frac{1}{L_{eff}} + AIGDW \cdot \frac{1}{W_{eff}}\right] \tag{1.41}$$

$$PIGCD[L] = PIGCD \cdot \left[1 + PIGCDL \cdot \frac{1}{L_{eff}}\right] \tag{1.42}$$

$$\begin{aligned} NDEPCV[L] = NDEPCV \cdot \Bigg[1 &+ NDEPCVL1 \cdot \frac{1}{L_{eff}^{NDEPCVLEXP1}} \\ &+ NDEPCVL2 \cdot \frac{1}{L_{eff}^{NDEPCVLEXP2}} + NDEPCVW \cdot \frac{1}{W_{eff}^{NDEPCVWEXP}} \\ &+ NDEPCVWL \cdot \frac{111}{(L_{eff} \cdot W_{eff})^{NDEPCVWLEXP}}\Bigg] \end{aligned} \tag{1.43}$$

$$VFBCV[L] = VFBCV \cdot \left[1 + VFBCVL \cdot \frac{1}{L_{eff}^{VFBCVLEXP}} + VFBCVW \cdot \frac{1}{W_{eff}^{VFBCVWEXP}} + VFBCVWL \cdot \frac{1}{(L_{eff} \cdot W_{eff})^{VFBCVWLEXP}}\right] \tag{1.44}$$

$$VSATCV[L] = VSATCV \cdot \left[1 + VSATCVL \cdot \frac{1}{L_{eff}^{VSATCVLEXP}} + VSATCVW \cdot \frac{1}{W_{eff}^{VSATCVWEXP}} + VSATCVWL \cdot \frac{1}{(L_{eff} \cdot W_{eff})^{VSATCVWLEXP}}\right] \tag{1.45}$$

$$PCLMCV[L] = PCLMCV \cdot \left[1 + PCLMCVL \cdot \frac{1}{L_{eff}^{PCLMCVLEXP}}\right] \tag{1.46}$$

$$K2[L] = K2 \cdot \left[1 + K2L \cdot \frac{1}{L_{eff}^{K2LEXP}} + K2W \cdot \frac{1}{W_{eff}^{K2WEXP}} + K2WL \cdot \frac{1}{(L_{eff} \cdot W_{eff})^{K2WLEXP}}\right] \tag{1.47}$$

$$PRWB[L] = PRWB \cdot \left[1 + PRWBL \cdot \frac{1}{L_{eff}^{PRWBLEXP}}\right] \tag{1.48}$$

$$RSW[L] = RSW \cdot \left[1 + RSWL \cdot \frac{1}{L_{eff}^{RSWLEXP}}\right] \tag{1.49}$$

$$RDW[L] = RDW \cdot \left[1 + RDWL \cdot \frac{1}{L_{eff}^{RDWLEXP}}\right] \tag{1.50}$$

$$RDSW[L] = RDSW \cdot \left[1 + RDSWL \cdot \frac{1}{L_{eff}^{RDSWLEXP}}\right] \tag{1.51}$$

1.5 Terminal Voltages

BSIM6 is a body referenced model.

$$V_t = \frac{K.T}{q} \tag{1.52}$$

$$V_g = V_g - V_b \tag{1.53}$$

$$V_d = V_d - V_b \tag{1.54}$$

$$V_s = V_s - V_b \tag{1.55}$$

$$V_{gs} = V_g - V_s \tag{1.56}$$

$$V_{gd} = V_g - V_d \tag{1.57}$$

$$V_{gb} = V_g - V_b \tag{1.58}$$

$$V_{ds} = V_d - V_s \tag{1.59}$$

$$V_{dsx} = \sqrt{V_{ds}^2 + 0.01} - 0.1 \tag{1.60}$$

$$V_{bsx} = -\left[V_s + \frac{1}{2}(V_{ds} - V_{dsx})\right] \tag{1.61}$$

1.6 Pinch-off Potential and Normalized Charge Calculation

1.6.1 Pinch-off Potential with Poly Depletion

$$\phi_b = \ln\left(\frac{n_{body}}{n_i}\right) \tag{1.62}$$

$$\gamma_0 = \frac{\sqrt{2 \cdot q \cdot \epsilon_{si} \cdot NDEP}}{C_{ox}\sqrt{nV_t}} \tag{1.63}$$

$$\gamma_g = \frac{\sqrt{2 \cdot q \cdot \epsilon_{si} \cdot NGATE}}{C_{ox}\sqrt{nV_t}} \tag{1.64}$$

$$\gamma^{'} = \gamma_0 \cdot \sqrt{nV_t} \tag{1.65}$$

$$\gamma_g^{'} = \gamma_g \cdot \sqrt{nV_t} \tag{1.66}$$

$$\delta_{PD} = \frac{NDEP}{NGATE} \tag{1.67}$$

$$\left(\frac{\gamma_0}{\gamma_g}\right)^2 = \left(\frac{\frac{\sqrt{2 \cdot q \cdot \epsilon_{si} \cdot NDEP}}{C_{ox}\sqrt{nV_t}}}{\frac{\sqrt{2 \cdot q \cdot \epsilon_{si} \cdot NGATE}}{C_{ox}\sqrt{nV_t}}}\right)^2 = \frac{NDEP}{NGATE} = \delta_{PD} \tag{1.68}$$

$$\gamma = \frac{\gamma_0}{1 + \delta_{PD}} \tag{1.69}$$

In accumulation and inversion under depletion approximation, the bulk charge is given as [2]

$$Q_b = -sign(\psi_s) \cdot \gamma^{'} \cdot C_{ox} \cdot \sqrt{V_t.(e^{-\frac{\phi_s}{V_t}} - 1) + \psi_s} \tag{1.70}$$

From potential balance equation including poly depletion,

$$V_G = V_{FB} + \psi_S - \frac{Q_i + Q_b}{C_{ox}} + \left(\frac{Q_i + Q_b}{\gamma_g.C_{ox}}\right)^2 \tag{1.71}$$

At pinch off,$\psi_S = \psi_P$ and $Q_i = 0$. Substituting in (1.70) and (1.71),

$$V_G - V_{FB} = \psi_P + \gamma^{'} \cdot \sqrt{V_t.(e^{-\frac{\phi_P}{V_t}} - 1) + \psi_P} + (\frac{\gamma^{'}}{\gamma_g^{'}})^2\left(V_t.(e^{-\frac{\phi_P}{V_t}} - 1) + \psi_P\right) \tag{1.72}$$

$$= \psi_P + \gamma^{'} \cdot \sqrt{V_t.(e^{-\frac{\phi_P}{V_t}} - 1) + \psi_P} + \delta_{PD}\left(V_t.(e^{-\frac{\phi_P}{V_t}} - 1) + \psi_P\right) \tag{1.73}$$

Normalizing it,

$$v_g - v_{fb} = \psi_p + \gamma_0 \cdot \sqrt{e^{-\psi_p} + \psi_p - 1} + \delta_{PD}\left(e^{-\psi_P} - 1 + \psi_p\right) \tag{1.74}$$

Explicit expression for ψ_p can be derived from above relation in the asymptotic form by inspecting the behavior in three different regions. First consider the depletion and inversion region of operation where $\psi_p >> 0$ so that $e^{-\psi_p}$ is very small. Let $\zeta_1 = e^{-\psi_p}$

$$v_g - v_{fb} = \psi_p + \gamma_0 \cdot \sqrt{\psi_p + \zeta_1 - 1} + \delta_{PD}\left(\zeta_1 - 1 + \psi_p\right) \tag{1.75}$$

Let

$$\sqrt{\psi_p + \zeta_1 - 1} = x \tag{1.76}$$

or

$$\psi_p = x^2 + 1 - \zeta_1 \tag{1.77}$$

Thus

$$v_g - v_{fb} = x^2 + 1 - \zeta_1 + \gamma_0.x + \delta_{PD}.x^2 \tag{1.78}$$

or

$$x^2 + \frac{\gamma_0}{1+\delta_{PD}} \cdot x + \frac{1-\zeta_1}{1+\delta_{PD}} - \frac{v_g - v_{fb}}{1+\delta_{PD}} = 0 \tag{1.79}$$

This gives

$$x = \left[\sqrt{\frac{v_g - v_{fb} - 1 + \zeta_1}{1+\delta_{PD}} + \left(\frac{\gamma_0}{2\cdot(1+\delta_{PD})}\right)^2} - \frac{\gamma_0}{2\cdot(1+\delta_{PD})}\right] \tag{1.80}$$

$$\psi_p = x^2 + 1 - \zeta_1 = \left[\sqrt{\frac{v_g - v_{fb} - 1 + \zeta_1}{1+\delta_{PD}} + \left(\frac{\gamma_0}{2\cdot(1+\delta_{PD})}\right)^2} - \frac{\gamma_0}{2\cdot(1+\delta_{PD})}\right]^2 + 1 - \zeta_1 \tag{1.81}$$

$$= \left[\sqrt{\frac{v_g - v_{fb} - 1 + \zeta_1}{1+\delta_{PD}} + \left(\frac{\gamma}{2}\right)^2} - \frac{\gamma}{2}\right]^2 + 1 - \zeta_1 \tag{1.82}$$

where $\gamma = \frac{\gamma_0}{1+\delta_{PD}}$
Similarly,
when ψ_p is close to 0

$$\psi_{p0} = \left[\frac{v_g - v_{fb}}{2} - 3(1 + \frac{\gamma}{\sqrt{2}})\right] + \sqrt{\left[\frac{v_g - v_{fb}}{2} - 3(1 + \frac{\gamma}{\sqrt{2}})\right]^2 + 6(v_g - v_{fb})} \tag{1.83}$$

and in accumulation where $\psi_p << 0$ ($\zeta_2 = \psi_p$),

$$\psi_p = -\ln\left[1 - \zeta_2 + \left(\frac{v_g - v_{fb} - \zeta_2}{\gamma}\right)^2\right] \tag{1.84}$$

The expression of ψ_p in inversion involves the exponential term $e^{-\psi_p}$ which can increase the overall computational time. To avoid that, it is modeled in inversion as

$$\psi_p = 1 + \left[\sqrt{\frac{v_g - v_{fb} - 1}{1 + \delta_{PD}} + (\frac{\gamma}{2})^2} - \frac{\gamma}{2}\right]^2 \tag{1.85}$$

Thus the pinch off potential is expressed as

$$\psi_p = \begin{cases} 1 + \left[\sqrt{v_g - v_{fb} - 1 + \left(\frac{\gamma}{2}\right)^2} - \frac{\gamma}{2}\right]^2 & \text{if } v_g - v_{fb} > \phi_b + \gamma\sqrt{\phi_b} \\ 1 + e^{-\psi_{p0}}\left[\sqrt{v_g - v_{fb} - 1 + e^{-\psi_{p0}} + \left(\frac{\gamma}{2}\right)^2} - \frac{\gamma}{2}\right]^2 & \text{if } \phi_b + \gamma\sqrt{\phi_b} \geq v_g - v_{fb} \geq 0 \\ -\ln\left[1 - \psi_{p0} + \left(\frac{v_g - v_{fb} - \psi_{p0}}{\gamma}\right)^2\right] & \text{if } v_g - v_{fb} < 0 \end{cases} \tag{1.86}$$

Note : Derivatives of ψ_p are continuous in all regions.

1.6.2 Normalized Charge Density

Inversion Charge [3], [4] : Normalized inversion charge density at source/drain is newly derived for BSIM6 and can be obtained as follows.
Charge sheet model approximates inversion charge density as

$$Q_i = -\gamma^{'}.C_{ox}.\sqrt{V_t}\left[\sqrt{\frac{\psi_S}{V_t} + e^{\frac{\psi_S - 2.\phi_F - V_{ch}}{V_t}}} - \sqrt{\frac{\psi_S}{V_t}}\right] \tag{1.87}$$

Using inversion charge linearization [4],

$$Q_i = n_q.C_{ox} \cdot (\psi_S - \psi_P) \tag{1.88}$$

or

$$\psi_S = \psi_P + \frac{Q_i}{n_q.C_{ox}} \tag{1.89}$$

Substituting ψ_S from (1.89) in (1.87),

$$-\frac{Q_i}{\gamma^{'}.C_{ox}.\sqrt{V_t}} = \left[\sqrt{\frac{\psi_P + \frac{Q_i}{n_q.C_{ox}}}{V_t} + e^{\frac{\psi_P + \frac{Q_i}{n_q.C_{ox}} - 2.\phi_F - V_{ch}}{V_t}}} - \sqrt{\frac{\psi_P + \frac{Q_i}{n_q.C_{ox}}}{V_t}}\right] \tag{1.90}$$

rearranging,

$$\left[-\frac{Q_i}{\gamma^{'}.C_{ox}.\sqrt{V_t}} + \sqrt{\frac{\psi_P + \frac{Q_i}{n_q.C_{ox}}}{V_t}}\right]^2 = \left[\sqrt{\frac{\psi_P + \frac{Q_i}{n_q.C_{ox}}}{V_t} + e^{\frac{\psi_P + \frac{Q_i}{n_q.C_{ox}} - 2.\phi_F - V_{ch}}{V_t}}}\right]^2 \tag{1.91}$$

$$e^{\frac{\psi_P + \frac{Q_i}{n_q.C_{ox}} - 2.\phi_F - V_{ch}}{V_t}} = \left(-\frac{Q_i}{\gamma^{'}.C_{ox}.\sqrt{V_t}}\right)^2 - 2.\left(\frac{Q_i}{\gamma.C_{ox}.\sqrt{V_t}}\right) \cdot \sqrt{\frac{\psi_P + \frac{Q_i}{n_q.C_{ox}}}{V_t}} \tag{1.92}$$

This reduces to

$$\frac{\psi_P + \frac{Q_i}{n_q.C_{ox}} - 2.\phi_F - V_{ch}}{V_t} = \ln\left[\left(-\frac{Q_i}{\gamma^{'}.C_{ox}.\sqrt{V_t}}\right)^2 - 2.\left(\frac{Q_i}{\gamma^{'}.C_{ox}.\sqrt{V_t}}\right) \cdot \sqrt{\frac{\psi_P + \frac{Q_i}{n_q.C_{ox}}}{V_t}}\right] \tag{1.93}$$

$$= \ln\left[-\frac{Q_i}{\gamma^{'}.C_{ox}.\sqrt{V_t}}\left(-\frac{Q_i}{\gamma^{'}.C_{ox}.\sqrt{V_t}} + 2 \cdot \sqrt{\frac{\psi_P + \frac{Q_i}{n_q.C_{ox}}}{V_t}}\right)\right] \tag{1.94}$$

Normalizing inversion charge to $-2V_t.n_q.C_{ox}$, all voltages to V_t and using $\gamma_0 = \gamma^{'}.\sqrt{V_t}$,

$$\psi_p - 2.q_i - 2.\phi_f - v_{ch} = \ln\left[\frac{2n_q.q_i}{\gamma_0}\left(\frac{2.n_q.q_i}{\gamma_0} + 2 \cdot \sqrt{\phi_p - 2q_i}\right)\right] \tag{1.95}$$

which gives

$$\ln(q_i) + \ln\left[\frac{2n_q}{\gamma_0}(q_i\frac{2n_q}{\gamma_0} + 2\sqrt{\psi_p - 2q_i})\right] + 2q_i = \psi_p - 2\phi_f - v_{ch} \tag{1.96}$$

This is a general equation which can be solved to give normalized inversion charge density. It can be further simplified by noting that the term $\left[\frac{2n_q}{\gamma_0}(q_i\frac{2n_q}{\gamma_0}+2\sqrt{\psi_p-2q_i})\right]$ never exceeds unity and therefore can be approximated by $\frac{4n_q}{\gamma_0}.\sqrt{\psi_p}$.
Thus (1.96) can be written as [5]

$$\ln(q_i)+\ln\left(\frac{4n_q}{\gamma_0}.\sqrt{\psi_p}\right)+2q_i=\psi_p-2\phi_f-v_{ch} \tag{1.97}$$

The procedure of obtaining initial guess for the solution of above equation for weak inversion is described below [6]. Note that to generalized the process, subscript "i" is dropped from the term q_i
Let $v=\psi_p-2\phi_f-v_{ch}-\ln(\frac{4n_q\sqrt{\psi_p}}{\gamma})=\ln q+2q$

$$v=\ln q+2q \tag{1.98}$$
$$=\ln q+2e^{\ln q} \tag{1.99}$$
$$=\ln q+\frac{1}{F(\ln q)} \tag{1.100}$$

Here in second term q has been used as $\ln(e^q)$. The function F is defined as

$$F=\frac{1}{2e^{\ln q}} \tag{1.101}$$
$$=\frac{1}{2e^{(}\ln q+\ln q_t-\ln q_t)} \tag{1.102}$$
$$=\frac{1}{2q_te^{\ln\frac{q}{q_t}}} \tag{1.103}$$
$$=\frac{1}{2q_t}e^{-\Delta} \tag{1.104}$$

Where $\Delta=\ln\frac{q}{q_t}$. Expanding (1.104) around $\Delta=0$ using Taylor series expansion (as $|2q|<<|\ln q|$),

$$F=\frac{1}{2q_t}.[1-e^{-0}.\Delta]] \tag{1.105}$$
$$=\frac{1}{2q_t}(1-\ln\frac{q}{q_t}) \tag{1.106}$$

substituting in (1.100),

$$v=\ln q+\frac{2q_t}{1-\ln q+\ln q_t} \tag{1.107}$$

This equation is solved for q. Let,

$$\ln q = x \tag{1.108}$$

$$v = x + \frac{2q_t}{1 + \ln q_t - x} \tag{1.109}$$

$$v(1 + \ln q_t) - vx - x(1 + \ln q_t) + x^2 - q_t = 0 \tag{1.110}$$

$$x = \frac{v + (1 + \ln q_t) - \sqrt{(v + (1 + \ln q_t)^2 - 4v(1 + \ln q_t) + 8q_t}}{2} \tag{1.111}$$

For subthreshold region, normalized inversion charge density will be $|q| << 1$ and $|\ln q| >> |2q|$. The initial value is taken at a point where $|\ln q| = 2.|2q|$ which gives

$$q_t = 0.301 \tag{1.112}$$

$$1 + \ln q_t = -0.201491 \tag{1.113}$$

substituting in (1.111),

$$x = \frac{v - 0.201491 - \sqrt{(v - 0.201491)^2 - 4v(-0.201491) + 8(0.301)}}{2} \tag{1.114}$$

$$x = \ln q = \frac{v - 0.201491 - \sqrt{(v + 0.402982)v + 2.446562}}{2} \tag{1.115}$$

Once the initial guess is known, the final value is obtained by using analytical method as shown below

$$n_{q0} = 1 + \frac{\gamma}{2\sqrt{\psi_p}} \tag{1.116}$$

$$v = \psi_p - 2\phi - v_{ch} - ln\left(4.0 \cdot \frac{n_{q0}}{\gamma} \cdot \sqrt{\psi_p}\right) \tag{1.117}$$

$$ln_{q0} = \frac{1}{2}\left[v - 0.201491 - \sqrt{v \cdot (v + 0.402982) + 2.446562}\right] \tag{1.118}$$

$$q_0 = e^{ln_{q0}} \tag{1.119}$$

if $ln_{q0} <= -80.0$

$$q_{s/d} = f = q_0 \cdot \left[1 + \psi_p - 2\phi - v_{ch} - ln_{q0} - \ln\left(2 \cdot \frac{n_{q0}}{\gamma}\left(2 \cdot q_0 \cdot \frac{n_{q0}}{\gamma} + 2 \cdot \sqrt{\psi_p}\right)\right)\right] \tag{1.120}$$

In this equation, if $\ln q_0$ becomes very large and negative then $q_0 = e^{\ln q_0}$ may be out of range of precision limit of the simulator. Therefore it is approximated as follows

if $\ln q_0 < -110$, $q_0 = e^{-100}$

if $\ln q_0 > -90$, $q_0 = e^{\ln q_0}$

else $q_0 = exp(-100 + 20(\frac{5}{64} + \frac{z}{2} + z^2(\frac{15}{16} - z^2(1.25 - z^2))))$

where $z = \frac{\ln q_0 + 100}{20}$.

The above polynomial provides smooth derivatives for q. For the derivation of polynomial coefficients, refer to Appendix A.

For $\ln q_0 > -80$

$$f = 2q_0 + \ln\left(2q_0\frac{n_q}{\gamma}(2q_0\frac{n_q}{\gamma} + 2\sqrt{\psi_p}\right) - (v_p - 2\phi_f - v_{ch}) \tag{1.121}$$

$$f' = 2 + \frac{1}{q_0} + \frac{\frac{n_{q0}}{\gamma} - \frac{1}{\sqrt{\psi_p}}}{\frac{n_{q0}}{\gamma} \cdot q_0 + \sqrt{\psi_p}} \tag{1.122}$$

$$q_1 = q_0 - \frac{f}{f'} \tag{1.123}$$

The accuracy of this initial guess is further improved by following procedure

$$f = 2q_1 + \ln\left(2q_1\frac{n_q}{\gamma}(2q_1\frac{n_q}{\gamma} + 2\sqrt{\psi_p}\right) - (v_p - 2\phi_f - v_{ch}) \tag{1.124}$$

$$f' = 2 + \frac{1}{q_1} + \frac{\frac{n_{q1}}{\gamma} - \frac{1}{\sqrt{\psi_p}}}{\frac{n_{q1}}{\gamma} \cdot q_1 + \sqrt{\psi_p}} \tag{1.125}$$

Applying Halley's method,

$$f'' = -\frac{1}{q_1^2} - \frac{1}{\left[(\psi_p)^{\frac{3}{2}}\right] \cdot \left[\frac{n_{q0}}{\gamma} \cdot q_1 + \sqrt{\psi_p}\right]} - \left[\frac{\frac{n_{q0}}{\gamma} - \frac{1}{\sqrt{\psi_p}}}{\frac{n_{q0}}{\gamma} \cdot q_1 + \sqrt{\psi_p}}\right]^2 \tag{1.126}$$

$$q_{s/d} = q_1 - \frac{f}{f'} \cdot \left(1 + \frac{f \cdot f''}{2 \cdot f'^2}\right) \tag{1.127}$$

1.7 Short Channel Effects

Vt Roll-off, DIBL, and Subthreshold Slope Degradation (Ref.: BSIM4 Model)

$$\psi_{st} = 0.4 + PHIN + \frac{kT}{q} \cdot \ln \frac{NDEP}{n_i} \tag{1.128}$$

$$PhistVbs = \psi_{st} - V_{bsx} \tag{1.129}$$

$$X_{dep} = \sqrt{\frac{2 \cdot \epsilon_{sub} \cdot PhistVbs}{q \cdot NDEP}} \tag{1.130}$$

$$n = 1 + \frac{CIT + NFACTOR + CDSCD \cdot V_{dsx} - CDSCB \cdot V_{bsx}}{C_{ox}} \tag{1.131}$$

$$V_t = \frac{k_b \cdot T}{q} \tag{1.132}$$

$$nV_t = n \cdot V_t \tag{1.133}$$

$$\Delta V_{th,VDNUD} = -K2 \cdot V_{bsx} \tag{1.134}$$

$$\Delta V_{th,DIBL} = -(ETA0 + ETAB \cdot V_{bsx}) \cdot V_{dsx} \tag{1.135}$$

$$\begin{aligned} \Delta V_{th,DITS} = & -n\frac{KT}{q} \cdot \ln\left(\frac{L_{eff}}{L_{eff} + DVTP0 \cdot (1 + \exp(-DVTP1 \cdot V_{ds})}\right) \\ & - \left(DVTP5 + \frac{DVTP2}{L_{eff}^{DVTP3}}\right) \cdot tanh\left(DVTP4 \cdot V_{dsx}\right) \end{aligned} \tag{1.136}$$

$$\Delta V_{th,all} = \Delta V_{th,VNUD} + \Delta V_{th,DIBL} + \Delta V_{th,DITS} \tag{1.137}$$

$$V_{gfb} = V_g - V_{fb} - \Delta V_{th,all} \tag{1.138}$$

Note: Short channel effect and Reverse short channel effect are modeled using NDEPL1, NDELEXP1, NDEPL2 and NDEPLEXP2 parameters. Width scaling of V_{th} is modeled using NDEPW and NDEPWEXP parameters.

1.8 Drain Saturation Voltage

The drain saturation voltage model is calculated after the source-side charge (q_s) has been calculated. V_{dseff} is subsequently used to compute the drain-side charge (q_d).

Electric Field Calculations

Electric Field is in MV/cm

$$\eta = \begin{cases} \frac{1}{2} \cdot ETAMOB & \text{for NMOS} \\ \frac{1}{3} \cdot ETAMOB & \text{for PMOS} \end{cases} \tag{1.139}$$

$$E_{effs} = 10^{-8} \cdot \left(\frac{q_{bs} + \eta \cdot q_{is}}{\epsilon_{ratio} \cdot Tox} \right) \tag{1.140}$$

Drain Saturation Voltage (V_{dsat}) Calculations (Ref. BSIM4 & EKV Model)

$$D_{mobs} = 1 + (UA + UC \cdot V_{bsx}) \cdot (E_{effs})^{EU} + \frac{UD}{\left[\frac{1}{2} \cdot \left(1 + \frac{q_{is}}{q_{bs}} \right) \right]^{UCS}} \tag{1.141}$$

$$T_0 = \begin{cases} \frac{1}{1 + PSATB \cdot V_{bsx}} & V_{bs \geq 0} \\ 1 - PSATB \cdot V_{bsx} & V_{bs} < 0 \end{cases} \tag{1.142}$$

$$\lambda_C = \frac{2 \cdot U0 \cdot nV_t}{(D_{mobs})^{PSAT} \cdot VSAT \cdot L_{eff}} \cdot [1 + PTWG \cdot \frac{10 \cdot PSATX \cdot qs \cdot T_0}{10 \cdot PSATX + qs \cdot T_0}] \tag{1.143}$$

$$q_{dsat} = \frac{\lambda_C}{2} \cdot \frac{q_s^2 + q_s}{1 + \frac{\lambda_C}{2} \cdot (1 + q_s)} \tag{1.144}$$

$$v_{dsat} = \psi_p - \frac{2\phi_b}{n} - 2q_{dsat} - \ln \left[\frac{2q_{dsat} \cdot n_q}{gam} \cdot \left(\frac{2q_{dsat} \cdot n_q}{gam} + \frac{gam}{n_q - 1} \right) \right] \tag{1.145}$$

$$V_{dsat} = v_{dsat} \cdot nV_t \tag{1.146}$$

$$V_{dssat} = V_{dsat} - V_s \tag{1.147}$$

$$V_{dseff} = \frac{V_{ds}}{\left[1 + \left(\frac{V_{ds}}{V_{dssat}} \right)^{1/DELTA} \right]^{DELTA}} \tag{1.148}$$

$$v_{deff} = \frac{V_{dseff} + V_s}{nV_t} \tag{1.149}$$

1.9 Mobility degradation with vertical field

(Ref. BSIM4 Model)

$$E_{effm} = 10^{-8} \cdot \left(\frac{q_{ba} + \eta \cdot q_{ia}}{\epsilon_{ratio} \cdot T_{ox}} \right) \tag{1.150}$$

Where q_{ia} and q_{ba} are the average inversion charge and bulk charge densities respectively.

$$D_{mob} = 1 + (UA + UC \cdot V_{bsx}) \cdot (E_{effm})^{EU} + \frac{UD}{\left[\frac{1}{2} \cdot \left(1 + \frac{q_{ia}}{q_{ba}}\right)\right]^{UCS}} \tag{1.151}$$

The D_{mob} goes into denominator of mobility expression.

1.10 Parasitic series resistance

1.10.1 Bias Dependent Internal Series Resistance ($R_{ds}(V)$)

The internal source-drain resistance ($R_{ds}(V)$) option can be invoked by setting the model selector $RDSMOD = 0$ (internal). The expressions for source/drain series resistances are as follows:

$$T_0 = 1 + PRWG \cdot q_{ia} \tag{1.152}$$

$$T_1 = PRWB \cdot (\sqrt{\phi_s - V_{bs}} - \sqrt{\phi_s}) \tag{1.153}$$

$$T_2 = \frac{1}{T_0} + T_1 \tag{1.154}$$

$$T_3 = \frac{1}{2}\left[T_2 + \sqrt{T_2^2 + 0.01}\right] \tag{1.155}$$

$$R_{ds}(V) = NF \cdot \left(R_{s,geo} + R_{d,geo} + W_{eff}^{WR}\left[RDSWMIN + RDSW \cdot T_3\right]\right) \tag{1.156}$$

$$D_r = 1.0 + \mu_0 \cdot C_{ox} \cdot \frac{W_{eff}}{L_{eff}} \cdot q_{ia} \cdot R_{ds} \tag{1.157}$$

$R_{s,geo}$ and $R_{d,geo}$ are the source and drain diffusion resistances, which are described later. And, D_r goes into the denominator of the final I_{ds} expression.

1.10.2 Bias Dependent External Series Resistance ($R_s(V)$ & $R_d(V)$)

The bias-dependent external resistance model is adopted from BSIM4 and can be invoked by setting model selector RDSMOD=1. BSIM4 and BSIM6 allow the source

extension resistance $R_s(V)$ and the drain extension resistance $R_d(V)$ to be external and asymmetric (i.e. $R_s(V)$ and $R_d(V)$ can be connected between the external and internal source and drain nodes, respectively; furthermore, $R_s(V)$ does not have to be equal to $R_d(V)$). This feature makes accurate RF CMOS simulation possible.
The source/drain series resistance is the sum of a bias-independent component and a bias-dependent component.

$$V_{gs,eff} = \frac{1}{2}\left[V_{gs} - V_{fbsdr} + \sqrt{(V_{gs} - V_{fbsdr})^2 + 10^{-2}}\right]$$
$$V_{gd,eff} = \frac{1}{2}\left[V_{gd} - V_{fbsdr} + \sqrt{(V_{gd} - V_{fbsdr})^2 + 10^{-2}}\right] \tag{1.158}$$
$$R_{source} = \frac{1}{W_{eff}^{WR} \cdot NF} \cdot \left(RSWMIN + RSW \cdot \left[-PRWB \cdot V_{bs} + \frac{1}{1 + PRWG_i \cdot V_{gs,eff}}\right]\right) + R_{s,geo} \tag{1.159}$$
$$R_{drain} = \frac{1}{W_{eff}^{WR} \cdot NF} \cdot \left(RDWMIN + RDW \cdot \left[-PRWB \cdot V_{bd} + \frac{1}{1 + PRWG_i \cdot V_{gd,eff}}\right]\right) + R_{d,geo} \tag{1.160}$$

$R_{s,geo}$ and $R_{d,geo}$ are the source and drain diffusion resistances, which are described below.

1.10.3 Sheet resistance model

The resistances $R_{s,geo}$ and $R_{d,geo}$ are simply calculated as the sheet resistances ($RSHS$,$RSHD$) times the number of squares (NRS,NRD):

$$R_{s,geo} = NRS \cdot RSHS$$
$$R_{d,geo} = NRD \cdot RSHD \tag{1.161}$$

1.11 Output Conductance [1]

Channel Length Modulation (CLM)

$$E_{sat} = \frac{2 \cdot VSAT}{\frac{U0}{D_{mob}}} \tag{1.162}$$

$$F = \begin{cases} 1 & \text{for } FPROUT \leq 0 \\ \frac{1}{1+\frac{FPROUT \cdot \sqrt{L_{eff}}}{qia+2 \cdot nV_t}} & \text{for } FPROUT > 0 \end{cases} \tag{1.163}$$

$$C_{clm} = \begin{cases} PCLM \cdot \left(1 + PCLMG \cdot \frac{q_{ia}}{E_{sat} \cdot L_{eff}}\right) \frac{1}{F} & \text{for } PCLMG > 0 \\ \frac{PCLM}{\cdot \left(1 - PCLMG \cdot \frac{q_{ia}}{E_{sat} \cdot L_{eff}}\right)} \frac{1}{F} & \text{for } PCLMG < 0 \end{cases} \tag{1.164}$$

$$V_{asat} = V_{dssat} + E_{satL} \tag{1.165}$$

$$M_{CLM} = 1 + C_{clm} \ln \left[1 + \frac{V_{ds} - V_{dseff}}{V_{asat}} \cdot \frac{1}{C_{clm}}\right] \tag{1.166}$$

Drain Induced Barrier Lowering (DIBL)

$$PVAGfactor = \begin{cases} 1 + PVAG \cdot \frac{q_{im}}{E_{sat} L_{eff}} & \text{for } PVAG > 0 \\ \frac{1}{1 - PVAG \cdot \frac{q_{im}}{E_{sat} L_{eff}}} & \text{for } PVAG < 0 \end{cases} \tag{1.167}$$

$$\theta_{rout} = PDIBLC \tag{1.168}$$

$$V_{ADIBL} = \frac{q_{ia} + 2kT/q}{\theta_{rout}} \cdot \left(1 - \frac{V_{dssat}}{V_{dssat} + q_{ia} + 2kT/q}\right) \cdot PVAGfactor \cdot \frac{1}{1 + PDIBLCB \cdot V_{bsx}} \tag{1.169}$$

$$M_{DIBL} = \left(1 + \frac{V_{ds} - V_{dseff}}{V_{ADIBL}}\right) \tag{1.170}$$

Note: Length scaling parameters for PDIBLC are PDIBLCL and PDIBLCLEXP.

Drain Induced Threshold Shift (DITS)

$$V_{ADITS} = \frac{1}{PDITS} \cdot F \cdot [1 + (1 + PDITSL \cdot L_{eff}) \exp(PDITSD \cdot V_{ds})] \tag{1.171}$$

$$M_{DITS} = \left(1 + \frac{V_{ds} - V_{dseff}}{V_{ADITS}}\right) \tag{1.172}$$

Substrate Current induced Body Effect (SCBE)

$$litl = \sqrt{(\epsilon_{sub}/\epsilon_{ox}) \cdot T_{ox} \cdot XJ} \tag{1.173}$$

$$V_{ASCBE} = \frac{L_{eff}}{PSCBE2} \cdot \exp\left(\frac{PSCBE1 \cdot litl}{V_{ds} - V_{dseff}}\right) \tag{1.174}$$

$$M_{SCBE} = \left(1 + \frac{V_{ds} - V_{dseff}}{V_{ASCBE}}\right) \tag{1.175}$$

$$M_{oc} = M_{DIBL} \cdot M_{CLM} \cdot M_{DITS} \cdot M_{SCBE} \tag{1.176}$$

M_{oc} is multiplied to I_{ds} in the final drain current expression.

1.12 Velocity Saturation

Current Degradation Due to Velocity Saturation

$$T_1 = 2 \cdot \lambda_C \cdot (q_s - q_{deff}) \tag{1.177}$$

$$\lambda_C = \frac{2 \cdot U0 \cdot nV_t}{(D_{mobs})^{PSAT} \cdot VSAT \cdot L_{eff}} \cdot [1 + PTWG \cdot \frac{10 \cdot PSATX \cdot qs \cdot T_0}{10 \cdot PSATX + qs \cdot T_0}] \tag{1.178}$$

$$D_{vsat} = \frac{1}{2}\left[\sqrt{1 + T_1^2} + \frac{1}{T_1} \cdot \ln(T_1 + \sqrt{1 + T_1^2})\right] \tag{1.179}$$

$$D_{ptwg} = D_{vsat} \tag{1.180}$$

$$D_{tot} = D_{mob} \cdot D_{vsat} \cdot D_r \tag{1.181}$$

where D_r is the effect of internal resistance (R_{dsi}) on current, defined as

$$D_r = \begin{cases} 1 & \text{if } RDSMOD = 1 \\ 1 + U0 \cdot C_{ox} \cdot \frac{W_{eff}}{L_{eff}} \cdot q_{ia} \cdot R_{dsi} & \text{if } RDSMOD = 0 \end{cases} \tag{1.182}$$

1.13 Effective Mobility

$$\mu_{eff} = \frac{U0}{D_{tot}} \tag{1.183}$$

1.14 Drain Current Model

1.14.1 Without Velocity Saturation

The drain current expression is derived as follows,

$$I_{ds} = I_{drift} + I_{diff} \tag{1.184}$$

$$I_{ds} = -W_{eff}.Q_i \cdot \mu_{eff}\frac{d\psi_s}{dx} + W \cdot \mu_{eff} \cdot V_t\frac{dQ_i}{dx} \tag{1.185}$$

from charge linearization, $\psi_s = \psi_p + \frac{Q_i}{n_q.C_{ox}}$. Thus

$$I_{ds} = \mu_{eff}.W_{eff} \cdot \left[-\frac{Q_i}{n_q.C_{ox}} + V_t\right]\frac{dQ_i}{dx} \tag{1.186}$$

normalizing inversion charge to $-2n_qC_{ox}V_t$ and using $\xi = \frac{x}{L}$,

$$I_{ds} = \mu_{eff}.\frac{W_{eff}}{L_{eff}} \cdot \left[-\frac{(-2.n_q.C_{ox}.V_t.q)}{n_q.C_{ox}} + V_t\right]\frac{d(-2.n_q.C_{ox}.V_t.q)}{d\xi} \tag{1.187}$$

$$= -2 \cdot n_q \cdot \mu_{eff} \cdot \frac{W_{eff}}{L_{eff}} \cdot C_{ox} \cdot nV_t^2 \cdot (2q+1)\frac{dq}{d\xi} \tag{1.188}$$

Total drain current,

$$I_{DS} = \int_0^1 I_{ds}\, d\xi = -2 \cdot n_q \cdot \mu_{eff} \cdot \frac{W_{eff}}{L_{eff}} \cdot C_{ox} \cdot nV_t^2 \cdot \int_{q_s}^{q_d} (2q+1)dq \tag{1.189}$$

which gives

$$I_{DS} = 2 \cdot n_q \cdot \mu_{eff} \cdot \frac{W_{eff}}{L_{eff}} \cdot C_{ox} \cdot nV_t^2 \cdot [(q_s - q_{deff})(q_s + q_{deff} + 1)] \tag{1.190}$$

n_q is the slope factor in charge based model and nV_t is $n.\frac{KT}{q}$ with n given by (1.131).

1.14.2 Including Velocity Saturation

As the device is getting smaller and smaller, the lateral electric field strength and therefore kinetic energy of the carriers increases. On reaching optical phonon energy

levels, they releases optical phonon by virtue of reduction in kinetic energy and therefore loses velocity [7]. The effect of velocity saturation on mobility is captured as follows

$$\mu = \frac{\mu_{eff}}{\sqrt{1 + (\frac{E}{E_c})^2}} \tag{1.191}$$

$$= \frac{\mu_{eff}}{\sqrt{1 + (\frac{1}{E_c} \cdot \frac{d\psi_s}{dx})^2}} \tag{1.192}$$

from (1.188) and (1.192),

$$I_{ds} = -2 \cdot n_q \cdot \frac{\mu_{eff}}{\sqrt{1 + (\frac{1}{E_c} \cdot \frac{d\psi_s}{dx})^2}} \cdot \frac{W_{eff}}{L_{eff}} \cdot C_{ox} \cdot nV_t^2 \cdot (2q+1)\frac{dq}{d\xi} \tag{1.193}$$

$$= z \cdot \frac{(2q+1)\frac{dq}{d\xi}}{\sqrt{1 + (\frac{1}{E_c} \cdot \frac{d\psi_s}{dx})^2}} \tag{1.194}$$

with $z = -2\mu_{eff} \cdot n_q \cdot \frac{W_{eff}}{L_{eff}} \cdot C_{ox} \cdot nV_t^2$
Total current,

$$I_{DS} = \int_0^1 I_{ds}\, d\xi = z \cdot \int_{q_s}^{q_d} \frac{(2q+1)}{\sqrt{1 + (\frac{1}{E_c} \cdot \frac{d\psi_s}{dx})^2}} dq \tag{1.195}$$

$$I_{DS} \int_0^1 \sqrt{1 + \left(\frac{1}{E_c} \cdot \frac{d\psi_s}{dx}\right)^2}\, d\xi = z \cdot \int_{q_s}^{q_d} (2q+1) dq \tag{1.196}$$

from (1.190),

$$\int_{q_s}^{q_d} (2q+1) dq = -(q_s - q_{deff})(q_s + q_{deff} + 1) \tag{1.197}$$

Now consider the LHS of (1.196). Using charge linearization, $\psi_s = \psi_p + \frac{Q_i}{n_q.C_{ox}}$,

$$\frac{1}{E_c}\frac{d\psi_s}{dx} = \frac{1}{E_c.n_q.C_{ox}}\frac{Q_i}{dx} = -\frac{2V_t}{E_c.L}\frac{dq}{d\xi} = -\lambda_c \cdot \frac{dq}{d\xi} \tag{1.198}$$

Let

$$D_{vsat} = \int \sqrt{1 + \left(\frac{1}{E_c} \cdot \frac{d\psi_s}{dx}\right)^2} d\xi$$

It is evaluated by assuming that lateral electric field ($-\frac{d\psi_s}{d\xi}$) increases linearly from 0 at source to $2 \cdot \left(\frac{\psi_{s,D} - \psi_{s,S}}{L}\right)$ at drain [8] i.e.

$$-\frac{d\psi_s}{dx} = 2 \cdot \frac{\psi_{s,D} - \psi_{s,S}}{L} \cdot \frac{x}{L} = 2 \cdot \frac{\psi_{s,D} - \psi_{s,S}}{L} \cdot \xi \tag{1.199}$$

From charge linearization (1.89),

$$\psi_{s,S} = \psi_P + \frac{Q_S}{n_q.C_{ox}} = \psi_P - 2V_t.q_s \tag{1.200}$$

$$\psi_{s,D} = \psi_P + \frac{Q_D}{n_q.C_{ox}} = \psi_P - 2V_t.q_d \tag{1.201}$$

$$\psi_{s,D} - \psi_{s,S} = 2.V_t(q_s - q_d) \tag{1.202}$$

substituting in (1.199),

$$-\frac{d\psi_s}{dx} = 2 \cdot \frac{2.V_t(q_s - q_d)}{L^2} \cdot x = 2 \cdot \frac{2.V_t(q_s - q_d)}{L} \cdot \xi \tag{1.203}$$

$$-\frac{1}{E_c}\frac{d\psi_s}{dx} = 2 \cdot \frac{2.V_t}{E_c L} \cdot (q_s - q_d)\xi = 2\lambda_c(q_s - q_d)\xi \tag{1.204}$$

where $\lambda_c = \frac{2V_t}{E_c.L}$. Thus D_{vsat} can be given as

$$D_{vsat} = \int \sqrt{1 + \left(\frac{1}{E_c} \cdot \frac{d\psi_s}{dx}\right)^2} d\xi \tag{1.205}$$

$$= \int \sqrt{1 + (2\lambda_c(q_s - q_d)\xi)^2} d\xi = \int \sqrt{1 + (2\lambda_c.\Delta q \cdot \xi)^2} d\xi \tag{1.206}$$

$$= \frac{1}{2}\left[\sqrt{1 + (2.\lambda_c.\Delta q)^2} + \frac{1}{2.\lambda_c.\Delta q}.\ln\left(2.\lambda_c.\Delta q + \sqrt{1 + (2.\lambda_c.\Delta q)^2}\right)\right] \tag{1.207}$$

with $\Delta q = q_s - q_d$. From (1.196), (1.197) and (1.207),

$$I_{DS} = 2 \cdot n_q \cdot \mu_{eff} \cdot \frac{W_{eff}}{L_{eff}} \cdot C_{ox} \cdot nV_t^2 \cdot [(q_s - q_{deff})(q_s + q_{deff} + 1)].M_{oc} \tag{1.208}$$

where $\mu_{eff} = \frac{U0}{D_{tot}}$ and $D_{tot} = D_{mod}.D_{vsat}.D_r$

1.15 Impact Ionization Model

The impact ionization current model in BSIM6 is the same as that in BSIM4, and is modeled by

$$I_{ii} = ALPHA0 \cdot (V_{ds} - V_{dseff}) \cdot exp\Big(- \frac{BETA0}{V_{ds} - V_{dseff}}\Big) \cdot \frac{I_{ds}}{M_{SCBE}} \tag{1.209}$$

where parameters $ALPHA0$ and $BETA0$ are impact ionization coefficients. ALPHA0L and ALPHA0LEXP are length scaling parameters for ALPHA0.

Note: The order of ALPHA0 in BSIM6 = 10^6 X order of ALPHA0 in BSIM4

1.16 GIDL/GISL Current Model

GIDL/GISL currents are set using model selector GIDLMOD=1. The GIDL/GISL current and its body bias effect are modeled by

$$\begin{aligned} I_{GIDL} &= AGIDL \cdot W_{eff} \cdot NF \cdot \frac{V_{ds} - V_{gse} - EGIDL}{3 \cdot T_{oxe}} \\ &\quad \cdot exp\left(- \frac{3 \cdot T_{oxe} \cdot BGIDL}{V_{ds} - V_{gse} - EGIDL}\right) \cdot \frac{V_{db}^3}{CGIDL + V_{db}^3} \end{aligned} \tag{1.210}$$

$$\begin{aligned} I_{GISL} &= AGISL \cdot W_{eff} \cdot NF \cdot \frac{-V_{ds} - V_{gde} - EGISL}{3 \cdot T_{oxe}} \\ &\quad \cdot exp\left(- \frac{3 \cdot T_{oxe} \cdot BGISL}{-V_{ds} - V_{gde} - EGISL}\right) \cdot \frac{V_{sb}^3}{CGISL + V_{sb}^3} \end{aligned} \tag{1.211}$$

where $AGIDL$, $BGIDL$, $CGIDL$ and $EGIDL$ are model parameters for the drain side and $AGISL$, $BGISL$, $CGISL$ and $EGISL$ are the model parameters for the source side. $CGIDL$ and $CGISL$ account for the body-bias dependence of I_{GIDL} and I_{GISL} respectively.W_{eff} and NF are the effective width of the source/drain diffusions and the number of fingers. Further explanation of W_{eff} and NF can be found in the chapter of the layout-dependence model. Check scaling parameters in the parameter list at the end.

I_{GIDL}/I_{GISL} can be switched off by setting $GIDLMOD = 0$.

1.17 Gate Tunneling Current Model

As the gate oxide thickness is scaled down to $3nm$ and below, gate leakage current due to carrier direct tunneling becomes important. This tunneling happens between the gate and silicon beneath the gate oxide. To reduce the tunneling current, high-k dielectrics are being used in place of gate oxide. In order to maintain a good interface with substrate, multi-layer dielectric stacks are being used. The BSIM6 gate tunneling model (taken from BSIM4) has been shown to work for multi-layer gate stacks as well. The tunneling carriers can be either electrons or holes, or both, either from the conduction band or valence band, depending on (the type of the gate and) the bias regime. In BSIM6, the gate tunneling current components include the tunneling current between gate and substrate (I_{gb}), and the current between gate and channel (I_{gc}), which is partitioned between the source and drain terminals by $I_{gc} = I_{gcs} + I_{gcd}$. The third component happens between gate and source/drain diffusion regions (I_{gs} and I_{gd}). Figure 1 shows the schematic gate tunneling current flows.

1.17.1 Model Selectors

Two global selectors are provided to turn on or off the tunneling components. **IGCMOD** = 1 turns on I_{gc}, I_{gs}, and I_{gd}; **IGBMOD** = 1 turns on I_{gb}. When the selectors are set to zero, no gate tunneling currents are modeled.

$$V_{ox} = nVt \cdot (v_g - v_{fb} - \psi_p + q_s + q_{deff}) \tag{1.212}$$

$$V_{oxacc} = \frac{1}{2}\left(-V_{ox} + \sqrt{V_{ox}^2 + 10^{-4}}\right) \tag{1.213}$$

$$V_{oxdepinv} = \frac{1}{2}\left(V_{ox} + \sqrt{V_{ox}^2 + 10^{-4}}\right) \tag{1.214}$$

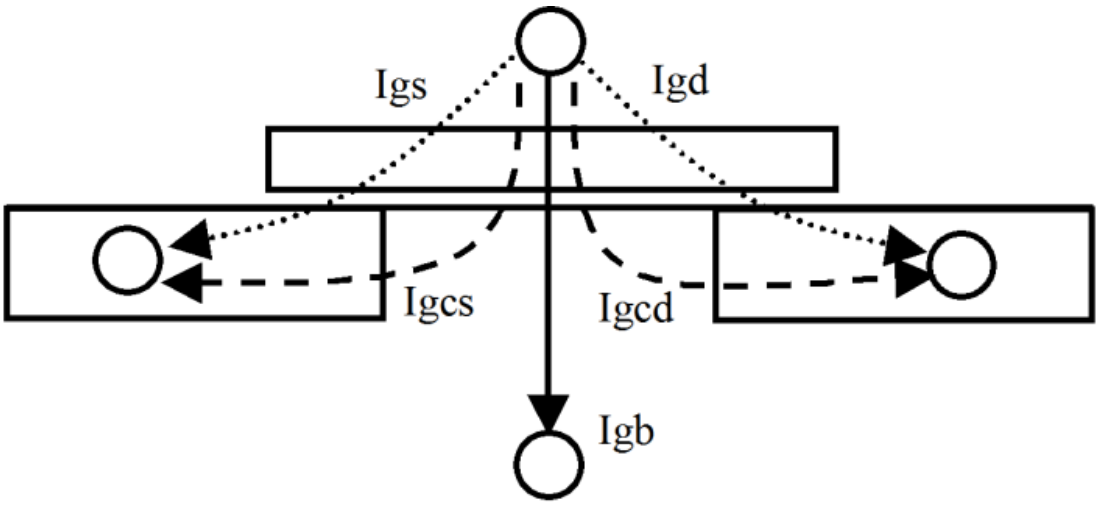

Figure 1: Schematic gate current components flowing between MOSFET terminals.

Eq. (1.213) and (1.214) are valid and continuous from accumulation through depletion to inversion.

1.17.2 Equations for Tunneling Currents

Note: All gate tunneling current equations use operating temperature in the calculations.

Gate-to-Substrate Current ($I_{gb} = I_{gbacc} + I_{gbinv}$): I_{gbacc}, determined by ECB (Electron tunneling from Conduction Band), is significant in accumulation and given by

$$\begin{aligned} I_{gbacc} &= NF \cdot W_{eff} L_{eff} \cdot A \cdot T_{oxRatio} \cdot V_{gb} \cdot V_{aux} \cdot i_{gtemp} \\ &\quad \cdot exp[-B \cdot TOXE(AIGBACC - BIGBACC \cdot V_{oxacc}) \cdot (1 + CIGBAC \cdot V_{oxacc})] \end{aligned} \tag{1.215}$$

where the physical constants $A = 4.97232e-7\ A/V^2$, $B = 7.45669e11(g/F - s^2)^{0.5}$,

and

$$T_{oxRatio} = \left(\frac{TOXREF}{TOXE}\right)^{NTOX} \cdot \frac{1}{TOXE^2} \tag{1.216}$$

$$V_{aux} = NIGBACC \cdot V_t \cdot log\left(1 + exp\left(-\frac{V_{oxacc}}{NIGBACC \cdot V_t}\right)\right) \tag{1.217}$$

I_{gbinv}, determined by EVB (Electron tunneling from Valence Band), is significant in inversion and given by

$$\begin{aligned} I_{gbinv} &= NF \cdot W_{eff}L_{eff} \cdot A \cdot T_{oxRatio} \cdot V_{gb} \cdot V_{aux} \cdot i_{gtemp} \\ &\cdot exp[-B \cdot TOXE(AIGBINV - BIGBINV \cdot V_{oxdepinv}) \cdot (1 + CIGBINVV_{oxdepinv})] \end{aligned} \tag{1.218}$$

where A = 3.75956e-7 A/V^2, B = 9.82222e11 $(g/F - s^2)^{0.5}$, and

$$V_{aux} = NIGBINV \cdot V_t \cdot log\left(1 + exp\left(\frac{V_{oxdepinv} - EIGBINV}{NIGBINV \cdot V_t}\right)\right) \tag{1.219}$$

$$I_{gb} = I_{gbacc} + I_{gbinv} \tag{1.220}$$

Gate-to-Channel Current (I_{gc0}) and Gate-to-S/D (I_{gs} and I_{gd}): I_{gc0}, determined by ECB for NMOS and HVB (Hole tunneling from Valence Band) for PMOS at $V_{ds} = 0$, is formulated as

$$\begin{aligned} I_{gc0} &= NF \cdot W_{eff}L_{eff} \cdot A \cdot T_{oxRatio} \cdot V_{gse} \cdot V_{aux} \cdot i_{gtemp} \\ &\cdot exp[-B \cdot TOXE(AIGC - BIGC \cdot V_{oxdepinv}) \cdot (1 + CIGCV_{oxdepinv})] \end{aligned} \tag{1.221}$$

where A = 4.97232 A/V^2 for NMOS and 3.42537 A/V^2 for PMOS, B = 7.45669e11 $(g/F - s^2)^0.5$ for NMOS and 1.16645e12 $(g/F - s^2)^{0.5}$ for PMOS.

$$V_{aux} = n_q \cdot nVt \cdot (q_s + q_{deff}) \tag{1.222}$$

Partition of I_{gc}: To consider the drain bias effect, I_{gc} is split into two components, I_{gcs} and I_{gcd}, that is $I_{gc} = I_{gcs} + I_{gcd}$, and

$$I_{gcs} = I_{gc0} \cdot \frac{PIGCD \cdot V_{dseffx} + exp(-PIGCD \cdot V_{dseffx}) - 1 + 10^{-4}}{PIGCD \cdot {V_{dseffx}}^2 + 2 \cdot 10^{-4}} \tag{1.223}$$

and

$$I_{gcd} = I_{gc0} \cdot \frac{1 - (PIGCD \cdot V_{dseffx} + 1) \cdot exp(-PIGCD \cdot V_{dseffx}) + 10^{-4}}{PIGCD \cdot {V_{dseffx}}^2 + 2 \cdot 10^{-4}} \tag{1.224}$$

where

$$V_{dseffx} = \sqrt{V_{dseff} + 0.01} - 0.1 \tag{1.225}$$

At $V_{ds} = 0$, $I_{gcs} = I_{gcd} = \frac{1}{2} I_{gc0}$. Thus I_{gc0} is the gate to channel current I_{gc} at $V_{ds} = 0$.

I_{gs} and I_{gd}: I_{gs} represents the gate tunneling current between the gate and the source diffusion region, while I_{gd} represents the gate tunneling current between the gate and the drain diffusion region. I_{gs} and I_{gd} are determined by ECB for NMOS and HVB for PMOS, respectively.

$$\begin{aligned} I_{gs} &= NF \cdot W_{eff} DLCIG \cdot A \cdot T_{oxRatioEdge} \cdot V_{gs} \cdot V_{gs}^{'} \cdot i_{gtemp} \\ &\quad \cdot exp[-B \cdot TOXE \cdot POXEDGE \cdot (AIGS - BIGS \cdot V_{gs}^{'}) \cdot (1 + CIGSV_{gs}^{'})] \end{aligned} \tag{1.226}$$

and

$$\begin{aligned} I_{gd} &= NF \cdot W_{eff} DLCIGD \cdot A \cdot T_{oxRatioEdge} \cdot V_{gd} \cdot V_{gd}^{'} \cdot i_{gtemp} \\ &\quad \cdot exp[-B \cdot TOXE \cdot POXEDGE \cdot (AIGD - BIGD \cdot V_{gd}^{'}) \cdot (1 + CIGDV_{gd}^{'})] \end{aligned} \tag{1.227}$$

where A = 4.97232 A/V^2 for NMOS and 3.42537 A/V^2 for PMOS, B = 7.45669e11 $(g/F - s^2)^{0.5}$ for NMOS and 1.16645e12 $(g/F - s^2)^{0.5}$ for PMOS, and

$$T_{oxRatioEdge} = \left(\frac{TOXREF}{TOXE \cdot POXEDGE} \right)^{NTOX} \cdot \frac{1}{(TOXE \cdot POXEDGE)^2} \tag{1.228}$$

$$V_{gs}^{'} = \sqrt{(V_{gs} - V_{fbsd})^2 + 10^{-4}} \tag{1.229}$$

$$V_{gd}^{'} = \sqrt{(V_{gd} - V_{fbsd})^2 + 10^{-4}} \tag{1.230}$$

Vfbsd is the flat-band voltage between gate and S/D diffusions calculated as

If $NGATE > 0.0$

$$V_{fbsd} = \frac{k_B T}{q} log\left(\frac{NGATE}{NSD}\right) + VFBSDOFF \tag{1.231}$$

Else $V_{fbsd} = 0.0$.

1.18 Gate resistance and Body resistance network Model

1.18.1 Gate Electrode Electrode and Intrinsic-Input Resistance (IIR) Model

General Description: BSIM6 provides four options for modeling gate electrode resistance (bias-independent) and intrinsic-input resistance (IIR, bias-dependent). The IIR model considers the relaxation-time effect due to the distributive RC nature of the channel region, and therefore describes the first-order non-quasi-static effect. Thus, the IIR model should not be used together with the charge-deficit NQS model at the same time. The model selector RGATEMOD is used to choose different options.

Model Option and Schematic: There are four model selectors for gate resistance network.

RGATEMOD = 0 (zero-resistance): In this case, no gate resistance is generated (see Figure 2).

RGATEMOD = 1 (constant-resistance): In this case, only the electrode gate resistance (bias-independent) is generated by adding an internal gate node. *Rgeltd* is given by

$$Rgeltd = \frac{RSHG \cdot (XGW + \frac{W_{effci}}{3 \cdot NGCON})}{NGCON \cdot (L_{drawn} - XGL) \cdot NF} \tag{1.232}$$

RGATEMOD = 2 (IIR model with variable resistance): In this case, the gate resistance is the sum of the electrode gate resistance *Rgeltd* (1.232) and the intrinsic-input resistance R_{ii} as given by (1.233). An internal gate node will be generated.

$$\frac{1}{R_{ii}} = XRCRG1.NF \cdot \left(\frac{I_{ds}}{V_{dseff}} + XRCRG2 \cdot \frac{W_{eff}\mu_{eff}C_{oxeff}V_t}{L_{eff}}\right)$$

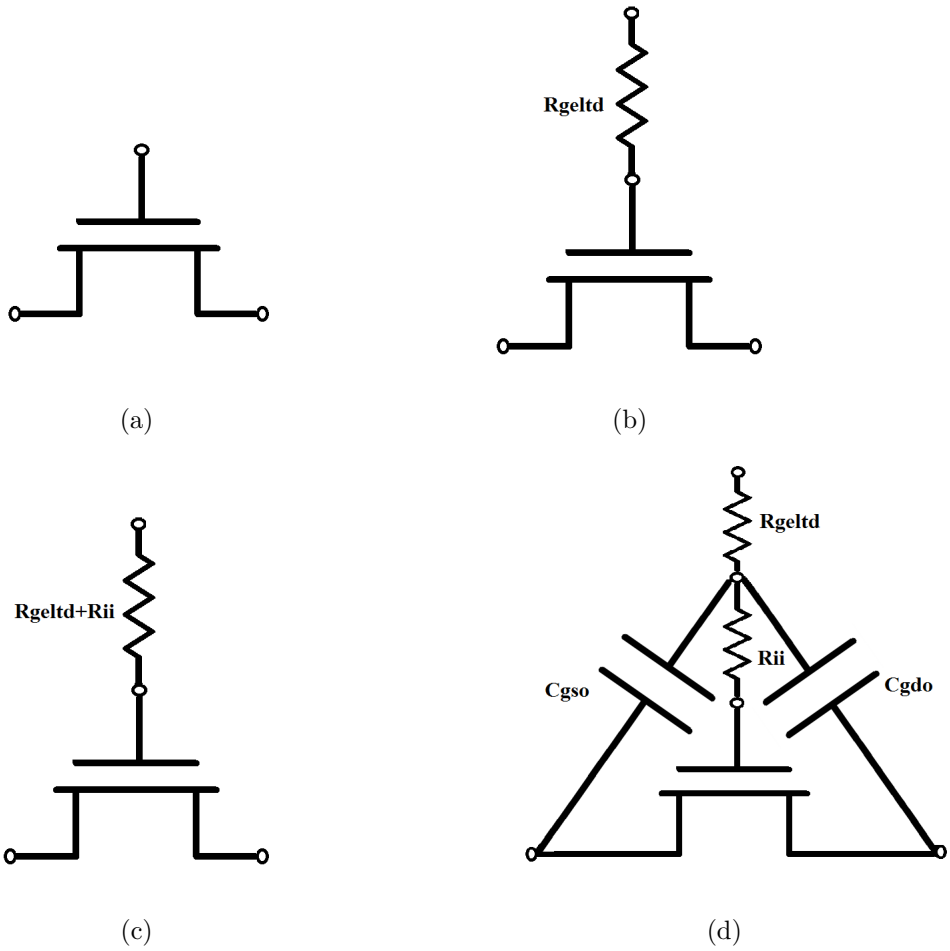

Figure 2: Gate resistance network for (a) $RGATEMOD = 0$ (b) $RGATEMOD = 1$ (b) $RGATEMOD = 2$ (d) $RGATEMOD = 3$.

or

$$\frac{1}{R_{ii}} \approx XRCRG1.NF \cdot \left(\mu_{eff} \left(\frac{W_{eff}}{L_{eff}} \right) C_{ox} \cdot q_{ia} + XRCRG2 \cdot \frac{W_{eff}\mu_{eff}C_{oxeff}V_t}{L_{eff}} \right) \tag{1.233}$$

RGATEMOD = 3 (IIR model with two nodes): In this case, the gate electrode resistance *Rgeltd* is in series with the intrinsic-input resistance R_{ii} through two internal gate nodes, so that the overlap capacitance current will not pass through the intrinsic-input resistance.

1.18.2 Substrate Resistance Network

General Description: For CMOS RF circuit simulation, it is essential to consider the high frequency coupling through the substrate. BSIM6 offers a flexible built-in substrate resistance network. This network is constructed such that little simulation efficiency penalty will result. Note that the substrate resistance parameters should be extracted for the total device, not on a per-finger basis.

Model Selector and Topology The model selector **RBODYMOD** can be used to turn on or turn off the resistance network.

RBODYMOD = 0 (Off):

No substrate resistance network is generated at all.

RBODYMOD = 1 (On):

All five resistances *RBPS*, *RBPD*, *RBPB*, *RBSB*, and *RBDB* in the substrate network as shown schematically below are present simultaneously.

A minimum conductance, GBMIN, is introduced in parallel with each resistance and therefore to prevent infinite resistance values, which would otherwise cause poor convergence. GBMIN is merged into each resistance to simplify the representation of the model topology. Note that the intrinsic model substrate reference point in this case is the internal body node **bNodePrime**, into which the impact ionization current I_{ii} and the GIDL current I_{GIDL} flow.

RBODYMOD = 2 (On : Scalable Substrate Network):

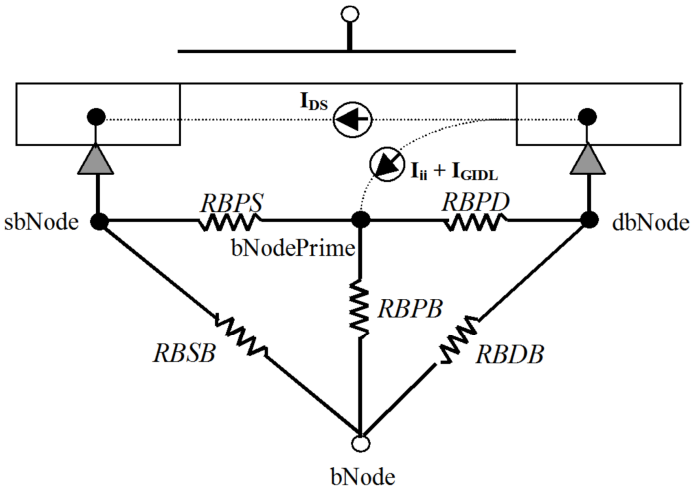

Figure 3: Topology with the substrate resistance network turned on.

The schematic is similar to **RBODYMOD** = 1 but all the five resistors in the substrate network are now scalable with a possibility of choosing either five resistors, three resistors or one resistor as the substrate network.

The resistors of the substrate network are scalable with respect to channel length (L), channel width (W) and number of fingers (NF). The scalable model allows to account for both horizontal and vertical contacts.

The scalable resistors RBPS and RBPD are evaluated through

$$RBPS = RBPS0 \cdot \left(\frac{L}{10^{-6}}\right)^{RBPSL} \cdot \left(\frac{W}{10^{-6}}\right)^{RBPSW} \cdot NF^{RBPSNF} \quad (1.234)$$

$$RBPD = RBPD0 \cdot \left(\frac{L}{10^{-6}}\right)^{RBPDL} \cdot \left(\frac{W}{10^{-6}}\right)^{RBPDW} \cdot NF^{RBPDNF} \quad (1.235)$$

The resistor RBPB consists of two parallel resistor paths, one to the horizontal contacts and other to the vertical contacts. These two resistances are scalable and RBPB is given

by a parallel combination of these two resistances.

$$RBPBX = RBPBX0 \cdot \left(\frac{L}{10^{-6}}\right)^{RBPBXL} \cdot \left(\frac{W}{10^{-6}}\right)^{RBPBXW} \cdot NF^{RBPDNF} \quad (1.236)$$

$$RBPBY = RBPBY0 \cdot \left(\frac{L}{10^{-6}}\right)^{RBPBYL} \cdot \left(\frac{W}{10^{-6}}\right)^{RBPBYW} \cdot NF^{RBPDNF} \quad (1.237)$$

$$RBPB = \frac{RBPBX \cdot RBPBY}{RBPBX + RBPBY} \quad (1.238)$$

The resistors RBSB and RBDB share the same scaling parameters but have different scaling prefactors. These resistors are modeled in the same way as RBPB. The equations for RBSB are shown below. The calculation for RBDB follows RBSB.

$$RBSBX = RBSBX0 \cdot \left(\frac{L}{10^{-6}}\right)^{RBSBXL} \cdot \left(\frac{W}{10^{-6}}\right)^{RBSBXW} \cdot NF^{RBSDNF} \quad (1.239)$$

$$RBSBY = RBSBY0 \cdot \left(\frac{L}{10^{-6}}\right)^{RBSBYL} \cdot \left(\frac{W}{10^{-6}}\right)^{RBSBYW} \cdot NF^{RBSDNF} \quad (1.240)$$

$$RBSB = \frac{RBSBX \cdot RBSBY}{RBSBX + RBSBY} \quad (1.241)$$

Similarly, the equations for $RBDB$ is as follows

$$RBDBX = RBDBX0 \cdot \left(\frac{L}{10^{-6}}\right)^{RBDBXL} \cdot \left(\frac{L}{10^{-6}}\right)^{RBDBXW} \cdot (NF)^{RBDBXNF} \quad (1.242)$$

$$RBDBY = RBDBY0 \cdot \left(\frac{L}{10^{-6}}\right)^{RBDBYL} \cdot \left(\frac{L}{10^{-6}}\right)^{RBDBYW} \cdot (NF)^{RBDBYNF} \quad (1.243)$$

$$RBDB = \frac{RBDBX \times RBDBY}{RBDBX + RBDBY} \quad (1.244)$$

The implementation of **RBODYMOD** = 2 allows the user to chose between the 5-R network (with all five resistors), 3-R network (with RBPS, RBPD and RBPB) and 1-R network (with only RBPB).

If the user does not provide both the scaling parameters RBSBX0 and RBSBY0 for RBSB or both the scaling parameters RBDBX0 and RBDBY0 for RBDB, then the conductances for both RBSB and RBDB are set to GBMIN. This converts the 5-R schematic to 3-R schematic where the substrate network consists of the resistors RBPS, RBPD and RBPB. RBPS, RBPD and RBPB are then calculated using (1.234), (1.235), and (1.238).

If the user chooses not to provide either of RBPS0 or RBPD0, then the 5-R schematic is converted to 1-R network with only one resistor RBPB. The conductances for RBSB and RBDB are set to GBMIN. The resistances RBPS and RBPD are set to 1e-3 Ohm. The resistor RBPB is then calculated using (1.238).

In all other situations, 5-R network is used with the resistor values calculated from the equations aforementioned.

1.19 Noise Modeling

The following noise sources in MOSFETs are modeled in BSIM6 for SPICE noise ananlysis: flicker noise (also known as 1/f noise), channel thermal noise and induced gate noise and their correlation, thermal noise due to physical resistances such as the source/ drain, gate electrode, and substrate resistances, and shot noise due to the gate dielectric tunneling current.

Noise models in BSIM 6.0.0	**Origin**
Flicker noise model	BSIM4 Unified Model (FNOIMOD=1)
Thermal noise(TNOIMOD=0)	BSIM4 (TNOIMOD=0)
Thermal noise (TNOIMOD=1)	BSIM4 (TNOIMOD=2)
Gate current shot noise	BSIM4 gate current noise
Noise associated with parasitic resistances	BSIM4 parasitic resistance noise

1.19.1 Flicker Noise Models

BSIM6's flicker noise model is same as FNOIMOD=1 in BSIM4. The unified physical flicker noise model is smooth over all bias regions.

The physical mechanism for the flicker noise is trapping/detrapping-related charge fluctuation in oxide traps, which results in fluctuations of both mobile carrier numbers and mobilities in the channel. The unified flicker noise model captures this physical process. In the inversion region, the noise density is expressed as [9]

$$\begin{aligned} S_{id,inv}(f) &= \frac{kTq^2\mu_{eff}I_{ds}}{C_{oxe}L_{effNOI}^2 f^{EF}\cdot 10^{10}}\left(NOIA\cdot log\left(\frac{N_0+N^*}{N_l+N^*}\right)\right. \\ &\left. NOIB\cdot(N_0-N_l)+\frac{NOIC}{2}(N_0^2-N_l^2)\right) \\ &\frac{kTI_{ds}^2\Delta L_{clm}}{W_{eff}L_{effNOI}^2 f^{EF}\cdot 10^{10}}\left(\frac{NOIA+NOIB\cdot N_l+NOIC\cdot N_l^2}{(N_l+N^*)^2}\right) \end{aligned} \quad (1.245)$$

where $L_{effNOI} = L_{eff} - 2\cdot LINTNOI$, μ_{eff} is the effective mobility at the given bias condition, and L_{eff} and W_{eff} are the effective channel length and width, respectively. The parameter N_0 is the charge density at the source side given by

$$N_0 = \frac{2n_qC_{ox}V_tq_s}{q} \quad (1.246)$$

The parameter N_l is the charge density at the drain end given by

$$N_l = \frac{2n_qC_{ox}V_tq_{deff}}{q} \quad (1.247)$$

and N* is given by

$$N^* = \frac{V_t\big(C_{ox}+C_d+CIT\big)}{q} \quad (1.248)$$

where CIT is a model parameter from DC IV and C_d is the depletion capacitance.

ΔL_{clm} is the channel length reduction due to channel length modulation and given by

$$\begin{aligned} \Delta L_{clm} &= litl\cdot log\left(\frac{\frac{V_{ds}-V_{dseff}}{litl}+EM}{E_{sat}}\right) \\ E_{sat} &= \frac{2VSAT}{\mu_{eff}} \end{aligned} \quad (1.249)$$

In the subthreshold region, the noise density is written as

$$S_{id,subVt}(f) = \frac{NOIA \cdot k \cdot T \cdot I_{ds}^2}{W_{eff} L_{eff} f^{EF} N^{*2} \cdot 10^{10}} \tag{1.250}$$

The total flicker noise density is

$$S_{id}(f) = \frac{S_{id,inv} \cdot S_{id,subVt}}{S_{id,inv} + S_{id,subVt}} \tag{1.251}$$

1.19.2 Channel Thermal Noise

There are two channel thermal noise models in BSIM6. One is a charge-based model (default model) similar to that used in BSIM3v3.2 and BSIM4.7.0 (TNOIMOD=0). The other is the holistic model similar to BSIM4.7.0 (TNOIMOD=2). These two models can be selected through the model selector TNOIMOD.

TNOIMOD = 0 (Charge based Model): The noise current is given by

$$Q_{inv} = |Q_{s,intrinsic} + Q_{d,intrinsic}| \times NFIN_{total} \tag{1.252}$$

$$\overline{i_d^2} = \begin{cases} NTNOI \cdot \frac{4kT\Delta f}{R_{ds} + \frac{L_{eff}^2}{\mu_{eff} Q_{inv}}} & \text{if RDSMOD} = 0 \\ NTNOI \cdot \frac{4kT\Delta f}{L_{eff}^2} \cdot \mu_{eff} Q_{inv} & \text{if RDSMOD} = 1 \end{cases} \tag{1.253}$$

where $R_{ds}(V)$ is the bias-dependent LDD source/drain resistance, and the parameter NTNOI is introduced for more accurate fitting of short-channel devices. Q_{inv} is the total inversion charge in the channel.

TNOIMOD = 1 (Holistic Model): In this thermal noise model (similar to TNOIMOD = 2 in BSIM4.7.0), all the short-channel effects and velocity saturation effect incorporated in the IV model are automatically included, hence the name "holistic thermal noise model". In this thermal noise model both the gate and the drain noise are implemented as current noise sources. The drain current noise flows from drain to source; whereas the induced gate current noise flows from the gate to the source. The correlation between the two noise sources is independently controllable and can be tuned

using the parameter RNOIC, although the use of default value 0.395 is recommended when measured data is not available. As illustrated in Fig. 4, TNOIMOD=1 shows good physical behavior in both the weak and strong inversion regions. The white noise gamma factor $\gamma_{WN} = \frac{S_{Id}}{4kTg_{d0}}$ shows a value of 1 at low V_{ds}, as expected. At high V_{ds}, it correctly goes to 2/3 for strong inversion and 1/2 in sub-threshold [10]. The relevant formulations of TNOIMOD=2 are given below. For more details, see Ph.D. thesis of Darsen Lu and BSIM4 manual.

$$\beta_{tnoi} = RNOIA \cdot \left[1.0 + TNOIA \cdot L_{eff} \cdot \left(\frac{q_{ia}}{E_{sat,noi}L_{eff}}\right)^2\right] \tag{1.254}$$

$$\theta_{tnoi} = RNOIB \cdot \left[1.0 + TNOIB \cdot L_{eff} \cdot \left(\frac{q_{ia}}{E_{sat,noi}L_{eff}}\right)^2\right] \tag{1.255}$$

$$c_{tnoi} = RNOIC \cdot \left[1.0 + TNOIC \cdot L_{eff} \cdot \left(\frac{q_{ia}}{E_{sat,noi}L_{eff}}\right)^2\right] \tag{1.256}$$

$$\tag{1.257}$$

$$S_{id} = 4KT \cdot \mu C_{ox}\frac{W_{eff}}{L_{vsat}}V_t D_{ptwg}M_{oc}\left[\frac{q_s + q_{deff}}{2} + \frac{(q_s - q_{deff})^2}{12\left(\frac{1+q_s+q_{deff}}{2}\right)}\right] \cdot (3 \cdot \beta_{tnoi}^2) \tag{1.258}$$

$$S_{ig} = 4KT \cdot \frac{1}{12 \cdot NF \cdot W_{eff}\mu_{eff} \cdot D_{ptwg}M_{oc}C_{ox} \cdot V_t}\frac{L_{vsat}^3}{L_{eff}^2} \cdot \left[\frac{\frac{q_s+q_{deff}}{2}}{\left(\frac{1+q_s+q_{deff}}{2}\right)^2}\right.$$
$$\left. - \frac{6\left(\frac{1+q_s+q_{deff}}{2}\right)(q_s - q_{deff})^2}{60\left(\frac{1+q_s+q_{deff}}{2}\right)^4} + \frac{(q_s - q_{deff})^4}{144\left(\frac{1+q_s+q_{deff}}{2}\right)^5}\right] \cdot (\frac{15}{4} \cdot \theta_{tnoi}^2) \tag{1.259}$$

$$S_{ig,id} = -j\omega \cdot 4KT \cdot \mu C_{ox}D_{ptwg}M_{oc}V_t(\frac{L_{vsat}}{L_{eff}}) \cdot \left[\frac{(q_s - q_{deff})}{12\left(\frac{1+q_s+q_{deff}}{2}\right)} - \frac{(q_s - q_{deff})^3}{144\left(\frac{1+q_s+q_{deff}}{2}\right)^3}\right] \cdot \frac{c_{tnoi}}{0.395} \tag{1.260}$$

$$c = \frac{S_{ig,id}}{\sqrt{S_{ig}} \cdot \sqrt{S_{id}}} \tag{1.261}$$

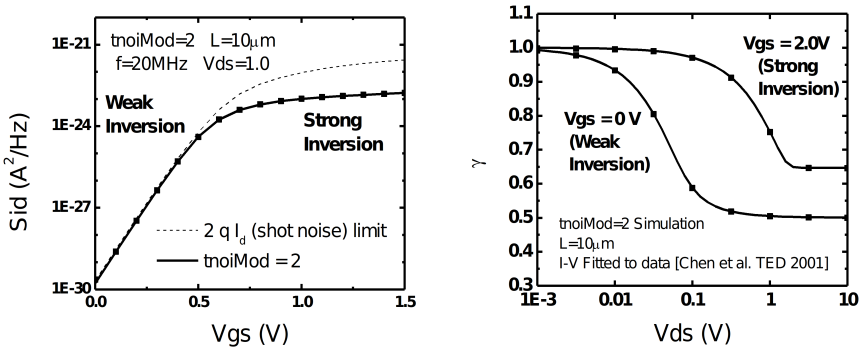

Figure 4: TNOIMOD=1 shows good physical behavior at high and low V_{ds} from sub-threshold to strong inversion regions.

1.19.3 Gate Current Shot Noise

$$\overline{i_{gs}^2} = 2q(I_{gcs} + I_{gs}) \tag{1.262}$$

$$\overline{i_{gd}^2} = 2q(I_{gcd} + I_{gd}) \tag{1.263}$$

$$\overline{i_{gb}^2} = 2qI_{gbinv} \tag{1.264}$$

1.19.4 Resistor Noise

The noise associated with each parasitic resistors in BSIM6 are calculated

If $RDSMOD = 1$ then

$$\frac{\overline{i_{RS}^2}}{\Delta f} = 4kT \cdot \frac{1}{R_{source}} \tag{1.265}$$

$$\frac{\overline{i_{RD}^2}}{\Delta f} = 4kT \cdot \frac{1}{R_{drain}} \tag{1.266}$$

If $RGATEMOD = 1$ then

$$\frac{\overline{i_{RG}^2}}{\Delta f} = 4kT \cdot \frac{1}{R_{geltd}} \tag{1.267}$$

2 Asymmetric MOS Junction Diode Models

2.1 Junction Diode IV Model

In BSIM6, there is only one diode model (DIOMOD=2 from BSIM4), which includes resistance and breakdown. BSIM6 models the diode breakdown with current limiting in both forward IJTHSFWD or IJTHDFWD and reverse operations XJBVS, XJBVD, BVS, and BVD.

Source/Body Junction Diode The equations for the source-side diode are as follows:

$$I_{bs} = I_{sbs}\Big[exp\Big(\frac{V_{bs}}{NJS \cdot V_t}\Big) - 1\Big] \cdot f_{breakdown} + V_{bs} \cdot G_{min} \tag{2.1}$$

where I_{sbs} is the total saturation current consisting of the components through the gate-edge (Jsswgs) and isolation-edge sidewalls (Jssws) and the bottom junction (Jss),

$$I_{sbs} = A_{seff} J_{ss}(T) + P_{seff} J_{ssws}(T) + W_{effcj} \cdot NF \cdot J_{sswgs}(T) \tag{2.2}$$

where the calculation of the junction area and perimeter is discussed in section Layout-Dependent Parasitics Models, and the temperature-dependent current density model is given in Section Temperature Dependence of Junction Diode IV. The exponential term in equation given below is linearized at both the limiting current IJTHSFWD in the forward-bias mode and the limiting current IJTHSREV in the reverse-bias mode. In (2.1), $f_{breakdown}$ is given by

$$f_{breakdown} = 1 + XJBVS \cdot exp\Big(-\frac{(BVS + V_{bs})}{NJS \cdot V_t}\Big) \tag{2.3}$$

$if XJBVS \leq 0.0$, it is reset to 1.0.

Drain/Body Junction Diode The equations for the drain-side diode are as follows:

$$I_{bd} = I_{sbd}\Big[\exp\Big(\frac{V_{bd}}{NJD \cdot V_t}\Big) - 1\Big] \cdot f_{breakdown} + V_{bd} \cdot G_{min} \tag{2.4}$$

where I_{sbs} is the total saturation current consisting of the components through the gate-edge (Jsswgs) and isolation-edge sidewalls (Jssws) and the bottom junction (Jss),

$$I_{sbd} = A_{deff} J_{sd}(T) + P_{deff} J_{sswd}(T) + W_{effcj} \cdot NF \cdot J_{sswgd}(T) \tag{2.5}$$

where the calculation of the junction area and perimeter is discussed in Section Layout-Dependent Parasitics Models, and the temperature-dependent current density model is given in Section Temperature Dependence of Junction Diode IV. The exponential term in (2.6) is linearized at both the limiting current IJTHDFWD in the forward-bias mode and the limiting current IJTHDREV in the reverse-bias mode. In (2.1), $f_{breakdown}$ is given by

$$f_{breakdown} = 1 + XJBVD \cdot exp\Big(- \frac{\cdot(BVD + V_{bd})}{NJD \cdot V_t}\Big) \tag{2.6}$$

$if XJBVD \leq 0.0$, it is reset to 1.0.

Total Junction Source/Drain Diode Including Tunneling Total diode current including the carrier recombination and trap-assisted tunneling current in the space-charge region is modeled by:

$$\begin{aligned} I_{bs\_totle} &= I_{bs} \\ &- W_{effcj} \cdot NF \cdot J_{tsswgs}(T) \cdot \Big[exp\Big(\frac{-V_{bs}}{NJTSSWG(T) \cdot Vtm0} \cdot \frac{VTSSWGS}{VTSSWGS - V_{bs}}\Big)\Big] \\ &- P_{s,deff} J_{tssws}(T) \Big[exp\Big(\frac{-V_{bs}}{NJTSSW(T) \cdot Vtm0} \cdot \frac{VTSSWS}{VTSSWS - V_{bs}}\Big) - 1\Big] \\ &- A_{s,deff} J_{tss}(T) \Big[exp\Big(\frac{-V_{bs}}{NJTS(T) \cdot Vtm0} \frac{VTSS}{VTSS - V_{bs}}\Big) - 1\Big] + g_{min} \cdot V_{bs} \end{aligned} \tag{2.7}$$

$$\begin{aligned} I_{bd\_totle} &= I_{bd} \\ &- W_{effcj} \cdot NF \cdot J_{tsswgd}(T) \cdot \Big[exp\Big(\frac{-V_{bd}}{NJTSSWGD(T) \cdot Vtm0} \cdot \frac{VTSSWGD}{VTSSWGD - V_{bd}}\Big)\Big] \\ &- P_{d,deff} J_{tsswd}(T) \Big[exp\Big(\frac{-V_{bd}}{NJTSSWD(T) \cdot Vtm0} \cdot \frac{VTSSWD}{VTSSWD - V_{bd}}\Big) - 1\Big] \\ &- A_{d,deff} J_{tsd}(T) \Big[exp\Big(\frac{-V_{bd}}{NJTD(T) \cdot Vtm0} \frac{VTSD}{VTSD - V_{bd}}\Big) - 1\Big] + g_{min} \cdot V_{bd} \end{aligned} \tag{2.8}$$

2.2 Junction Diode CV Model

Source and drain junction capacitances consist of three components: the bottom junction capacitance, sidewall junction capacitance along the isolation edge, and sidewall junction capacitance along the gate edge. An analogous set of equations are used for both sides but each side has a separate set of model parameters.

Source/Body Junction Diode The source-side junction capacitance can be calculated by

$$C_{bs} = A_{seff}C_{jbs} + P_{seff}C_{jbssw} + W_{effcj} \cdot NF \cdot C_{jbsswg} \tag{2.9}$$

where C_{jbs} is the unit-area bottom S/B junciton capacitance, C_{jbssw} is the unit-length S/B junction sidewall capacitance along the isolation edge, and C_{jbsswg} is the unit-length S/B junction sidewall capacitance along the gate edge. The effective area and perimeters in (2.9) are given in Section Layout-Dependent Parasitics Models.

Cjbs is calculated by

$$C_{jbs} = \begin{cases} CJS(T) \cdot \left(1 - \frac{V_{bs}}{PBS(T)}\right)^{-MJS} & \text{if } \frac{V_{bs}}{PBS(T)} \leq x_0 \\ CJS(T) \cdot \frac{1}{(1-x_0)^{MJS}} \cdot \left[1 + MJS\left(1 + \frac{\frac{V_{bs}}{PBS} - 1}{1-x_0}\right)\right] & \text{otherwise} \end{cases} \tag{2.10}$$

where the value of x_0 is taken as 0.9.

Cjbssw is calculated by

$$C_{jbssw} = \begin{cases} CJSWS(T) \cdot \left(1 - \frac{V_{bs}}{PBSWS(T)}\right)^{-MJSWS} & \text{if } \frac{V_{bs}}{PBSWS(T)} \leq x_0 \\ CJSWS(T) \cdot \frac{1}{(1-x_0)^{MJSWS}} \cdot \left[1 + MJSWS\left(1 + \frac{\frac{V_{bs}}{PBSWS(T)} - 1}{1-x_0}\right)\right] & \text{otherwise} \end{cases} \tag{2.11}$$

where the value of x_0 is taken as 0.9.

Cjbsswg is calculated by

$$C_{jbsswg} = \begin{cases} CJSWGS(T) \cdot \left(1 - \frac{V_{bs}}{PBSWGS(T)}\right)^{-MJSWGS} & \text{if } \frac{V_{bs}}{PBSWGS(T)} \leq \\ CJSWGS(T) \cdot \frac{1}{(1-x_0)^{MJSWGS}} \cdot \left[1 + MJSWGS\left(1 + \frac{\frac{V_{bs}}{PBSWGS(T)} - 1}{1-x_0}\right)\right] & \text{otherwise} \end{cases} \tag{2.12}$$

where the value of x_0 is taken as 0.9.

Drain/Body Junction Diode The drain-side junction capacitance can be calculated by

$$C_{bd} = A_{deff}C_{jbd} + P_{deff}C_{jbdsw} + W_{effcj} \cdot NF \cdot C_{jbdswg} \tag{2.13}$$

where Cjbd is the unit-area bottom D/B junciton capacitance, Cjbdsw is the unit-length D/B junction sidewall capacitance along the isolation edge, and Cjbdswg is the unit-length D/B junction sidewall capacitance along the gate edge. The effective area and perimeters in (2.13) are given in Section Layout-Dependent Parasitics Models.

Cjbd is calculated by

$$C_{jbd} = \begin{cases} CJD(T) \cdot \left(1 - \frac{V_{bs}}{PBD(T)}\right)^{-MJD} & \text{if } \frac{V_{bs}}{PBD(T)} \leq x_0 \\ CJD(T) \cdot \frac{1}{(1-x_0)^{MJD}} \cdot \left[1 + MJD\left(1 + \frac{\frac{V_{bs}}{PBD} - 1}{1-x_0}\right)\right] & \text{otherwise} \end{cases} \tag{2.14}$$

where the value of x_0 is taken as 0.9.

Cjbdsw is calculated by

$$C_{jbdsw} = \begin{cases} CJSWD(T) \cdot \left(1 - \frac{V_{bs}}{PBSWD(T)}\right)^{-MJSWS} & \text{if } \frac{V_{bs}}{PBSWD(T)} \leq x_0 \\ CJSWD(T) \cdot \frac{1}{(1-x_0)^{MJSWD}} \cdot \left[1 + MJSWD\left(1 + \frac{\frac{V_{bs}}{PBSWD(T)} - 1}{1-x_0}\right)\right] & \text{otherwise} \end{cases} \tag{2.15}$$

where the value of x_0 is taken as 0.9.

Cjbdswg is calculated by

$$C_{jbdswg} = \begin{cases} CJSWGD(T) \cdot \left(1 - \frac{V_{bs}}{PBSWGD(T)}\right)^{-MJSWGD} & \text{if } \frac{V_{bs}}{PBSWGD(T)} \\ CJSWGD(T) \cdot \frac{1}{(1-x_0)^{MJSWGD}} \cdot \left[1 + MJSWGD\left(1 + \frac{\frac{V_{bs}}{PBSWGD(T)} - 1}{1-x_0}\right)\right] & \text{otherwise} \end{cases} \tag{2.16}$$

where the value of x_0 is taken as 0.9.

3 Layout dependent Parasitics Models

3.1 Layout-Dependent Parasitics Models

BSIM6 provides a comprehensive and versatile geometry/layout-dependent parasitcs model taken from BSIM4. It supports modeling of series (such as isolated, shared, or merged source/ drain) and multi-finger device layout, or a combination of these two configurations. This model has impact on every BSIM6 sub-models except the substrate resistance network model. Note that the narrow-width effect in the per-finger device with multi-finger configuration is accounted for by this model. A complete list of model parameters and selectors can be found at the end.

3.1.1 Geometry Definition

Figure 5 schematically shows the geometry definition for various source/drain connections and source/drain/gate contacts. The layout parameters shown in this figure will be used to calculate resistances and source/drain perimeters and areas.

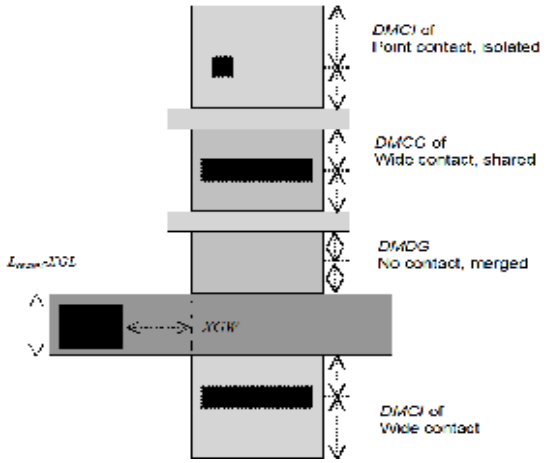

Figure 5: Definition for layout parameters.

3.1.2 Model Formulation and Options

Effective Junction Perimeter and Area: In the following, only the source-side case is illustrated. The same approach is used for the drain side. The effective junction perimeter on the source side is calculated by

If (PS is given)

if (**perMod**=0)

P_{seff}=PS

else

Else

P_{seff} computed from NF, DWJ, **geoMod**, DMCG, DMCI, DMDG, DMCGT, RSH, and MIN.

The effective junction area on the source side is calculated by

If (AS is given)

$A_{seff} = AS$

Else

A_{seff} computed from NF, DWJ, **geoMod**, DMCG, DMCI, DMDG, DMCGT, RSH, and MIN.

In the above, P_{seff} and A_{seff} will be used to calculate junction diode IV and CV. P_{seff} does not include the gate-edge perimeter.

Source/Drain Diffusion Resistance: The source diffusion resistance is calculated by
If(number of sources NRS is given)
ELSE if(**rgeoMod**=0)
Source diffusion resistance R_{sdiff} is not generated.
Else
R_{sdiff} computed from NF, DWJ, **geoMod**, DMCG, DMCI, DMDG, DMCGT, RSH, and MIN.

where the number of source squares NRS is an instance parameter. Similarly, the drain diffusion resistance is calculated by
If(number of sources NRD is given)
ELSE if(**rgeoMod**=0)
Drain diffusion resistance R_{ddiff} is not generated.
Else
R_{ddiff} computed from NF, DWJ, **geoMod**, DMCG, DMCI, DMDG, DMCGT, RSH, and MIN.

Gate Electrode Resistance: The gate electrode resistance with multi-finger configuration is modeled by

$$Rgeltd = \frac{RSHG \cdot \left(XGW + \frac{W_{effci}}{3NGCON}\right)}{NGCON \cdot \left(L_{drawn} - XGL\right) \cdot NF} \tag{3.1}$$

Option for Source/Drain Connections: Table 1 lists the options for source/drain connections through the model selector **geoMod**. For multi-finger devices, all inside S/D diffusions are assumed shared.

Option for Source/Drain Contacts: Table 2 lists the options for source/drain contacts through the model selector **rgeoMod**.

geomod	End Source	End drain	Note
0	isolated	isolated	NF=Odd
1	isolated	shared	NF=Odd, Even
2	shared	shared	NF=Odd, Even
3	shared	isolated	NF=Odd, Even
4	isolated	merged	NF=Odd
5	shared	merged	NF=Odd, Even
6	merged	isolated	NF=Odd
7	merged	shared	NF=Odd, Even
8	merged	merged	NF=Odd
9	sha/iso	shared	NF=Even
10	shared	sha/iso	NF=Even

Table 1: geoMod options.

rgeoMod	End-source contact	End-drain contact
0	No R_{sdiff}	No R_{ddiff}
1	wide	wide
2	wide	point
3	point	wide
4	point	point
5	wide	merged
6	point	merged
7	merged	wide
8	merged	point

Table 2: **rgeoMod** options.

4 Temperature dependence Models

4.1 Temperature Dependence Model

Accurate modeling of the temperature effects on MOSFET characteristics is important to predict circuit behavior over a range of operating temperatures (T). The operating temperature might be different from the nominal temperature (TNOM) at which the BSIM6 model parameters are extracted. This chapter presents the BSIM6 temperature dependence models for threshold voltage, mobility, saturation velocity, source/drain resistance, and junction diode IV and CV.

4.1.1 Length Scaling of Temperature parameters

$$UTE = UTE \cdot \left(1 + UTEL\frac{1}{L_{eff}}\right) \tag{4.1}$$

$$UA1 = UA1 \cdot \left(1 + UA1L\frac{1}{L_{eff}}\right) \tag{4.2}$$

$$UD1 = UD1 \cdot \left(1 + UD1L\frac{1}{L_{eff}}\right) \tag{4.3}$$

$$AT = AT \cdot \left(1 + ATL\frac{1}{L_{eff}}\right) \tag{4.4}$$

$$PTWGT = PTWGT \cdot \left(1 + PTWGTL\frac{1}{L_{eff}}\right) \tag{4.5}$$

$$\tag{4.6}$$

4.1.2 Temperature Dependence of Threshold Voltage

The temperature dependence of V_{th} is modeled by

$$\begin{aligned}
V_{th}(T) &= V_{th}(TNOM) + \left(KT1 + \frac{KT1L}{L_{eff}} + KT2 \cdot V_{breff}\right) \cdot \left(\left(\frac{T}{TNOM}\right)^{KT1EXP} - 1\right) \\
V_{fb}(T) &= V_{fb}(TNOM) - KT1 \cdot \left(\frac{T}{TNOM} - 1\right) \qquad (4.7) \\
VFBSDOFF(T) &= VFBSDOFF(TNOM) \cdot [1 + TVFBSDOFF \cdot (T - TNOM)] \\
NFACTOR(T) &= NFACTOR(TNOM) + TFACTOR \cdot \left(\frac{T}{TNOM} - 1\right) \qquad (4.8) \\
ETA0(T) &= ETA0(TNOM) + TETA0\left(\frac{T}{TNOM} - 1\right) \qquad (4.9)
\end{aligned}$$

4.1.3 Temperature Dependence of Mobility

$$\begin{aligned}
U0(T) &= U0(TNOM) \cdot (T/TNOM)^{UTE} \qquad (4.10) \\
UA(T) &= UA(TNOM)[1 + UA1 \cdot (T - TNOM)] \qquad (4.11) \\
UC(T) &= UC(TNOM)[1 + UC1 \cdot (T - TNOM)] \qquad (4.12) \\
UD(T) &= UD(TNOM) \cdot (T/TNOM)^{UD1} \qquad (4.13) \\
UCS(T) &= UCS(TNOM) \cdot (T/TNOM)^{UCSTE} \qquad (4.14) \\
& \qquad (4.15)
\end{aligned}$$

4.1.4 Temperature Dependence of Saturation Velocity

$$VSAT(T) = VSAT(TNOM) \cdot (T/TNOM)^{-AT} \qquad (4.16)$$

4.1.5 Temperature Dependence of LDD Resistance

$$\begin{aligned}
rdstemp &= (T/TNOM)^{PRT} \qquad (4.17) \\
& \qquad (4.18)
\end{aligned}$$

RDSMOD = 0 (internal source/drain LDD resistance)

$$RDSW(T) = RDSW(TNOM) \cdot rdstemp \tag{4.19}$$
$$RDSWMIN(T) = RDSWMIN(TNOM) \cdot rdstemp \tag{4.20}$$

RDSMOD = 1 (external source/drain LDD resistance)

$$RDW(T) = RDW(TNOM) \cdot rdstemp \tag{4.21}$$
$$RDWMIN(T) = RDWMIN(TNOM) \cdot rdstemp) \tag{4.22}$$
$$RSW(T) = RSW(TNOM) \cdot rdstemp \tag{4.23}$$
$$RSWMIN(T) = RSWMIN(TNOM) \cdot rdstemp \tag{4.24}$$

4.1.6 Temperature Dependence of Junction Diode IV

- **Source-side diode** The source-side diode is turned off if both A_{seff} and P_{seff} are zero. Otherwise, the source-side saturation current is given by

$$I_{sbs} = A_{seff} J_{ss}(T) + P_{seff} J_{ssws}(T) + W_{effcj} \cdot NF \cdot J_{sswgs}(T) \tag{4.25}$$

where

$$\begin{aligned} J_{ss}(T) &= JSS(TNOM) \cdot exp\left(\frac{\frac{E_g(TNOM)}{v_t(TNOM)} - \frac{E_g(T)}{v_t(T)} + XTIS \cdot ln\left(\frac{T}{TNOM}\right)}{NJS} \right) \\ J_{ssws}(T) &= JSSWS(TNOM) \cdot exp\left(\frac{\frac{E_g(TNOM)}{v_t(TNOM)} - \frac{E_g(T)}{v_t(T)} + XTIS \cdot ln\left(\frac{T}{TNOM}\right)}{NJS} \right) \\ J_{sswgs}(T) &= JSSWGS(TNOM) \cdot exp\left(\frac{\frac{E_g(TNOM)}{k_b \cdot TNOM} - \frac{E_g(T)}{k_b \cdot T} + XTIS \cdot ln\left(\frac{T}{TNOM}\right)}{NJS} \right) \end{aligned} \tag{4.26}$$

where Eg is given in Temperature Dependences of Eg and ni.

- **Drain-side diode** The drain-side diode is turned off if both A_{seff} and P_{seff} arezero. Otherwise, the drain-side saturation current is given by

$$I_{sbd} = A_{deff} J_{sd}(T) + P_{deff} J_{sswd}(T) + W_{effcj} \cdot NF \cdot J_{sswgd}(T) \tag{4.27}$$

where

$$\begin{aligned}
J_{sd}(T) &= JSD(TNOM) \cdot exp\left(\frac{\frac{E_g(TNOM)}{k_b \cdot TNOM} - \frac{E_g(T)}{k_b \cdot T} + XTID \cdot ln\left(\frac{T}{TNOM}\right)}{NJD} \right) \\
J_{sswd}(T) &= JSSWD(TNOM) \cdot exp\left(\frac{\frac{E_g(TNOM)}{k_b \cdot TNOM} - \frac{E_g(T)}{k_b \cdot T} + XTID \cdot ln\left(\frac{T}{TNOM}\right)}{NJD} \right) \\
J_{sswgd}(T) &= JSSWGD(TNOM) \cdot exp\left(\frac{\frac{E_g(TNOM)}{k_b \cdot TNOM} - \frac{E_g(T)}{k_b \cdot T} + XTID \cdot ln\left(\frac{T}{TNOM}\right)}{NJD} \right)
\end{aligned} \tag{4.28}$$

4.1.7 Temperature Dependence of Junction Diode CV

– Source-side diode: The temperature dependences of zero-bias unit-length/area junction capacitances on the source side are modeled by

$$CJS(T) = CJS(TNOM) + TCJ \cdot (T - TNOM) \tag{4.29}$$
$$CJSWS(T) = CJSWS(TNOM) + TCJSW \cdot (T - TNOM) \tag{4.30}$$
$$CJSWGS(T) = CJSWGS(TNOM) + TCJSWG \cdot (T - TNOM) \tag{4.31}$$

The temperature dependences of the built-in potentials on the source side are modeled by

$$PBS(T) = PBS(TNOM) - TPB \cdot (T - TNOM) \tag{4.32}$$
$$PBSWS(T) = PBSWS(TNOM) - TPBSW \cdot (T - TNOM) \tag{4.33}$$
$$PBSWGS(T) = PBSWGS(TNOM) - TPBSWG \cdot (T - TNOM) \tag{4.34}$$

– Drain-side diode: The temperature dependences of zero-bias unit-length/area junction capacitances on the drain side are modeled by

$$CJS(T) = CJS(TNOM)[1 + TCJ \cdot (T - TNOM)] \quad (4.35)$$

$$CJSWS(T) = CJSWS(TNOM) + TCJSW \cdot (T - TNOM) \quad (4.36)$$

$$CJSWGS(T) = CJSWGS(TNOM)[1 + TCJSWG \cdot (T - TNOM)] \quad (4.37)$$

The temperature dependences of the built-in potentials on the drain side are modeled by

$$PBD(T) = PBD(TNOM) - TPB \cdot (T - TNOM) \quad (4.38)$$

$$PBSWD(T) = PBSWD(TNOM) - TPBSW \cdot (T - TNOM) \quad (4.39)$$

$$PBSWGD(T) = PBSWGD(TNOM) - TPBSWG \cdot (T - TNOM) \quad (4.40)$$

- **trap-assisted tunneling (TAT) and recombination current**

$$
\begin{aligned}
J_{tsswgs}(T) &= J_{tsswgs}(TNOM)\cdot\left(\sqrt{\frac{JTWEFF}{W_{effcj}}}+1\right)\\
&\cdot\quad exp\left[\frac{-E_g(TNOM)}{k_bT}\cdot X_{tsswgs}\cdot\left(1-\frac{T}{TNOM}\right)\right] \qquad (4.41)\\
J_{tssws}(T) &= J_{tssws}(TNOM)\cdot exp\left[\frac{-E_g(TNOM)}{k_bT}\cdot X_{tssws}\cdot\left(1-\frac{T}{TNOM}\right)\right]\\
J_{tss}(T) &= J_{tss}(TNOM)\cdot exp\left[\frac{-E_g(TNOM)}{k_bT}\cdot X_{tss}\cdot\left(1-\frac{T}{TNOM}\right)\right]\\
J_{tsswgd}(T) &= J_{tsswgd}(TNOM)\cdot\left(\sqrt{\frac{JTWEFF}{W_{effcj}}}+1\right)\\
&\cdot\quad exp\left[\frac{-E_g(TNOM)}{k_bT}\cdot X_{tsswgd}\cdot\left(1-\frac{T}{TNOM}\right)\right] \qquad (4.42)\\
J_{tsd}(T) &= J_{tsd}(TNOM)\cdot exp\left[\frac{-E_g(TNOM)}{k_bT}\cdot X_{tsd}\cdot\left(1-\frac{T}{TNOM}\right)\right]\\
NJTSSWG(T) &= NJTSSWG(TNOM)\cdot\left[1+TNJTSSWG\big(\frac{T}{TNOM}-1\big)\right]\\
NJTSSW(T) &= NJTSSW(TNOM)\cdot\left[1+TNJTSSW\big(\frac{T}{TNOM}-1\big)\right]\\
NJTS(T) &= NJTS(TNOM)\cdot\left[1+TNJTS\big(\frac{T}{TNOM}-1\big)\right]\\
NJTSSWGD(T) &= NJTSSWGD(TNOM)\cdot\left[1+TNJTSSWGD\big(\frac{T}{TNOM}-1\big)\right]\\
NJTSSWD(T) &= NJTSSWD(TNOM)\cdot\left[1+TNJTSSWD\big(\frac{T}{TNOM}-1\big)\right]\\
NJTSSWD(T) &= NJTSSWD(TNOM)\cdot\left[1+TNJTSSWD\big(\frac{T}{TNOM}-1\big)\right]\\
NJTSD(T) &= NJTSD(TNOM)\cdot\left[1+TNJTSD\big(\frac{T}{TNOM}-1\big)\right]
\end{aligned}
\qquad (4.43)
$$

4.1.8 Temperature Dependences of E_g and n_i

- Energy-band gap of channel (E_g): The temperature dependence of E_g is modeled by

$$Eg0 = BG0SUB - \frac{TBGASUB \times Tnom^2}{Tnom + TBGBSUB} \tag{4.44}$$

$$E_g = BG0SUB - \frac{TBGASUB \times T^2}{T + TBGBSUB} \tag{4.45}$$

- Intrinsic carrier concentration of non-silicon channel (n_i)

$$n_i = NI0SUB \times \left(\frac{T}{Tnom}\right)^{(3/2)} \times exp\left(\frac{Eg}{2\frac{kTnom}{q}} - \frac{Eg}{2\frac{kT}{q}}\right) \tag{4.46}$$

5 Stress effect Model Development

5.1 Stress Effect Model

CMOS feature size aggressively scaling makes shallow trench isolation(STI) very popular active area isolation process in advanced technologies. Recent years, strain channel materials have been employed to achieve high device performance. The mechanical stress effect induced by these process causes MOSFET performance function of the active area size(OD: oxide definition) and the location of the device in the active area. And the necessity of new models to describe the layout dependence of MOS parameters due to stress effect becomes very urgent in advance CMOS technologies. Influence of stress on mobility has been well known since the 0.13um technology. The stress influence on saturation velocity is also experimentally demonstrated. Stress-induced enhancement or suppression of dopant diffusion during the processing is reported. Since the doping profile may be changed due to different STI sizes and stress, the threshold voltage shift and changes of other second-order effects, such as DIBL and body effect, were shown in process integration. BSIM4 considers the influence of stress on mobility, velocity saturation, threshold voltage, body effect, and DIBL effect.

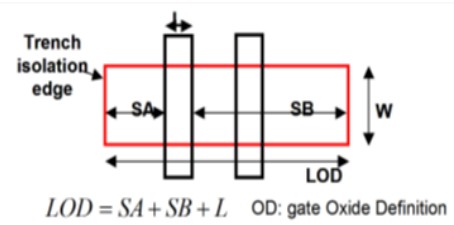

Figure 6: the typical layout of a MOSFET

5.1.1 Stress Effect Model Development

Experimental analysis show that there exist at least two different mechanisms within the influence of stress effect on device characteristics. The first one is mobility-related and is induced by the band structure modification. The second one is Vth-related as a result of doping profile variation. Both of them follow the same 1/LOD trend but reveal different L and W scaling. We have derived a phenomenological model based on these findings by modifying some parameters in the BSIM model. Note that the following equations have no impact on the iteration time because there are no voltage-controlled components in them.

Mobility-related Equations: This model introduces the first mechanism by adjusting the U0 and Vsat according to different W, L and OD shapes. Define mobility relative change due to stress effect as :

$$\rho_{\mu_{eff}} = \Delta\mu_{eff}/\mu_{effo} = (\mu_{eff} - \mu_{effo})/\mu_{effo} = \frac{\mu_{eff}}{\mu_{effo}} - 1 \tag{5.1}$$

So,

$$\frac{\mu_{eff}}{\mu_{effo}} = 1 + \rho_{\mu_{eff}} \tag{5.2}$$

Figure 6 shows the typical layout of a MOSFET on active layout surrounded by STI isolation. SA, SB are the distances between isolation edge to Poly from one and the other side, respectively. 2D simulation shows that stress distribution can be expressed by a simple function of SA and SB. Assuming that mobility relative change is propotional to stress distribution. It can be described as function of SA, SB(LOD effect), L, W, and

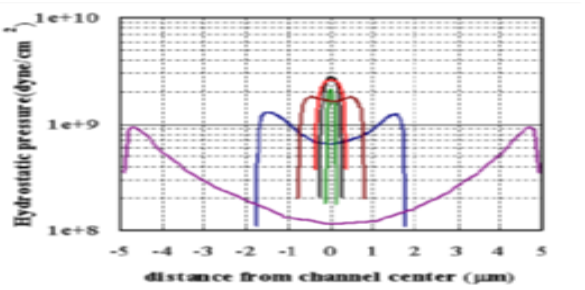

Figure 7: Stress distribution within MOSFET channel using 2D simulation

T dependence:

$$\rho_{\mu_{eff}} = \frac{KU0}{Kstress_u0} \cdot \left(Inv\_sa + Inv\_sb\right) \tag{5.3}$$

where:

$$Inv\_sa = \frac{1}{SA + 0.5 \cdot L_{drawn}} \tag{5.4}$$

$$Inv\_sb = \frac{1}{SB + 0.5 \cdot L_{drawn}} \tag{5.5}$$

$$\begin{aligned} Kstress\_u0 = & \left(1 + \frac{LKU0}{(L_{drawn} + XL)^{LLODKU0}}\right. \\ & + \frac{WKU0}{(W_{drawn} + XW + WLOD)^{WLODKU0}} \\ & \left. + \frac{PKU0}{(L_{drawn} + XL)^{LLODKU0} \cdot (W_{drawn} + XW + WLOD)^{WLODKU0}}\right) \\ & \times \left(1 + TKU0 \cdot \left(\frac{Temperature}{TNOM} - 1\right)\right) \end{aligned} \tag{5.6}$$

So that:

$$\mu_{eff} = \frac{1 + \rho_{\mu_{eff}}(SA, SB)}{1 + \rho_{\mu_{eff}}(SA_{ref}, SB_{ref})} \mu_{effo} \tag{5.7}$$

$$\nu_{sattemp} = \frac{1 + KVSAT \cdot \rho_{\mu_{eff}}(SA, SB)}{1 + KVSAT \cdot \rho_{\mu_{eff}}(SA_{ref}, SB_{ref})} \nu_{sattempo} \tag{5.8}$$

and SA_{ref}, SB_{ref} are reference distances between OD edge to poly from one and the other side.

Vth-related Equations: Vth0 (threshold voltage without stress effect), K2 and ETA0 are modified to cover the doping profile change in the devices with different LOD. They use the same 1/LOD formulas as shown in earlier sections, but different equations for W and L scaling:

$$\begin{aligned} VTH0 &= VTH0_{original} + \frac{KVTH0}{Kstress\_vth0} \cdot \left(Inv\_sa + Inv\_sb - Inv\_sa_{ref} - Inv\_sb_{ref}\right) \\ K2 &= K2_{original} + \frac{STK2}{Kstress\_vth0^{LODK2}} \cdot \left(Inv\_sa + Inv\_sb - Inv\_sa_{ref} - Inv\_sb_{ref}\right) \\ ETA0 &= ETA0_{original} + \frac{STETA0}{Kstress\_vth0^{LODETA0}} \cdot \left(Inv\_sa + Inv\_sb - Inv\_sa_{ref} - Inv\_sb_{ref}\right) \end{aligned} \tag{5.9}$$

where:

$$Inv\_sa_{ref} = \frac{1}{SA_{ref} + 0.5 \cdot L_{drawn}} \tag{5.10}$$

$$Inv\_sbref = \frac{1}{SB_{ref} + 0.5 \cdot L_{drawn}} \tag{5.11}$$

$$\begin{aligned} Kstress\_vth0 = \Bigg(1 &+ \frac{LKVTH0}{(L_{drawn} + XL)^{LLODKVTH}} \\ &+ \frac{WKVTH0}{(W_{drawn} + XW + WLOD)^{WLODKVTH}} \\ &+ \frac{PKVTH0}{(L_{drawn} + XL)^{LLODKVTH} \cdot (W_{drawn} + XW + WLOD)^{WLODKVTH}}\Bigg) \end{aligned} \tag{5.12}$$

Multiple Finger Device: For multiple finger device, the total LOD effect is the average of LOD effect to every finger. That is(see Figure 8) for the layout for multiple

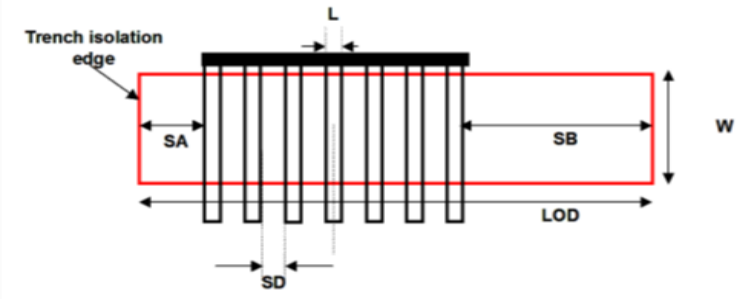

Figure 8: Layout of multiple finger MOSFET

finger device):

$$Inv\_sa = \frac{1}{NF}\sum_{i=0}^{NF-1}\frac{1}{SA + 0.5\cdot L_{drawn} + i\cdot(SD + L_{drawn})} \tag{5.13}$$

$$Inv\_sb = \frac{1}{NF}\sum_{i=0}^{NF-1}\frac{1}{SB + 0.5\cdot L_{drawn} + i\cdot(SD + L_{drawn})} \tag{5.14}$$

$$\tag{5.15}$$

5.1.2 Effective SA and SB for Irregular LOD

General MOSFET has an irregular shape of active area shown in Figure 9 To fully describe the shape of OD region will require additional instance parameters. However, this will result in too many parameters in the net lists and would massively increase the read-in time and degrade the readability of parameters. One way to overcome this difficulty is the concept of effective SA and SB similar to [11]. Stress effect model as described earlier allows an accurate and efficient layout extraction of effective SA and

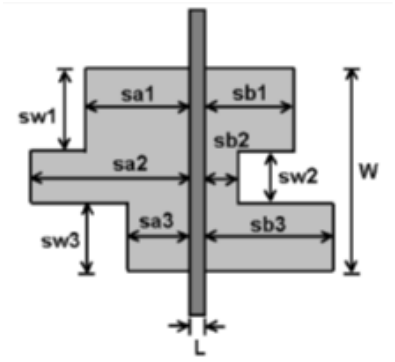

Figure 9: A typical layout of MOS devices with more instance parameters (swi, sai and sbi) in addition to the traditional L and W

SB while keeping fully compatibility of the LOD model. They are expressed as:

$$\frac{1}{SA_{eff} + 0.5 \cdot L_{drawn}} = \sum_{i=1}^{n} \frac{sw_i}{W_{drawn}} \cdot \frac{1}{sa_i + 0.5 \cdot L_{drawn}} \tag{5.16}$$

$$\frac{1}{SB_{eff} + 0.5 \cdot L_{drawn}} = \sum_{i=1}^{n} \frac{sw_i}{W_{drawn}} \cdot \frac{1}{sb_i + 0.5 \cdot L_{drawn}} \tag{5.17}$$

$$\tag{5.18}$$

6 Well Proximity Effect Model

7 Well Proximity Effect Model

Retrograde well profiles have several key advantages for highly scaled bulk complementary metal oxide semiconductor(CMOS) technology. With the advent of high-energy implanters and reduced thermal cycle processing, it has become possible to provide a relatively heavily doped deep nwell and pwell without affecting the critical device-related doping at the surface. The deep well implants provide a low resistance path and suppress parasitic bipolar gain for latchup protection, and can also improve soft error rate

and noise isolation. A deep buried layer is also key to forming triple-well structures for isolated-well NMOSFETs. However, deep buried layers can affect devices located near the mask edge. Some of the ions scattered out of the edge of the photoresist are implanted in the silicon surface near the mask edge, altering the threshold voltage of those devices [12]. It is observed a threshold voltage shifts of up to 100 mV in a deep boron retrograde pwell, a deep phosphorus retrograde nwell, and also a triple-well implementation with a deep phosphorus isolation layer below the pwell over a lateral distance on the order of a micrometer [12]. This effect is called well proximity effect. BSIM6 considers the influence of well proximity effect on threshold voltage, mobility, and body effect. This well proximity effect model is developed by the Compact Model Council [13].

7.1 Well Proximity Effect Model

Experimental analysis [12] shows that well proximity effect is strong function of distance of FET from mask edge, and electrical quantities influenced by it follow the same geometrical trend. A phenomenological model based on these findings has been developed by modifying some parameters in the BSIM model. Note that the following equations have no impact on the iteration time because there are no voltage controlled components in them. Well proximity affects threshold voltage, mobility and the body effect of the device. The effect of the well proximity can be described through the following equations :

$$\begin{aligned} Vth0 &= Vth0_{org} + KVTH0WE \cdot (SCA + WEB \cdot SCB + WEC \cdot SCC) \\ K2 &= K2_{org} + K2WE \cdot (SCA + WEB \cdot SCB + WEC \cdot SCC) \\ \mu_{eff} &= \mu_{eff,org} \cdot (1 + KU0WE \cdot (SCA + WEB \cdot SCB + WEB \cdot SCC)) \end{aligned} \quad (7.1)$$

where SCA, SCB, SCC are instance parameters that represent the integral of the first/second/third distribution function for scattered well dopant. The guidelines for calculating the instance parameters SCA, SCB, SCC have been developed by the Compact Model Council which can be found at the CMC website [13].

8 C-V Model

Inversion Charge : Total inversion charge (excluding velocity saturation, CLM and poly depletion) can be expressed explicitly in terms of normalized charge densities at source and drain sides as follows,

$$Q_I = W \cdot \int_0^L Q_i \; dx \tag{8.1}$$

$$= -WL \cdot C_{ox} \cdot V_t \int_0^1 2.n_q.q \; d\xi \tag{8.2}$$

$$-\frac{Q_I}{WL \cdot C_{ox} V_t} = q_I = 2.n_q \cdot \int_0^1 q \; d\xi \tag{8.3}$$

Here $\xi = \frac{x}{L}$. Inversion charge density is normalized to $-2.n_q.C_{ox}.V_t$ and voltages to V_t. From (1.189),

$$I_{ds} = -2 \cdot n_q \cdot \mu_{eff} \cdot \frac{W_{eff}}{L_{eff}} \cdot C_{ox} \cdot nV_t^2 \cdot (2q+1)\frac{dq}{d\xi} \tag{8.4}$$

Normalizing current with $2 \cdot n_q \cdot \mu_{eff} \cdot \frac{W_{eff}}{L_{eff}} \cdot C_{ox} \cdot nV_t^2$,

$$i = -(2q+1)\frac{dq}{d\xi} \tag{8.5}$$

which gives $d\xi = -\frac{(2q+1)}{i}dq = -\frac{(2q+1)}{(q_s-q_d)(1+q_s+q_d)}$. Substituting in (8.3)

$$q_I = -\frac{2n_q}{(q_s-q_d)(1+q_s+q_d)} \int_{q_s}^{q_d} q(2q+1) \; dq \tag{8.6}$$

$$= -\frac{2n_q}{(q_s-q_d)(1+q_s+q_d)} \left[\frac{2}{3}({q_d}^3 - {q_s}^3) + \frac{1}{2}({q_d}^2 - {q_s}^2)\right] \tag{8.7}$$

on rearranging,

$$q_I = n_q \cdot \left[q_s + q_d + \frac{1}{3} \cdot \frac{(q_s-q_d)^2}{1+q_s+q_d}\right] \tag{8.8}$$

Bulk Charge: Bulk charge density is given as

$$Q_b = -C_{ox} \cdot (V_G - V_{FB} - \psi_S) - Q_i \tag{8.9}$$

$$\tag{8.10}$$

using charge linearization

$$Q_b = -C_{ox} \cdot (V_G - V_{FB} - \psi_P) - Q_i \left(1 - \frac{1}{n_q}\right) \tag{8.11}$$

Total bulk charge,

$$Q_B = W \cdot \int_0^L Q_b \, dx \tag{8.12}$$

$$= -WL \cdot C_{ox} \cdot \left[V_G - V_{FB} - \psi_P + \left(1 - \frac{1}{n_q}\right) \cdot \int_0^1 \frac{Q_i}{C_{ox}} \, d\xi\right] \tag{8.13}$$

Normalizing the bulk charge to $-W.L.C_{ox}.V_t$,

$$q_B = v_g - v_{fb} - \psi_p - 2(n_q - 1) \cdot \int_0^1 q \, d\xi \tag{8.14}$$

We know that $i_{ds} = -(2q+1)\frac{dq}{d\xi}$ with i_{ds} given by (1.197). Thus $d\xi = -\frac{-(2q+1)}{i_{ds}} dq$,

$$q_B = v_g - v_{fb} - \psi_p + \frac{2(n_q - 1)}{i_{ds}} \cdot \int_{q_s}^{q_d} q(2q+1) \, dq \tag{8.15}$$

$$= v_g - v_{fb} - \psi_p + \frac{2(n_q - 1)}{(q_s - q_d)(1 + q_s + q_d)} \int_{q_s}^{q_d} \left[\frac{2q^3}{3} + \frac{q^2}{2}\right] \tag{8.16}$$

$$= v_g - v_{fb} - \psi_p + \frac{2(n_q - 1)}{(q_s - q_d)(1 + q_s + q_d)} \left[\frac{2}{3} \cdot (q_d - q_s)(q_d^2 + q_s^2 + q_s.q_d) + \frac{1}{2} \cdot (q_d - q_s)(q_d + q_s)\right] \tag{8.17}$$

which on rearrangement becomes,

$$q_B = v_g - v_{fb} - \psi_p - (n_q - 1)\left[q_s + q_d + \frac{1}{3} \cdot \frac{(q_s - q_d)^2}{1 + q_s + q_d}\right] \tag{8.18}$$

Bulk charge with poly depletion effect :

$$q_B = A + B + \frac{1}{3}.\frac{\Delta q^2}{C^3} \cdot \left[\frac{4}{8} \cdot \left(C^2 + P.Q\right) \cdot \frac{1}{1 + q_s + q_d} + \frac{2}{\gamma_g^2}\right] - n_q.\left[q_s + q_d + \frac{1}{3} \cdot \frac{(q_s - q_d)^2}{1 + q_s + q_d}\right] \tag{8.19}$$

where

$$P = \sqrt{\frac{1}{4} + \frac{v_g - v_{fb} - \psi_p + 2.q_s}{\gamma_g^2}} \tag{8.20}$$

$$Q = \sqrt{\frac{1}{4} + \frac{v_g - v_{fb} - \psi_p + 2.q_d}{\gamma_g^2}} \tag{8.21}$$

$$A = \frac{v_g - v_{fb} - \psi_p + 2.q_s}{1 + 2.\sqrt{\frac{1}{4} + \frac{v_g - v_{fb} - \psi_p + 2.q_s}{\gamma_g^2}}} \tag{8.22}$$

$$B = \frac{v_g - v_{fb} - \psi_p + 2.q_d}{1 + 2.\sqrt{\frac{1}{4} + \frac{v_g - v_{fb} - \psi_p + 2.q_s}{\gamma_g^2}}} \tag{8.23}$$

$$C = \sqrt{\frac{1}{4} + \frac{v_g - v_{fb} - \psi_p + 2.q_s}{\gamma_g^2}} + \sqrt{\frac{1}{4} + \frac{v_g - v_{fb} - \psi_p + 2.q_d}{\gamma_g^2}} \tag{8.24}$$

Source and Drain Charges

$$Q_s = \frac{n_q}{3}\left[2 \cdot q_s + q_{deff} + \frac{1}{2} \cdot \left(1 + \frac{4}{5} \cdot q_s + \frac{6}{5} \cdot q_{deff}\right)\left(\frac{q_s - q_{deff}}{1 + q_s + q_{deff}}\right)^2\right] \tag{8.25}$$

$$Q_d = \frac{n_q}{3}\left[q_s + 2 \cdot q_{deff} + \frac{1}{2} \cdot \left(1 + \frac{6}{5} \cdot q_s + \frac{4}{5} \cdot q_{deff}\right)\left(\frac{q_s - q_{deff}}{1 + q_s + q_{deff}}\right)^2\right] \tag{8.26}$$

$$\tag{8.27}$$

Quantum Mechanical Effect

$$X_{DC}^{inv} = \frac{ADOS \cdot (1.9 \cdot 10^{-9})}{1 + \left[\frac{Q_i + ETAQM \cdot Q_B}{QM0}\right]^{0.7 * BDOS}} \tag{8.28}$$

$$C_{ox}^{inv} = \frac{3.9 \cdot \epsilon_0}{TOXP \cdot \frac{3.9}{EPSROX} + \frac{X_{DC}^{inv}}{\epsilon_{ratio}}} \tag{8.29}$$

Intrinsic Charge expressions:

$$WLCOXVt_{inv} = NF \cdot Wact \cdot Lact \cdot C_{ox}^{inv} \cdot nVt \tag{8.30}$$

$$QBi = -NF \cdot Wact \cdot Lact \cdot \left(\frac{\epsilon_0 \cdot EPSROX}{TOXP} \right) \cdot nVt \cdot Qb \tag{8.31}$$

$$QSi = -WLCOXVt_{inv} \cdot Qs \tag{8.32}$$

$$QDi = -WLCOXVt_{inv} \cdot Qd \tag{8.33}$$

$$QGi = QSi + QDi + QBi \tag{8.34}$$

Bias-dependent overlap capacitance model

An accurate overlap capacitance model is essential. This is especially true for the drain side where the effect of the capacitance is amplified by the transistor gain. The overlap capacitance changes with gate to source and gate to drain biases. In LDD MOSFETs a substantial portion of the LDD region can be depleted, both in the vertical and lateral directions. This can lead to a large reduction of the overlap capacitance. This LDD region can be in accumulation or depletion. We use a single equation for both regions by using such smoothing parameters as $V_{gs,overlap}$ and $V_{gd,overlap}$ for the source and drain side, respectively. Unlike the case with the intrinsic capacitance, the overlap capacitances are reciprocal. In other words, $C_{gs,overlap} = C_{sg,overlap}$ and $C_{gd,overlap} = C_{dg,overlap}$.

The bias-dependent overlap capacitance model in BSIM6 is adopted from BSIM4. The overlap charge is given by:

$$\begin{aligned} \frac{Q_{gs,ov}}{NF \cdot W_{effCV}} &= CGSO \cdot V_{gs} + \\ & CGSL \cdot \left[V_{gs} - V_{fbsd} - V_{gs,overlap} - \frac{CKAPPAS}{2} \left(\sqrt{1 - \frac{4V_{gs,overlap}}{CKAPPAS}} - 1 \right) \right] \end{aligned} \tag{8.35}$$

$$\frac{Q_{gd,ov}}{NF \cdot W_{effCV}} = CGDO \cdot V_{gd} + CGDL \cdot \left[V_{gd} - V_{fbsd} - V_{gd,overlap} - \frac{CKAPPAD}{2} \left(\sqrt{1 - \frac{4V_{gd,overlap}}{CKAPPAD}} - 1 \right) \right] \tag{8.36}$$

$$V_{gs,overlap} = \frac{1}{2} \left[V_{gs} - V_{fbsd} + \delta_1 - \sqrt{(V_{gs} - V_{fbsd} + \delta_1)^2 + 4\delta_1} \right] \tag{8.37}$$

$$V_{gd,overlap} = \frac{1}{2} \left[V_{gd} - V_{fbsd} + \delta_1 - \sqrt{(V_{gd} - V_{fbsd} + \delta_1)^2 + 4\delta_1} \right] \tag{8.38}$$

$$\delta_1 = 0.02V \tag{8.39}$$

Outer Fringing Capacitance

The fringing capacitance consists of a bias-independent outer fringing capacitance and a bias-dependent inner fringing capacitance. Only the bias-independent outer fringing capacitance is modeled. If CF is not given then outer fringe capacitance is calculated as

$$CF = \frac{2 \cdot EPSROX \cdot \epsilon_0}{\pi} \cdot ln[CFRCOEFF \cdot (1 + \frac{0.4e-6}{TOX})] \tag{8.40}$$

9 Parameter Extraction Procedure

The objective of this section is to provide guidelines for the extraction of the main model parameters. The procedure is structured in such a way that parameters linked to specific psychical phenomena are extracted from analyses where these effects are prominent. Although parameter extraction is not always a straight-forward procedure, the aim is to minimize the effort invested and the number of the essential loops performed.

If all the steps of the described procedure are followed then a global model card is obtained which means that the model can be used across the entire width/length plane of the technology. If a local fitting is targeted, then only the parameters of Section 9.1 need to be extracted for each DUT. However, in that case binning is necessary if the model card is to be used for the entire geometry range of the technology. Irrespectively of the choice between global and local fitting, different model cards should be extracted for nmos and pmos devices or for different technologies.

Before proceeding to the extraction of any parameter, it is very important that **TNOM** is set to the value of the temperature at which the measurements were carried out. Also, it is recommended that if they are available, the values of the process parameters are provided. The most common process parameters are shown in Table 3.

Parameter Name	**Physical Description**
EPSROX	Relative Gate Dielectric Constant
EPSRSUB	Relative Dielectric Constant of the Channel
TOXE	Electrical Gate Equivalent Oxide Thickness
TOXP or **DTOX**	Physical Gate Equivalent Oxide Thickness
NDEP	Channel Doping Concentration
NGATE	Gate Doping Concentration
NSD	S/D Doping Concentration
XJ	S/D Jucntion Depth
XW/XL	Channel W/L Offset due to Mask/Etch Effect

Table 3: Process parameters which are recommended to be provided before parameter extraction.

9.1 Extraction of Geometry Independent Parameters

The first part of the model parameter extraction procedure is to extract the parameters that are related to the main physical phenomena, which define transistor's behavior, and are also geometry independent. For that, a wide and long channel device should be chosen. At this point, **WWIDE** and **LLONG** parameters must be assigned to the values of the width and length of this large chosen DUT. This ensures that once the behavior of the long/wide channel device is fitted, it cannot be further affected by the values scaling parameters that will be extracted in the next steps.

9.1.1 Gate Capacitance C_{GG} vs. V_G Analysis @ $V_S = 0\ V$, $V_D = 0\ V$ & $V_B = 0\ V$

At this step process parameters and parameters related to quantum mechanical effect are extracted. Even if values have been already assigned to process parameters, a fine tuning should be made in order to fit accurately the electrical behavior of the device. From C_{GG} vs. V_G analysis the following process parameters can be extracted: **NDEP**, **TOXE**, **VFB** and **NGATE**. Each of these parameters affects a different region or in a different way the C_{GG} capacitance, so they should be extracted accordingly. More specifically:

- **VFB** is defining the flat-band voltage of the device and it can be extracted by studying the region from depletion till the onset of strong-inversion.
- **NDEP** is affecting C_{GG} in the depletion region. If possible, **NDEP**, which defines the doping level, is better to be extracted from C_{GB} vs. V_G analysis (S and D terminals are grounded).
- **TOXE** is affecting the deep accumulation and strong-inversion regions.
- **NGATE** is related to the poly-silicon depletion effect, so it affects the slope of C_{GG} in the strong-inversion region.

Furthermore, the value of C_{OX} is affected by the Quantum Mechanical effect. So, the parameters: **ADOS**, **BDOS**, **QM0** and **ETAQM** are also extracted from C_{GG} vs. V_G analysis, when focusing at the slope of C_{GG} at the onset of the strong-inversion region.

9.1.2 Drain Current I_D vs. V_G Analysis @ $V_D = [V_{D,lin}, V_{D,sat}]$, $V_S = 0\ V$ & $V_B = 0\ V$

In this step, the V_G dependence of the drain current - I_D, is extracted. Different parameters are extracted in two different regions of operation, namely *linear mode* (i.e. $V_D \ll V_G - V_{TH}$) and *saturation* (i.e. $V_D \gg V_G - V_{TH}$). It is very important that during extraction in this step, both I_D and the transconductance - g_m (even $g_m^{'}$ and $g_m^{''}$) are extracted at once.

Linear Mode

- Focusing in *weak-inversion* region (I_D vs. V_G characteristic when y-axis is in logarithmic scale), **NFACTOR**, which is related to the sub-threshold slope of the I_D, can be extracted. Furthermore, a fine tuning of the **NDEP** and **VFB** parameters is performed. In case the values of **NDEP** and **VFB** obtained during the fitting of I_D vs. V_G characteristic differ much from those obtained during the fitting of C_{GG} vs. V_G characteristic (Section 9.1.1), parameters **NDEPCV** and **VFBCV** can be used for dynamic operation (CV) and **NDEP** and **VFB** for static operation (IV). In general, using different values for **NDEP** and **NDEPCV** for IV and CV operation is not recommended unless necessary.

- From *strong-inversion* region, the mobility **U0**, the parameter for the effective field **ETAMOB**, the parameters related to the effect of mobility reduction due to vertical field **UA** and **EU** and the parameters for the coulomb scattering effect **UD** and **UCS**, are extracted. Furthermore, the parameters for S/D series resistances are also extracted under the same bias conditions. If **RDSMOD = 0** (internal S/D series resistances), **RDSW** is extracted. Otherwise, **RSW** and **RDW** are extracted.

Saturation

- From *weak-inversion* region (I_D vs. V_G characteristic when y-axis is in logarithmic scale), **CDSCD** paramerer, which is linked to the dependence of the sub-threshold slope on drain bias, is extracted.

- Focusing in *strong-inversion* region, the parameters that are connected to the velocity saturation effect, namely **VSAT**, **PSAT**, **PTWG** and **PSATX**, can be extracted. **PSATX** does need to be changed.

Finally, from *accumulation* to *depletion* region, in both *linear mode* and *saturation*, the parameters related to GIDL effect are extracted. First, the selector **GIDLMOD** should be set to 1 to activate GIDL/GILS currents and then the parameters **AGIDL**, **BGIDL**, **CGIDL** and **EGIDL** are extracted. Ideally GIDL and GILS currents should be equal, so it is sufficient to extract **AGIDL**, **BGIDL**, **CGIDL** and **EGIDL** parametrers. But in case GIDL and GISL currents differ, then parameters **AGISL**, **BGISL**, **CGISL** and **EGISL** can also be used.

9.1.3 Gate Current I_G vs. V_G Analysis @ various V_D, $V_S = 0\ V$ & $V_B = 0\ V$

From I_G vs. V_G analysis, parameters related to the gate current can be extracted. First, the tunneling components should be activated by setting to 1 the selectors **IGCMOD** and **IGBMOD**. Different parameters are extracted in different regions of operation and more specifically:

Accumulation to weak-inversion Region

- **AIGBACC**, **BIGBACC**, **CIGBACC** and **NIGBACC**, which are linked to the gate-to-substrate current component determined by ECB.
- **AIGS**, **BIGS** and **CIGS**, which are linked to the tunneling current between the gate and the source diffusion region and **AIGD**, **BIGD** and **CIGD**, which are linked to the tunneling current between the gate and the drain diffusion region.
- **DLCIG** and **DLCIGD**, which are linked to the S/D overlap length for I_{GS} and I_{GD} respectively.

Weak to strong-inversion Region

- **AIGBINV**, **BIGBINV**, **CIGBINV**, **EIGBINV** and **NIGBINV**, which are linked to the gate-to-substrate current component determined by EVB.
- **AIGC**, **BIGC**, **CIGC**, **NIGC** and **PIGCD**, which are linked to the gate-to-channel current. **PIGCD** is expressing the V_D dependence of gate-to-channel current.

9.1.4 Drain Current I_D vs. V_D Analysis @ various V_G, $V_S = 0\ V$ & $V_B = 0\ V$

In this step, both I_D vs. V_D and output conductance - g_{ds} (even g'_{ds}) vs. V_D characteristics are studied at once. Different effects impact both the characteristics, so the parameters related to those effects are extracted. In detail,

- **DELTA**, which is a smoothing factor for the transition between V_{DS} and $V_{DS,sat}$.
- **PDITS** and **PDITSD**, linked to DITS effect.
- **PCLM**, **PCLMG** and **FPROUT** linked to the CLM effect.
- **PDIBLC**, linked to the impact of DIBL effect on R_{out}.
- **PVAG**, linked to the V_G dependence on Early voltage.

9.1.5 Gate Capacitance C_{GG} vs. V_G Analysis @ $V_{DS} \neq 0\ V$ & $V_B = 0\ V$

Velocity saturation (VS) and channel length modulation (CLM) effects not only affect the static behavior of the transistor but the dynamic as well. The extraction of **VSAT** and **PCLM** from I_D vs. V_G and I_D vs. V_D characteristics should be sufficient in order to capture these effects for CV operation. To verify that, C_{GG} vs. V_G characteristic for different $V_{DS} \neq 0\ V$, from linear mode to saturation must be studied. If different values for **VSAT** and **PCLM** are necessary for accurate fitting of the CV behavior at different V_D biases, then **VSATCV** and **PCLMCV** can be used.

9.1.6 Drain Current I_D vs. V_G Analysis @ $V_D = [V_{D,lin}, V_{D,sat}]$ & various V_B

In this step almost the same procedure as in Section 9.1.2 will be repeated in order to extract the parameters that are linked to the body effect. Similar to Section 9.1.2, it is also very important that during the extraction in this step both I_D and g_m are studied at once.

Linear Mode

- Focusing in *weak-inversion* region, **CDSCB**, which is linked to the V_B (or V_S) dependence of the sub-threshold slope, is extracted. Also **K2**, which is linked to the V_{TH} shift due to vertical non-uniform doping, is extracted in the same region.

- In *strong-inversion* region, **UC**, which is linked to the V_B (or V_S) dependence of mobility, is extracted. The parameter for V_B (or V_S) dependence of S/D series resistances, **PRWB**, is also extracted under the same bias conditions.

Saturation

- In *strong-inversion* region, the parameter that is connected to V_B (or V_S) dependence of the velocity saturation effect, i.e. **PSATB**, is extracted.

In order to validate that the values of the parameters, which are linked to V_B (or V_S) dependencies, are correctly extracted, it is useful to check I_D vs. V_D and g_{ds} vs. V_D characteristics @ various V_G & $V_B \neq 0\ V$ (or $V_S \neq 0\ V$) and, if needed, to fine tune the values of the parameters.

9.1.7 Fitting Verification

When all the extraction steps of this part have been performed, the fitting of the model should be checked for all the analyses carried out up to this point. Parameters can be fine tuned for better fitting in all regions.

9.2 Extraction of Short Channel Effects & Length Scaling Parameters

Once the behavior of the wide/long channel device has been accurately modeled, the next step is the extraction of the parameters that are either related to short channel effects or express the different length dependencies. So at this part, devices across the entire length range of the technology, from the shortest to the longest one, are studied simultaneously. In order to avoid the impact of narrow channel effects or of the width dependencies these devices should have the same **wide** channel. The extraction that is carried out follows the same flow as in Section 9.1, but now a set of devices with constant **wide** channel but different channel lengths is used.

9.2.1 Gate Capacitance C_{GG} vs. V_G Analysis @ $V_S = 0\ V$, $V_D = 0\ V$ & $V_B = 0\ V$

In this step, parameters related to overlap and fringing capacitances as well as those that are linked to the length dependence of doping concentration and flat-band voltage are extracted. More specifically:

- **NDEPL1**, **NDEPLEXP1**, **NDEPL2** and **NDEPLEXP2**, which are the length scaling parameters for the doping concentration, are extracted from C_{GG} in the depletion region. If possible, it is recommended that those parameters are extracted from C_{GB} vs. V_G analysis (S and D terminals are grounded).
- Extraction of parameters related to overlap and fringing capacitances is carried out by studying the entire range of V_G bias of C_{GG} vs. V_G characteristic. These parameters are: **CGSO**, **CGDO**, **CGBO**, **CGSL**, **CGDL**, **CKAPPAS**, **CKAPPAD** and **CF**. If possible, it is recommended that **CGSO**, **CGDO**, **CGBO** and **CF** are extracted from C_{GD} vs. V_G at low V_B (when S and D terminals are connected together and B terminal is grounded), while **CGSL**, **CGDL**, **CKAPPAS** and **CKAPPAD** are extracted from C_{GD} vs. V_G at high V_B (when S, D and B terminals are connected together).
- **DLC**, which is the channel-length offset parameter for the CV model, is extracted in the strong-inversion region of C_{GG}.
- **VFBCVL** and **VFBCVLEXP**, which express the length dependence of flat-band voltage at CV, are extracted from depletion region till the onset of strong-inversion. In order to be able to use **VFBCVL** and **VFBCVLEXP** parameters, **VFBCV** must be $\neq \mathbf{0}$.

9.2.2 Drain Current I_D vs. V_G Analysis @ $V_D = [V_{D,lin}, V_{D,sat}]$, $V_S = 0\ V$ & $V_B = 0\ V$

In this step, parameters related to short channel effects or to length dependencies of I_D vs. V_G, are extracted. Similar to the procedure described in Section 9.1.2, the parameters are divided in two groups, those which are extracted in *linear mode* (i.e. $V_D \ll V_G - V_{TH}$) and those which are extracted in *saturation* (i.e. $V_D \gg V_G - V_{TH}$). It is very important that during the extraction both I_D and g_m of all the devices are studied at once.

Linear Mode

- Focusing in *weak-inversion* region (I_D vs. V_G characteristic when y-axis is in logarithmic scale), **NFACTORL** and **NFACTORLEXP**, which are related to the length dependence of the sub-threshold slope of I_D vs. V_G, can be extracted. Furthermore, **LINT**, which is the channel length offset parameter, is used to fit both the sub-threshold slope and the V_{TH}. For fitting the V_{TH} of the devices also **DVTP0** and **UD** can prove to be useful. **UD** should be used only for fine tuning because it mainly affects the region above threshold. It is recommended that the parameters **NDEPL1**, **NDEPLEXP1**, **NDEPL1** and **NDEPLEXP1** keep the values extracted from the C_{GG} vs. V_G analysis (Section 9.2.1). But, if the fitting of the V_{TH} across the entire length range cannot be achieved without changing the values of **NDEPL1**, **NDEPLEXP1**, **NDEPL1** and **NDEPLEXP1**, then these parameters are used for static operation (IV) and **NDEPCVL1**, **NDEPCVLEXP1**, **NDEPCVL1** and **NDEPCVLEXP1** parameters are used for dynamic operation (CV).

- In *strong-inversion* region, the parameters related to the length dependence of: i) the mobility; **U0L** and **U0LEXP**, ii) the effect of mobility reduction due to vertical field; **UAL**, **UALEXP**, **EUL** and **EULEXP** and iii) the coulomb scattering effect; **UDL** and **UDLEXP**, are extracted. Furthermore, parameters for the length dependence of S/D series resistances, namely **RDSWL** and **RDSWLEXP** (when **RDSMOD = 0**) or **RSWL**, **RSWLEXP**, **RDWL** and **RDWLEXP** (when **RDSMOD = 1**), are also extracted under the same bias conditions.

Saturation

- In *weak-inversion* region (I_D vs. V_G characteristic when y-axis is in logarithmic scale), **CDSCDL** and **CDSCDLEXP** paramerers, which are linked to the length dependence of the sub-threshold slope dependence on drain bias, are extracted. Moreover, parameters for DIBL effect, which control V_{TH} when $V_{DS} \neq 0$, namely **ETA0** and **DSUB**, are also extracted in the same region.

- Focusing in *strong-inversion* region, the length scaling parameters linked to the velocity saturation effect, i.e **VSATL**, **VSATLEXP**, **PSATL**, **PSATLEXP**, **PTWGL** and **PTWGLEXP**, can be extracted.

Finally, from *accumulation* to *depletion* region, in both *linear mode* and *saturation*, the parameters **AGIDLL/AGISLL**, which are related the length dependence of GIDL effect (GIDL/GISL currents), are extracted.

9.2.3 I_G vs. V_G Analysis @ various V_D, $V_S = 0\ V$ & $V_B = 0\ V$

From I_G vs. V_G analysis, parameters related to the length dependence of gate current are extracted. These parameters are: **AIGCL**, **AIGSL**, **AIGDL** and **PIGCDL**.

9.2.4 I_D vs. V_D Analysis @ various V_G, $V_S = 0\ V$ & $V_B = 0\ V$

In this step, both I_D vs. V_D and g_{ds} vs. V_D characteristics should be studied at once. Similar to the procedure described in Section 9.2.4 the parameters that are extracted are:

- **DELTAL** and **DELTALEXP**, which are related to the length dependence of the smoothing factor for the transition between V_{DS} and $V_{DS,sat}$.
- **PDITSL**, linked to the length dependence of DITS effect.
- **PCLML**, **PCLMLEXP**, **FPROUTL** and **FPROUTLEXP** linked to the length dependence of CLM effect.
- **PDIBLCL** and **PDIBLCLEXP**, linked to the length dependence of the impact of DIBL effect on R_{out}.

It is very important to be mentioned here, that if the slope of g_{ds} vs. V_D characteristic at low levels of inversion is steeper than the measurements, then **ETA0** should be decreased and **DVTP1** can be used to achieve an accurate fit for the V_{TH} in *saturation*.

9.2.5 C_{GG} vs. V_G Analysis @ $V_{DS} \neq 0\ V$ & $V_B = 0\ V$

The extraction of the length scaling parameters of **VSAT** and **PCLM** from I_D vs. V_G and I_D vs. V_D characteristics (Steps 9.2.2 and 9.2.4) should be sufficient in order to capture VS and CLM effects for CV operation. To verify that, C_{GG} vs. V_G characteristic of all devices, for different $V_{DS} \neq 0\,V$, from linear mode to saturation, must be studied. If different values for **VSATL**, **VSATLEXP**, **PCLML** and **PCLMLEXP** are necessary

for accurate fitting of the CV behavior across L, then **VSATCVL**, **VSATCVLEXP**, **PCLMCVL** and **PCLMCVLEXP** can be used.

9.2.6 I_D vs. V_G Analysis @ $V_D = [V_{D,lin}, V_{D,sat}]$ & various V_B (or various V_S)

In this step almost the same procedure as in Section 9.1.6 will be repeated in order to extract the length scaling parameters that are linked to the body effect. Similar to Section 9.1.6, it is also very important that during the extraction in this step both I_D and g_m of all devices are studied at once.

Linear Mode

- Focusing in *weak-inversion* region, **K2L** and **K2LEXP**, which are linked to the length dependence V_{TH} shift due to vertical non-uniform doping, are extracted.
- In *strong-inversion* region, **UCL** and **UCLEXP**, which are linked to the length dependence of mobility reduction with V_B (or V_S) bias, are extracted. The parameters for the length dependence of S/D series resistances with V_B (or V_S) bias, namely **PRWBL** and **PRWBLEXP**, are also extracted under the same bias conditions.

Saturation

- In *weak-inversion* region (I_D vs. V_G characteristic when y-axis is in logarithmic scale), the parameters related to length dependence of DIBL effect dependence on V_B (or V_S) bias, namely **ETAB** and **ETABEXP**, are extracted.

In order to validate that the values of the length scaling parameters, which are linked to V_B (or V_S) dependencies, are correctly extracted, it is useful to check I_D vs. V_D and g_{ds} vs. V_D characteristics @ various V_G & $V_B \neq 0\ V$ (or $V_S \neq 0\ V$) and, if needed, to fine tune the values of the parameters.

9.2.7 Fitting Verification

When all the steps for the extraction of short channel effects and length scaling parameters have been performed, the fitting of the model should be checked for all the analyses carried out in Section 9.2 and parameters can be fine tuned for better fitting.

9.3 Extraction of Narrow Channel Effects & Width Scaling Parameters

The next step in the parameter extraction procedure is the extraction of the parameters that are either related to narrow channel effects or express the different width dependencies. So at this part, devices across the entire width range of the technology, from the narrowest to the widest one, are studied simultaneously. In order to avoid the impact of short channel effects or of the length dependencies these devices should have the same **long** channel. The extraction that is carried out follows the same flow as in Section 9.2, but now a set of devices with constant **long** channel but different channel widths is used.

9.3.1 Gate Capacitance C_{GG} vs. V_G Analysis @ $V_S = 0\ V$, $V_D = 0\ V$ & $V_B = 0\ V$

In this step, parameters related to the width dependencies of the CV behavior of the device, e.g. width dependence of the doping concentration and flat-band voltage, are extracted. More specifically:

- **NDEPW** and **NDEPWEXP**, which are the width scaling parameters for the doping concentration, are extracted from C_{GG} in the depletion region. If possible, it is recommended that those parameters are extracted from C_{GB} vs. V_G analysis (S and D terminals are grounded).
- **DWC**, which is the channel-width offset parameter for the CV model, is extracted in the strong-inversion region of C_{GG}.
- **VFBCVW** and **VFBCVWEXP**, which express the width dependence of flat-band voltage at CV, are extracted along the entire V_G bias range of C_{GG} characteristic. In order to be able to use **VFBCVW** and **VFBCVWEXP** parameters, **VFBCV** must be $\neq \mathbf{0}$.

9.3.2 Drain Current I_D vs. V_G Analysis @ $V_D = [V_{D,lin}, V_{D,sat}]$, $V_S = 0\ V$ & $V_B = 0\ V$

In this step, parameters related to width dependencies of I_D vs. V_G, are extracted. Similar to the procedure described in Section 9.1.2, the parameters are divided in two

groups, those which are extracted in *linear mode* (i.e. $V_D \ll V_G - V_{TH}$) and those which are extracted in *saturation* (i.e. $V_D \gg V_G - V_{TH}$). It is very important that during the extraction both I_D and g_m of all the devices are studied at once.

Linear Mode

- Focusing in *weak-inversion* region (I_D vs. V_G characteristic when y-axis is in logarithmic scale), **NFACTORW** and **NFACTORWEXP**, which are related to the width dependence of the sub-threshold slope of I_D vs. V_G, can be extracted. Furthermore, **WINT**, which is the channel width offset parameter, is used to fit both the sub-threshold slope and the V_{TH} across W. It is recommended that the parameters **NDEPW** and **NDEPWEXP** keep the values extracted from the C_{GG} vs. V_G analysis (Section 9.3.1). But, if the fitting of the V_{TH} across the entire width range cannot be achieved without changing the values of **NDEPW** and **NDEPWEXP**, then these parameters are used for static operation (IV) and **NDEPCVW** and **NDEPCVWEXP** parameters are used for dynamic operation (CV).
- In *strong-inversion* region, the parameters related to the width dependence of mobility reduction due to vertical field effect, namely **UAW**, **UAWEXP**, **EUW** and **EUWEXP**, are extracted.

Saturation

- Focusing in *strong-inversion* region, the width scaling parameters linked to the velocity saturation effect, i.e. **VSATW** and **VSATWEXP**, can be extracted.

Finally, from *accumulation* to *depletion* region, in both *linear mode* and *saturation*, the parameters **AGIDLW**/**AGISLW**, which are related the width dependence of GIDL effect (GIDL/GISL currents), are extracted.

In order to validate that the values of the width scaling parameters are correctly extracted, it is useful to check I_D vs. V_D and g_{ds} vs. V_D characteristics @ various V_G, $V_S = 0\ V$ & $V_B = 0\ V$ (or $V_S \neq 0\ V$) and, if needed, to fine tune the values of the parameters.

9.3.3 Gate Current I_G vs. V_G Analysis @ various V_D, $V_S = 0\ V$ & $V_B = 0\ V$

From I_G vs. V_G analysis, parameters related to the width dependence of gate current are extracted. These parameters are: **AIGCW**, **AIGSW** and **AIGDW**.

9.3.4 Gate Capacitance C_{GG} vs. V_G Analysis @ $V_{DS} \neq 0\ V$ & $V_B = 0\ V$

The extraction of the width scaling parameters of **VSATW** and **VSATWEXP** from I_D vs. V_G and I_D vs. V_D characteristics (Step 9.3.2) should be sufficient in order to capture VS for CV operation. To verify that, C_{GG} vs. V_G characteristic of all devices, for different $V_{DS} \neq 0\ V$, from linear mode to saturation, must be studied. If different values for **VSATW** and **VSATWEXP** are necessary for accurate fitting of the CV behavior across W, then **VSATCVW** and **VSATCVWEXP** can be used.

9.3.5 Drain Current I_D vs. V_G Analysis @ $V_D = [V_{D,lin}, V_{D,sat}]$ & various V_B (or various V_S)

In this step, from *weak-inversion* region of *linear mode*, **K2W** and **K2WEXP**, which are linked to the width dependence V_{TH} shift due to vertical non-uniform doping, can be extracted. For validation purposes, it is useful to check: i) I_D vs. V_G and g_m vs. V_G characteristics in *weak* and *strong-inversion* and for both *linear mode* and *saturation*, and ii) I_D vs. V_D and g_{ds} vs. V_D characteristics @ various V_G & $V_B \neq 0\ V$ (or $V_S \neq 0\ V$) and, if needed, extract **K2W** and **K2WEXP** to fit both (i) and (ii).

9.3.6 Fitting Verification

When all the extraction steps for the width scaling have been performed, the fitting of the model should be checked for all the analyses carried out in Section 9.3and parameters can be further tuned for better fitting.

9.4 Extraction of Parameters for Narrow/Short Channel Devices

The final part in the parameter extraction procedure from a geometrical point of view, is the extraction of the parameters for narrow/short channel devices. These devices have the minimum dimensions so it is more difficult to capture their behavior. Since the narrow/short channel device parameters can affect the already performed fitting across length and width, it is recommended that two different sets of devices are studied simultaneously, i.e. one set with a constant **short** channel but different channel widths

(from narrowest to widest) and one set with a constant **narrow** channel but different channel lengths (from the shortest to the longest one).

9.4.1 Gate Capacitance C_{GG} vs. V_G Analysis @ $V_S = 0\ V$, $V_D = 0\ V$ & $V_B = 0\ V$

In this step, geometry dependent parameters for modeling the CV behavior of the narrow/short channel devices, are extracted. More specifically:

- **NDEPWL** and **NDEPWLEXP**, which are used to fit the doping concentration of small channel devices, are extracted from C_{GG} in the depletion region. If possible, it is recommended that those parameters are extracted from C_{GB} vs. V_G analysis (S and D terminals are grounded).
- **LWLC** and **WWLC**, which are coefficients of length/width dependencies for CV model, are extracted in the strong-inversion region of C_{GG}.
- **VFBCVWL** and **VFBCVWLEXP**, which are used to fit the flat-band voltage at CV, are extracted from depletion till the onset of strong-inversion region of C_{GG} characteristic. In order to be able to use **VFBCVWL** and **VFBCVWLEXP** parameters, **VFBCV** must be $\neq \mathbf{0}$.

9.4.2 Drain Current I_D vs. V_G Analysis @ $V_D = [V_{D,lin}, V_{D,sat}]$, $V_S = 0\ V$ & $V_B = 0\ V$

In this step, geometry dependent parameters for modeling I_D of the narrow/short channel devices, are extracted. Similar to the procedure described in Section 9.1.2, the parameters are divided in two groups, those which are extracted in *linear mode* (i.e. $V_D \ll V_G - V_{TH}$) and those which are extracted in *saturation* (i.e. $V_D \gg V_G - V_{TH}$). It is very important that during the extraction both I_D and g_m of all the devices are studied at once.

Linear Mode

- Focusing in *weak-inversion* region (I_D vs. V_G characteristic when y-axis is in logarithmic scale), **NFACTORWL** and **NFACTORWLEXP**, which are used to fit the sub-threshold slope of I_D vs. V_G for small channel devices, can be extracted. It is recommended that the parameters **NDEPWL** and **NDEPWLEXP** keep the

values extracted from the C_{GG} vs. V_G analysis (Section 9.4.1). But, if the fitting of the V_{TH} for both sets of devices cannot be achieved without changing the values of **NDEPWL** and **NDEPWLEXP**, then these parameters are used for static operation (IV) and **NDEPCVWL** and **NDEPCVWLEXP** parameters are used for dynamic operation (CV).

- In *strong-inversion* region, the parameters which are used to model the effect of mobility reduction due to vertical field in small channel devices, namely **UAWL**, **UAWLEXP**, **EUWL** and **EUWLEXP**, are extracted.

Saturation

- Focusing in *strong-inversion* region, the parameters which are used to model to the velocity saturation effect in small channel devices, i.e. **VSATWL** and **VSATWLEXP**, can be extracted.

In order to validate that the values of the parameters, modeling the behavior of narrow/short channel devices, are correctly extracted, it is useful to check I_D vs. V_D and g_{ds} vs. V_D characteristics @ various V_G, $V_S = 0\ V$ & $V_B = 0\ V$ and, if needed, to fine tune the values of the parameters.

9.4.3 C_{GG} vs. V_G Analysis @ $V_{DS} \neq 0\ V$ & $V_B = 0\ V$

The extraction of the parameters, which are used to model to the velocity saturation effect in small channel devices, **VSATWL** and **VSATWEXP**, from I_D vs. V_G and I_D vs. V_D characteristics (Step 9.4.2) should be sufficient in order to capture VS for CV operation. To verify that, C_{GG} vs. V_G characteristic of all devices, for different $V_{DS} \neq 0\ V$, from linear mode to saturation, must be studied. If different values for **VSATWL** and **VSATWLEXP** are necessary for accurate fitting of the CV behavior for both sets of devices, then **VSATCVWL** and **VSATCVWLEXP** can be used.

9.4.4 Drain Current I_D vs. V_G Analysis @ $V_D = [V_{D,lin}, V_{D,sat}]$ & various V_B (or various V_S)

In this step, from *weak-inversion* region of *linear mode*, **K2WL** and **K2WLEXP**, which are linked to the V_{TH} shift due to vertical non-uniform doping in small channel

devices, can be extracted. For validation purposes, it is useful to check: i) I_D vs. V_G and g_m vs. V_G characteristics in *weak* and *strong-inversion* and for both *linear mode* and *saturation*, and ii) I_D vs. V_D and g_{ds} vs. V_D characteristics @ various V_G & $V_B \neq 0\ V$ (or $V_S \neq 0\ V$) and, if needed, extract **K2WL** and **K2WLEXP** to fit both (i) and (ii).

9.4.5 Fitting Verification

When all the steps for narrow/short channel devices have been performed, the fitting of the model should be checked for all the analyses carried out in Section 9.4and parameters can be fine tuned for better fitting.

9.5 Extraction of Temperature Dependence Parameters

Up to this point of the parameter extraction procedure, the temperature dependence of the parameters has been ignored since all the parameters were extracted at **TNOM**. In this part, the parameters that are related to the impact of temperature on the behavior of devices are extracted, and for that, data across the temperature range of the technology are necessary. The behavior of devices is studied with the same geometrical sequence as the previous steps, while the temperature dependence parameters are extracted in the same regions of operation as the parameters of the corresponding physical effects.

9.5.1 Wide & Long Channel Devices

The first step, in the extraction of temperature dependence parameters, is to extract the behavior of a long and wide channel device **@ different T** and for different analyses. It is recommended that the same device as the one in Section 9.1 is used. In detail:

I_D vs. V_G analysis @ $V_D = V_{D,lin}$, $V_S = 0\ V$ & $V_B = 0\ V$

- From *weak-inversion* region (I_D vs. V_G characteristic when y-axis is in logarithmic scale), the parameters **TBGASUB** and **TBGBSUB**, which control the temperature dependence of E_g, are extracted. Also, **TNFACTOR** is extracted in order to fit the sub-threshold slope of I_D in different T, while **KT1** and **KT1EXP** are extracted for fitting the V_{TH} across T.

- From *strong-inversion* region, the mobility temperature exponent, **UTE** and the temperature coefficients: i) for mobility reduction due to vertical field effect, namely **UA1** and **UD1**, ii) for coulomb scattering effect, **UCSTE** and iii) for S/D series resitances, **PRT**, are extracted.

I_D vs. V_G analysis @ $V_D = V_{D,sat}$, $V_S = 0\ V$ & $V_B = 0\ V$

- From *strong-inversion* region, the parameters that are used to model to the temperature dependence of velocity saturation effect, i.e. **AT** and **PTWGT**, are extracted.

It is very important that in the above analyses both I_D and g_m of all the devices are studied at once. Furthermore, from *accumulation* to *depletion* region, in both *linear mode* and *saturation* of I_D vs. V_G analysis, the parameter **TGIDL**, which controls the temperature dependence of GIDL effect, is extracted.

I_D vs. V_D Analysis @ various V_G, $V_S = 0\ V$ & $V_B = 0\ V$

From I_D vs. V_D analysis in different temperatures, **TDELTA**, which is related to the temperature dependence of the smoothing factor for the transition between V_{DS} and $V_{DS,sat}$, is extracted.

I_D vs. V_G Analysis @ $V_D = V_{D,lin}$ & various V_B (or various V_S)

- From weak-inversion region (I_D vs. V_G characteristic when y-axis is in logarithmic scale) **KT2**, which is linked to the temperature dependence of V_{TH} shift due to vertical non-uniform doping with $V_B (or V_S)$ bias, is extracted.
- From *strong-inversion* region, the temperature coefficient for mobility reduction with $V_B (or V_S)$ bias, namely **UC1**, is extracted.

For validation purposes, it is useful to check: i) I_D vs. V_G and g_m vs. V_G characteristics in *weak* and *strong-inversion* and for both *linear mode* and *saturation*, and ii) I_D vs. V_D and g_{ds} vs. V_D characteristics @ various V_G & $V_B \neq 0\ V$ (or $V_S \neq 0\ V$) and, if needed, extract **KT2** and **UC1** to fit both (i) and (ii).

9.5.2 Length Scaling of Wide Channel Devices

The following step in the extraction of temperature dependence parameters, is to study the temperatures dependences across L. For this, data **@ different T** of a set of devices with constant **wide** channel but different channel lengths are used.

I_D vs. V_G analysis @ $V_D = V_{D,lin}$, $V_S = 0\ V$ & $V_B = 0\ V$

- From *weak-inversion* region (I_D vs. V_G characteristic when y-axis is in logarithmic scale), the parameter **KT1L** is extracted for fitting the V_{TH} across L, at different T.
- From *strong-inversion* region, the length scaling parameters for: i) mobility temperature exponent, **UTEL** and for the temperature coefficients or mobility reduction due to vertical field effect, namely **UA1L** and **UD1L**, are extracted.

I_D vs. V_G analysis @ $V_D = V_{D,sat}$, $V_S = 0\ V$ & $V_B = 0\ V$

- From *weak-inversion* region (I_D vs. V_G characteristic when y-axis is in logarithmic scale), the parameter **TETA0**, which is related to the temperature dependence of DIBL effect and thus is controlling the V_{TH} in saturation, is extracted.
- From *strong-inversion* region, the parameters that are used to model the temperature dependence of velocity saturation effect across L, i.e. **ATL** and **PTWGTL**, are extracted.

It is very important that in the above analyses both I_D and g_m of all the devices are studied at once. For validating that the values of length scaling parameters for temperature dependence parameters are extracted correctly, it is useful to check also I_D vs. V_D and g_{ds} vs. V_D characteristics and, if needed, to fine tune their value by repeating Step 9.5.2.

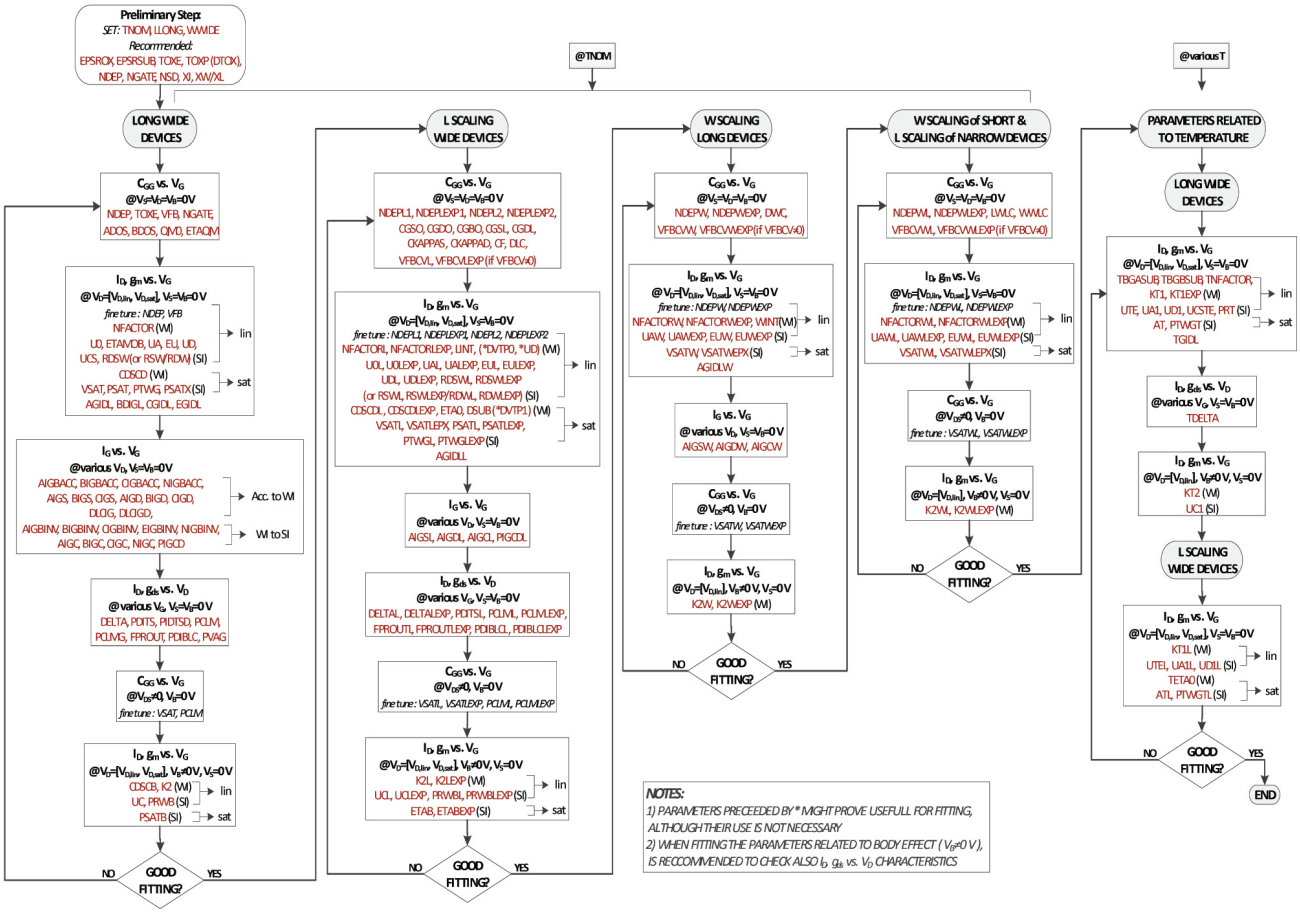

Figure 10: Parameters Extraction Procedure.

10 Instance Parameters

Name	Unit	Default	Min	Max	Description
L	m	10u	-	-	Designed Gate Length
W	m	10u	-	-	Designed Gate Width (per finger)
NF	-	1	1	-	Number of fingers
NRS	-	1	-	-	Number of source diffusion squares
NRD	-	1	-	-	Number of drain diffusion squares
VFBSDOFFV	-	0	-	-	Source-Drain flat band offset
MINZ	-	0	0	1	Minimize either no. of drain or source ends
XGW	m	0	0	-	Distance from gate contact center to dev edge
NGCON	-	1	1	2	Number of gate contacts
RGATEMOD	-	0	0	2	Gate resistance model selector
RBODYMOD	-	0	0	2	Substrate resistance network model selector
GEOMOD	-	0	0	10	same as BSIM4
RGEOMOD	-	0	0	8	Bias independent parasitic resistance model selector (same as BSIM4)
RBPB	Ohm	50	1mV	-	Resistance between bNodePrime and bNode
RBPD	Ohm	50	1mV	-	Resistance between bNodePrime and dbNode
RBPS	Ohm	50	1mV	-	Resistance between bNodePrime and sbNode
RBDB	Ohm	50	1mV	-	Resistance between dbNode and bNode
RBSB	Ohm	50	1mV	-	Resistance between sbNode and bNode
SA	-	0	0	-	Distance between OD edge from Poly from one side
SB	-	0	0	-	Distance between OD edge from Poly from other side
SD	-	0	0	-	Distance between neighboring fingers
SCA	-	0	0	-	Integral of the first distribution function for scatted well dopant
SCB	-	0	0	-	Integral of second distribution function for scattered well dopant
SCC	-	0	0	-	Integral of third distribution function for scattered well dopant
SC	-	0	0	-	Distance to a single well edge

AS	m^2	0	0	-	Source to Substrate Junction Area
AD	m^2	0	0	-	Drain to Substrate Junction Area
PS	m	0	0	-	Source to Substrate Junction Perimeter
PD	m	0	0	-	Drain to Substrate Junction Perimeter

11 Model Controllers and Process Parameters

Note: binnable parameters are marked as: $^{(b)}$

Name	**Unit**	**Default**	**Min**	**Max**	**Description and Scaling Parameters**
TYPE	-	1	-1	1	NMOS=1, PMOS=-1
GEOMOD	-	0	0	10	same as BSIM4
RGEOMOD	-	0	0	8	Bias independent parasitic resistance model selector (same as BSIM4)
RGATEMOD	-	0	0	2	Gate resistance Model selector
RBODYMOD	-	0	0	2	Substrate resistance network model selector
RDSMOD	-	0	0	1	Internal RDS:0, External RDS:1
COVMOD	-	0	0	1	Bias-independent overlap capacitance:0, Bias-dependent overlap capacitance:1
GIDLMOD	-	0	0	1	Turn off GIDL model:0, Turn-on GIDL model:1
PERMOD	-	1	0	1	Whether PS/PD (when given) includes the gate-edge perimeter 1: (including the gate-edge perimeter) 0: (not including the gate-edge perimeter)
XL	m	0	-	-	L offset for channel length due to mask/etch effect
XW	m	0	-	-	W offset for channel length due to mask/etch effect
LINT$^{(b)}$	m	0	-	-	Length reduction parameter (dopant diffusion effect)
WINT$^{(b)}$	m	0	-	-	Width reduction parameter (dopant diffusion effect)

DLC$^{(b)}$	m	0	-	-	Length reduction parameter for CV (dopant diffusion effect)
DWC$^{(b)}$	m	0	-	-	Width reduction parameter for CV (dopant diffusion effect)
TOX	m	3.0n	-	-	SiO_2 equivalent gate dielectric thickness
NDEP$^{(b)}$	m^{-3}	1e24	-	-	channel (body) doping concentration. Global Scaling Parameters - NDEPL1, NDEPLEXP1, NDEPL2, NDEPLEXP2, NDEPW, NDEPWEXP, NDEPWL, NDEPWLEXP
NSD$^{(b)}$	m^{-3}	1e26	2e25	1e27	S/D doping concentration
NGATE$^{(b)}$	m^{-3}	5e25	-	-	parameter for Poly Gate doping. Set $NGATE = 0$ for metal gates
VFB$^{(b)}$	V	-0.5	-	-	Flat band Voltage
EPSROX	-	3.9	1	-	relative dielectric constant of the gate insulator
EPSRSUB	-	11.9	1	-	relative dielectric constant of the channel material
NI0SUB	m^{-3}	1.1e16	-	-	intrinsic carrier concentration of channel at 300.15K
XJ$^{(b)}$	m	1.5e-7	-	-	S/D junction depth
DMCG		0	0	-	Distance of Mid-Contact to Gate edge
DMCI		DMCG	0	-	Distance of Mid-Contact to Isolation
DMDG		0	0	-	Distance of Mid-Diffusion to Gate edge
DMCGT		0	0	-	Distance of Mid-Contact to Gate edge in Test

12 Basic Model Parameters

Note: binnable parameters are marked as: $^{(b)}$

Name	Unit	Default	Min	Max	Description
LLONG	m	$10\mu m$	-	-	Length of extracted long channel device
WWIDE	m	$10\mu m$	-	-	Width of extracted long channel device
CIT$^{(b)}$	F/m^2	1e-8	0	-	Interface trap capacitance
NFACTOR$^{(b)}$		0	0	-	Subthreshold Swing factor. Global Scaling Parameters - NFACTORL, NFACTORLEXP, NFACTORW, NFACTORWEXP, NFACTORWL
CDSCD$^{(b)}$	F/m^2	7e-3	0	-	Drain-bias sensitivity of Subthreshold Swing. Global Scaling Parameters - CDSCDL, CDSCDLEXP
CDSCB$^{(b)}$	F/m^2	7e-3	0	-	Body-bias sensitivity of Subthreshold Swing. Global Scaling Parameters - CDSCBL, CDSCBLEXP
DVTP0$^{(b)}$	-	1e-10	-	-	Coefficient of drain-inducred V_{th} shift for long channel devices with pocket implant
DVTP1$^{(b)}$	-	0	-	-	Coefficient of drain-inducred V_{th} shift for long channel devices with pocket implant
DVTP2$^{(b)}$	-	0	-	-	Coefficient of drain-inducred V_{th} shift for long channel devices with pocket implant
DVTP3$^{(b)}$	-	0	-	-	Coefficient of drain-inducred V_{th} shift for long channel devices with pocket implant
DVTP4$^{(b)}$	-	0	-	-	Coefficient of drain-inducred V_{th} shift for long channel devices with pocket implant

DVTP5$^{(b)}$	-	0	-	-	Coefficient of drain-inducred V_{th} shift for long channel devices with pocket implant
PHIN$^{(b)}$	V	0.045	-	-	Vertical nonuniform doping effect on surface potential
K2$^{(b)}$	V	0	-	0	Vth shift due to nonuniform vertical doping. Global Scaling Parameters - K2L, K2LEXP, K2W, K2WEXP
ETA0$^{(b)}$	-	0.08	-	-	DIBL coefficient
DSUB$^{(b)}$	-	0.375	> 0	-	DIBL exponent coefficient
ETAB$^{(b)}$	-	-0.07	-	-	Body bias sensitivity to DIBL effect. Global Scaling Parameters - ETABLEXP
U0$^{(b)}$	$m^2/V-s$	67e-3	-	-	Low field mobility. Global Scaling Parameters - U0L, U0LEXP
ETAMOB	-	1.0	-	-	effective field parameter
UA$^{(b)}$	$(cm/MV)^{EU}$	0.001	> 0.0	-	Phonon / surface roughness scattering. Global Scaling Parameters - UAL, UALEXP, UAW, UAWEXP, UAWL
EU$^{(b)}$	cm/MV	1.5	> 0.0	-	Phonon / surface roughness scattering. Global Scaling Parameters - EUL, EULEXP, EUW, EUWEXP, EUWL
UD$^{(b)}$	cm/MV	0.001	> 0.0	-	Columbic scattering. Global Scaling Parameters - UDL, UDLEXP
UCS$^{(b)}$	-	2.0	1	2	Columbic scattering.
UC$^{(b)}$	-	0.001	≥ 0.0	-	Body-bias sensitivity on mobility. Global Scaling Parameters - UCL, UCLEXP
VSAT$^{(b)}$	m/s	1e6	-	-	Saturation velocity. Global Scaling Parameters - VSATL, VSALEXP, VSATW, VSATWEXP
DELTA$^{(b)}$	-	0.125	> 0	0.5	Smoothing factor for Vds to Vdsat. Global Scaling Parameters - DELTAL, DELTALEXP

PSAT	-	1.0	0.25	1.0	Velocity saturation exponent. Global Scaling Parameters - PSATL, PSATLEXP
PTWG$^{(b)}$	V^{-2}	0	-	-	Correction factor for velocity saturation. Global Scaling Parameters - PTWGL, PTWGLEXP
PSATX	-	1	0.25	4	Fine tuning of PTWG effect
PSATB	-	0	-	-	Velocity saturation exponent for non-zero V_{bs}
PCLM$^{(b)}$	-	0.013	> 0.0	-	Channel Length Modulation (CLM) parameter. Global Scaling Parameters - PCLML, PCLMLEXP
PCLMG	-	0	-	-	Gate bias dependent parameter for channel Length Modulation (CLM)
PSCBE1$^{(b)}$	-	4.24e8	–	-	Substrate current body-effect coefficient
PSCBE2$^{(b)}$	-	1.0e-8	–	-	Substrate current body-effect coefficient
PDITS$^{(b)}$	-	0	–	-	Drain-induced Vth shift
PDITSL	-	0	–	-	L dependence of Drain-induced Vth shift
PDITSD$^{(b)}$	-	0	–	-	VDS dependence of Drain-induced Vth shift
RSWMIN$^{(b)}$	$\Omega - \mu_m^{WR}$	0.0	0.0	-	source extension resistance per unit width at high V_{gs}
RSW$^{(b)}$	$\Omega - \mu_m^{WR}$	10	0.0	-	Zero bias source extension resistance per unit width. Global Scaling Parameters - RSWL, RSWLEXP
RDWMIN$^{(b)}$	$\Omega - \mu_m^{WR}$	0.0	0.0	-	Drain extension resistance per unit width at high V_{gs}
RDW$^{(b)}$	$\Omega - \mu_m^{WR}$	10	0.0	-	Zero bias drain extension resistance per unit width. Global Scaling Parameters - RDWL, RDWLEXP

RDSWMIN$^{(b)}$	$\Omega - \mu_m^{WR}$	0.0	0.0	-	LDD resistance per unit width at high $V_{gs} for RDSMOD = 0$
RDSW$^{(b)}$	$\Omega - \mu_m^{WR}$	10	0.0	-	Zero bias LDD resistance per unit width for RDSMOD=0. Global Scaling Parameters - RDSWL, RDSWLEXP
PRWG$^{(b)}$	V^{-1}	1	0	-	gate bias dependence of S/D extension resistance
PRWB$^{(b)}$	V^{-1}	0	0	-	body bias dependence of S/D extension resistance. Global Scaling Parameters - PRWBL, PRWBLEXP
WR$^{(b)}$	-	1.0	-	-	W dependence parameter of S/D extension resistance
RSH	Ω	0	0	-	Sheet resistance
PDIBLC$^{(b)}$	-	2e-4	0	-	DIBL effect on Rout. Global Scaling Parameters - PDIBLCL, PDIBLCLEXP
PDIBLCB$^{(b)}$	-	0	0	-	Body-bias sensitivity on DIBL
PVAG$^{(b)}$	-	1	-	-	V_{gs} dependence on early voltage
FPROUT$^{(b)}$	-	0	0	-	g_{ds} degradation factor due to pocket implant. Global Scaling Parameters - FPROUTL, FPROUTLEXP
AGIDL$^{(b)}$	-	0	-	-	Pre-exponential coefficient for GIDL. Global Scaling Parameters - AGIDLL, AGIDLW
BGIDL$^{(b)}$	-	2.3e-9	-	-	exponential coefficient for GIDL
CGIDL$^{(b)}$	-	0.5	-	-	exponential coefficient for GIDL
EGIDL$^{(b)}$	-	0.8	-	-	band bending parameter for GIDL
AGISL$^{(b)}$	-	0	-	-	Pre-exponential coefficient for GISL (AGISL$<$ 0 means GISL parameters will same as GIDL parameters). Global Scaling Parameters - AGISLL, AGISLW
BGISL$^{(b)}$	-	2.3e-9	-	-	exponential coefficient for GISL

CGISL$^{(b)}$	-	0.5	-	-	exponential coefficient for GISL
EGISL$^{(b)}$	-	0.8	-	-	band bending parameter for GISL
ALPHA0$^{(b)}$	-	0.0	-	-	First parameter of impact ionization current. Global Scaling Parameters - ALPHA0L, ALPHA0LEXP
BETA0$^{(b)}$	-	0.0	-	-	First V_{ds} dependent parameter of impact ionization current
AIGC$^{(b)}$	$(Fs^2/g)^{0.5}$	1.36e-2 (NMOS) and 9.8e-3 (PMOS)	-	-	Parameter for I_{gcs} and I_{gcd}. Global Scaling Parameters - AIGCL, AIGCW
BIGC$^{(b)}$	$(Fs^2/g)^{0.5}$	1.71e-3 (NMOS) and 7.59e-4 (PMOS)	-	-	Parameter for I_{gcs} and I_{gcd}
CIGC$^{(b)}$	$(Fs^2/g)^{0.5}$	0.075 (NMOS) and 0.03 (PMOS)	-	-	Parameter for I_{gcs} and I_{gcd}
AIGS$^{(b)}$	$(Fs^2/g)^{0.5}$	1.36e-2 (NMOS) and 9.8e-3 (PMOS)	-	-	Parameter for I_{gs} . Global Scaling Parameters - AIGSL, AIGSW
BIGS$^{(b)}$	$(Fs^2/g)^{0.5}$	1.71e-3 (NMOS) and 7.59e-4 (PMOS)	-	-	Parameter for I_{gs}

CIGS$^{(b)}$	$(Fs^2/g)^{0.5}$	0.075 (NMOS) and 0.03 (PMOS)	-	-	Parameter for I_{gs}
DLCIG$^{(b)}$	m	LINT	-	-	Source/Drain overlap length for I_{gs}
AIGD$^{(b)}$	$(Fs^2/g)^{0.5}$	1.36e-2 (NMOS) and 9.8e-3 (PMOS)	-	-	Parameter for I_{gd}. Global Scaling Parameters - AIGDL, AIGDW
BIGD$^{(b)}$	$(Fs^2/g)^{0.5}$	1.71e-3 (NMOS) and 7.59e-4 (PMOS)	-	-	Parameter for I_{gd}
CIGD$^{(b)}$	$(Fs^2/g)^{0.5}$	0.075 (NMOS) and 0.03 (PMOS)	-	-	Parameter for I_{gd}
DLCIGD$^{(b)}$	m	DLCIG	-	-	Source/Drain overlap length for I_{gd}
POXEDGE$^{(b)}$	-	1.0	-	-	Factor for the gate oxide thickness in source/drain overlap regions
PIGCD$^{(b)}$	-	1.0	-	-	V_{ds} dependence of I_{gcs} and I_{gcd}. Global Scaling Parameters - PIGCDL, PIGCDLEXP
NTOX$^{(b)}$	-	1.0	-	-	Exponent for the gate oxide ratio
TOXREF	m	3.0e-9	-	-	Nominal gate oxide thickness for gate dielectric tunneling current model only
VFBSDOFF$^{(b)}$	V	0.0	-	-	Flatband Voltage Offset Parameter

NDEPCV$^{(b)}$	m^{-3}	NDEP	-	-	channel (body) doping concentration for CV. Global Scaling Parameters - NDEPCVL1, NDEPCVLEXP1, NDEPCVL2, NDEPCVLEXP2, NDEPCVW, NDEPCVWEXP, NDEPCVWL, NDEPCVWLEXP
VFBCV$^{(b)}$	m^{-3}	VFB	-	-	channel (body) doping concentration for CV. Global Scaling Parameters - VFBCVL, VFBCVLEXP, VFBCVW, VFBCVWEXP, VFBCVWL, VFBCVWLEXP
VSATCV$^{(b)}$	m/s	VSAT	-	-	Saturation velocity for CV. Global Scaling Parameters - VSATCVL, VSACVLEXP, VSATCVW, VSATCVWEXP
PCLMCV$^{(b)}$	-	PCLM	> 0.0	-	Channel Length Modulation (CLM) parameter for CV. Global Scaling Parameters - PCLMCVL, PCLMCVLEXP
CF$^{(b)}$	F/m	0	0.0	-	Outer fringe cap
CFRCOEFF$^{(b)}$	F/m	1	1	-	Outer fringe cap coefficient
CGSO	F/m	calculated	0.0	-	Non LDD region source-gate overlap capacitance per unit channel width
CGDO	F/m	calculated	0.0	-	Non LDD region drain-gate overlap capacitance per unit channel width
CGSL$^{(b)}$	F/m	0	0.0	-	Overlap capacitance between gate and lightly-doped source region
CGDL$^{(b)}$	F/m	0	0.0	-	Overlap capacitance between gate and lightly-doped drain region
CKAPPAS$^{(b)}$	V	0.6	0.02	-	Coefficient of bias-dependent overlap capacitance for the source side
CKAPPAD$^{(b)}$	V	0.6	0.02	-	Coefficient of bias-dependent overlap capacitance for the drain side
CGBO	F/m	0	0.0	-	Gate-substrate overlap capacitance per unit channel length

ADOS	-	0	0	-	Quantum mechanical effect prefactor cum switch in inversion
BDOS	-	1.0	0	-	Charge centroid parameter - slope of CV curve under QME in inversion
QM0	-	1e-3	> 0.0	-	Charge centroid parameter - starting point for QME in inversion
ETAQM	-	0.54	0	-	Bulk charge coefficient for charge centroid in inversion

13 High-Speed/RF Model Parameters

Name	**Description**	**Default**
XRCRG1 (b)	Parameter forParameter for distributed channel-resistance effect for both intrinsic-input resistance and charge-deficit NQS models(Warning message issued if binned XRCRG1 ≤ 0.0) distributed channel-resistance effect for both intrinsic-input resistance and charge-deficit NQS models(Warning message issued if binned XRCRG1 ≤ 0.0)	12.0
XRCRG2 (b)	Parameter to account for the excess channel diffusion resistance for both intrinsic input resistance and charge-deficit NQS models	1.0
RBPB (Also an instance parameter)	Resistance connected between bNodePrime and bNode	50.0ohm
RBPD (Also an instance parameter)	Resistance connected between bNodePrime and dbNode (If less than 1.0e-3ohm, reset to 1.0e-3ohm)	50.0ohm
RBPS (Also an instance parameter)	Resistance connected between bNodePrime and sbNode (If less than 1.0e-3ohm, reset to 1.0e-3ohm)	50.0ohm
RBDB (Also an instance parameter)	Resistance connected between dbNode and bNode	50.0ohm

RBSB (Also an instance parameter)	Resistance connected between sbNode and bNode	50.0ohm
GBMIN	Conductance in parallel with each of the five substrate resistances to avoid potential numerical instability due to unreasonably too large a substrate resistance (Warning message issued if less than 1.0e-20 mho)	1.0e-12mho
RBPS0	Scaling prefactor for RBPS	50 Ohms
RBPSL	Length Scaling parameter for RBPS	0.0
RBPSW	Width Scaling parameter for RBPS	0.0
RBPSNF	Number of fingers Scaling parameter for RBPS	0.0
RBPD0	Scaling prefactor for RBPD	50 Ohms
RBPDL	Length Scaling parameter for RBPD	0.0
RBPDW	Width Scaling parameter for RBPD	0.0
RBPDNF	Number of fingers Scaling parameter for RBPD	0.0
RBPBX0	Scaling prefactor for RBPBX	100 Ohms
RBPBXL	Length Scaling parameter forRBPBX	0.0
RBPBXW	Width Scaling parameter for RBPBX	0.0
RBPBXNF	Number of fingers Scaling parameter for RBPBX	0.0
RBPBY0	Scaling prefactor for RBPBY	100 Ohms
RBPBYL	Length Scaling parameter forRBPBY	0.0
RBPBYW	Width Scaling parameter for RBPBY	0.0
RBPBYNF	Number of fingers Scaling parameter for RBPBY	0.0
RBSBX0	Scaling prefactor for RBSBX	100 Ohms
RBSBY0	Scaling prefactor for RBSBY	100 Ohms
RBDBX0	Scaling prefactor for RBDBX	100 Ohms
RBDBY0	Scaling prefactor for RBDBY	100 Ohms
RBSDBXL	Length Scaling parameter for RBSBX and RBDBX	0.0

RBSDBXW	Width Scaling parameter for RBSBX and RBDBX	0.0
RBSDBXNF	Number of fingers Scaling parameter for RBSBX and RBDBX	0.0
RBSDBYL	Length Scaling parameter for RBSBY and RBDBY	0.0
RBSDBYW	Width Scaling parameter for RBSBY and RBDBY	0.0
RBSDBYNF	Number of fingers Scaling parameter for RBSBY and RBDBY	0.0

14 Flicker and Thermal Noise Model Parameters

Parameter Name	**Description**	**Default Value**
NOIA	Flicker noise parameter A	$6.25e41(eV)^{-1}s^{1-EF}m^{-3}$ for NMOS; $6.188e40(eV)^{-1}s^{1-EF}m^{-3}$ for PMOS
NOIB	Flicker noise parameter B	$3.125e26(eV)^{-1}s^{1-EF}m^{-1}$ for NMOS; $1.5e25(eV)^{-1}s^{1-EF}m^{-1}$ for PMOS
NOIC	Flicker noise parameter C	$8.75(eV)^{-1}s^{1-EF}m$
EM	Saturation field	4.1e7V/m
AF	Flicker noise exponent	1.0
EF	Flicker noise frequency exponent	1.0
KF	Flicker noise coefficient	$0.0^{A2-EF}s^{1-EF}$
LINTNOI	Length Reduction Parameter Offset	0.0 m
NTNOI	Noise factor for short-channel devices for TNOIMOD=0 only	1.0
TNOIA	Coefficient of channel-length dependence of total channel thermal noise	1.5
TNOIB	Channel-length dependence parameter for channel tRNOIChermal noise partitioning	3.5
TNOIC	Length dependent parameter for Correlation Coefficient	0
RNOIA	Thermal Noise Coefficient	0.577
RNOIB	Thermal Noise Coefficient	0.5164
RNOIC	Correlation Coefficient parameter	0.395

15 Layout-Dependent Parasitic Model Parameters

Parameter Name	**Description**	**Default Value**
DMCG	Distance from S/D contact center to the gate edge	0.0m
DMCI	Distance from S/D contact center to the isolation edge in the channel-length direction	DMCG
DMDG	Same as DMCG but for merged device only	0.0m
DMCGT	DMCG of test structures	0.0m
NF (instance parameter only)	Number of device fingers (Fatal error if less than one)	1
DWJ	Offset of the S/D junction width	DWC (in CVmodel)
MIN (instance parameter only)	Whether to minimize the number of drain or source diffusions for even-number fingered device	0 (minimize the drain diffusion number)
XGW(Also an instance parameter)	Distance from the gate contact to the channel edge	0.0m
XGL	Offset of the gate length due to variations in patterning	0.0m
XL	Channel length offset due to mask/ etch effect	0.0m
XW	Channel width offset due to mask/etch effect	0.0m
NGCON(Also an instance parameter)	Number of gate contacts (Fatal error if less than one; if not equal to 1 or 2, warning message issued and reset to 1)	1

16 Asymmetric Source/Drain Junction Diode Model Parameters

Parameter Name (separate for source and drain side as indicated in the names)	**Description**	**Default Value**
IJTHSREV IJTHDREV	Limiting current in reverse bias region (If not positive, reset to 0.1A)	IJTHSREV = 0.1A, IJTHDREV = IJTHSREV
IJTHSFWD IJTHDFWD	Limiting current in forward bias region (If not positive, reset to 0.1A)	IJTHSFWD = 0.1A, IJTHDFWD = IJTHSFWD
XJBVS XJBVD	Fitting parameter for diode breakdown	XJBVS = 1.0, XJBVD = XJBVS
BVS BVD	Breakdown voltage (If not positive, reset to 10.0V)	BVS = 10.0V, BVD = BVS
JSS JSD	Bottom junction reverse saturation current density	JSS= 1.0e-4A/m2, JSD = JSS
JSWS JSWD	Isolation-edge sidewall reverse saturation current density	JSWS = 0.0A/m, JSWD = JSWS
JSWGS JSWGD	Gate-edge sidewall reverse saturation current density	JSWGS =0.0A/m, JSWGD = JSWGS
JTSS JTSD	Bottom trap-assisted saturation current density	JTSS = 0.0A/m JTSD = JTSS
JTSSWS JTSSWD	STI sidewall trap-assisted saturation current density	JTSSWS = 0.0A/m2 JTSSWD = JTSSWS
JTSSWGS JTSSWGD	Gate-edge sidewall trap-assisted saturation current density	JTSSWGS = 0.0A/m JTSSWGD = JTSSWGS
JTWEFF	Trap-assistant tunneling current density width dependence	0.0
NJTS NJTSD	Non-ideality factor for JTSS and JTSD	NJTS = 20.0 NJTSD = NJTS

NJTSSW NJTSSWD	Non-ideality factor for JTSSWS and JTSSWD	NJTSSW = 20.0 NJTSSWD = NJTSSW
NJTSSWG NJTSSWGD	Non-ideality factor forJTSSWGS and JTSSWGD	NJTSSWG = 20.0 NJTSSWGD = NJTSSWG
XTSS, XTSD	Power dependence of JTSS, JTSD on temperature	XTSS = 0.02 XTSD = 0.02
XTSSWS, XTSSWD	Power dependence of JTSSWS, JTSSWD on temperature	XTSSWS =0.02 XTSSWD = 0.02
XTSSWGS, XTSSWGD	Power dependence of JTSSWGS, JTSSWGD on temperature	XTSSWGS = 0.02 XTSSWGD = 0.02
VTSS VTSD	Bottom trap-assisted voltage dependent parameter	VTSS = 10V VTSD = VTSS
VTSSWS VTSSWD	STI sidewall trap-assisted voltage dependent parameter	VTSSWS =10V VTSSWD =VTSSWS
VTSSWGS VTSSWGD	Gate-edge sidewall trap-assisted voltage dependent parameter	VTSSWGS = 10V VTSSWGD =VTSSWGS
TNJTS TNJTSD	Temperature coefficient for NJTS and NJTSD	TNJTS=0.0 TNJTSD =TNJTS
TNJTSSW TNJTSSWD	Temperature coefficient for NJTSSW and NJTSSWD	TNJTSSW= 0.0 TNJTSSWD =TNJTSSW
TNJTSSWG TNJTSSWGD	Temperature coefficient for NJTSSWG and NJTSSWG	TNJTSSWG =0.0 TNJTSSWGD = TNJTSSWG
CJS CJD	Bottom junction capacitance per unit area at zero bias	CJS=5.0e-4 F/m2 CJD=CJS
MJS MJD	Bottom junction capacitance grating coefficient	MJS=0.5 MJD=MJS
MJSWS MJSWD	Isolation-edge sidewall junction capacitance grading coefficient	MJSWS =0.33 MJSWD =MJSWS
CJSWS CJSWD	Isolation-edge sidewall junction capacitance per unit area	CJSWS= 5.0e-10 F/m CJSWD =CJSWS
CJSWGS CJSWGD	Gate-edge sidewall junction capacitance per unit length	CJSWGS =CJSWS CJSWGD =CJSWS

MJSWGS MJSWGD	Gate-edge sidewall junction capacitance grading coefficient	MJSWGS =MJSWS MJSWGD =MJSWS
PB	Bottom junction built-in potential	PBS=1.0V PBD=PBS
PBSWS PBSWD	Isolation-edge sidewall junction built-in potential	PBSWS =1.0V PBSWD =PBSWS
PBSWGS PBSWGD	Gate-edge sidewall junction built-in potential	PBSWGS =PBSWS PBSWGD =PBSWS

17 Temperature Dependence Parameters

Parameter Name	**Description**	**Default Value**
TNOM	Temperature at which parameters are extracted	27^0C
DTEMP	Variability handle for temperature	0
UTE (b)	Mobility temperature exponent	-1.5
UCSTE(b)	Temperature coefficient of coulombic mobility	-4.775e-3
KT1 (b)	Temperature coefficient for threshold voltage	-0.11V
KT1EXP	Temperature exponent for threshold voltage	1.0
KT1L (b)	Channel length dependence of the temperature coefficient for threshold voltage	0.0Vm
KT2(b)	Body-bias coefficient of Vth temperature effect	0.022
UA1 (b)	Temperature coefficient for UA	1.0e-9m/V
UC1 (b)	Temperature coefficient for UC	0.056V-1 for MOBMOD=1; 0.056e-9m/V^2 for MOBMOD=0 and 2
UD1 (b)	Temperature coefficient for UD	$0.0(1/m)^2$
AT (b)	Temperature coefficient for saturation velocity	3.3e4m/s
PTWGT	Temperature coefficient for PTWG	0.0
PRT (b)	Temperature coefficient for Rdsw	0.0ohm-m
NJS, NJD	Emission coefficients of junction for source and drain junctions, respectively	NJS=1.0; NJD=NJS
XTIS, XTID	Junction current temperature exponents for source and drain junctions, respectively	XTIS=3.0; XTID=XTIS
TPB	Temperature coefficient of PB	0.0V/K
TPBSW	Temperature coefficient of PBSW	0.0V/K
TPBSWG	Temperature coefficient of PBSWG	0.0V/K
TCJ	Temperature coefficient of CJ	0.0K-1
TCJSW	Temperature coefficient of CJSW	0.0K-1
TCJSWG	Temperature coefficient of CJSWG	0.0K-1

TVFBSDOFF	Temperature coefficient of VFBSDOFF	0.0K-1
TNFACTOR(b)	Temperature coefficient of NFACTOR	0.0
TETA0 (b)	Temperature coefficient of ETA0	0.0

18 Stress Effect Model Parameters

Parameter Name	**Description**	**Default Value**
SA (Instance Parameter)	Distance between OD edge to Poly from one side (If not given or($\leq$ 0), stress effect will be turned off)	0.0
SB (Instance Parameter)	Distance between OD edge to Poly from other side (If not given or($\leq$ 0), stress effect will be turned off)	0.0
SD (Instance Parameter)	Distance between neighbouring fingers (For NF>1 :If not given or($\leq$ 0), stress effect will be turned off)	0.0
SAref	Reference distance between OD and edge to poly of one side (>0.0)	1E-06[m]
SBref	Reference distance between OD and edge to poly of the other side (>0.0)	1E-06[m]
WLOD	Width parameter for stress effect	0.0[m]
KU0	Mobility degradation/enhancement coefficient for stress effect	0.0[m]
KVSAT	Saturation velocity degradation/ enhancement parameter for stress effect ($1 \leq kvsat \leq 1$)	0.0[m]
TKU0	Temperature coefficient of KU0	0.0
LKU0	Length dependence of ku0	0.0
WKU0	Width dependence of ku0	0.0
PKU0	Cross-term dependence of ku0	0.0
LLODKU0	Length parameter for u0 stress effect (>0)	0.0
WLODKU0	Width parameter for u0 stress effect (>0)	0.0
KVTH0	Threshold shift parameter for stress effect	0.0[Vm]
LKVTH0	Length dependence of kvth0	0.0
WKVTH0	Width dependence of kvth0	0.0
PKVTH0	Cross-term dependence of kvth0	0.0
LLODVTH	Length parameter for Vth stress effect (>0)	0.0
WLODVTH	Width parameter for Vth stress effect (>0)	0.0
STK2	K2 shift factor related to Vth0 change	0.0[m]

LODK2	K2 shift modification factor for stress effect (>0)	0.0
STETA0	eta0 shift factor related to Vth0 change	0.0[m]
LODETA0	eta0 shift modification factor for stress effect (>0)	1.0

19 Well-Proximity Effect Parameters

Parameter Name	Description	Default Value
SCA (Instance Parameter)	Integral of the first distribution function for scattered well dopant (If not given , calculated)	0.0
SCB (Instance Parameter)	Integral of the second distribution function for scattered well dopant (If not given , calculated)	0.0
SCC (Instance Parameter)	Integral of the third distribution function for scattered well dopant (If not given , calculated)	0.0
SC (Instance Parameter)	Distance to a single well edge (If not given or $\leq$ 0.0, turn off WPE)	0.0[m]
WEB	Coefficient for SCB (>0.0)	0.0
WEC	Coefficient for SCC (>0.0)	0.0
KVTH0WE(b)	Threshold shift factor for well proximity effect	0.0
K2WE (b)	K2 shift factor for well proximity effect	0.0
KU0WE (b)	Mobility degradation factor for well proximity effect	0.0
SCREF	Reference distance to calculate SCA, SCB and SCC (<0)	1e-6[m]

20 Parameter equivalence between BSIM6 & BSIM4

The equivalent parameters are the closest match between two models. There values may be different in two models.

Region	**BSIM6 Parameter Name**	**BSIM4 Parameter Name**	**Comment**
Core Parameters	GEOMOD	GEOMOD	
	RGEOMOD	RGEOMOD	
	RDSMOD	RDSMOD	
	COVMOD	COVMOD	
	L	L	
	W	W	
	XL	XL	
	XW	XW	
	LINT	LINT	
	WINT	WINT	
	DLC	DLC	
	DWC	DWC	
	TOXE	TOXE	
	TOXP	TOXP	
	NF	NF	
	NDEP	NDEP or VTH0/VTHO	
	NGATE	NGATE	
	VFB, VFBCV	VFB, VFBCV	
Material properties	EASUB	-	Corresponds
	NI0SUB	-	to BSIM4
	EPSRSUB	-	mtrlmod=1
	EPSROX	-	
Threshold Voltage	NDEPL1, NDEPLEXP1, NDEPL2, NDEPLEXP2	DVT0, DVT1, DVT2, LPE0	Length scaling
	NDEPW, NDEPWEXP, NDEPWL, NDEPWLEXP	DVT0W, DVT1W, DVT2W, K3, W0	Width and Narrow-short Scaling
	K2W	K3B	

	DVTP0, DVTP1, DVTP2, DVTP3, DVTP4, DVTP5	same as BSIM4	
	PHIN	PHIN	
	ETA0	ETA0	
	ETAB	ETAB	
	DSUB	DSUB	
	K2	K2	
	K2L, L2LEXP	K1, LPEB	
Subthreshold Swing	CIT	CIT	
	NFACTOR	CDSC	
	CDSCD	CDSCD	
	CDSCB	CDSCB	
	NFACTOR	NFACTOR	
Drain Saturation Voltage	VSAT, DELTA	VSAT, DELTA	
Mobility Model	U0	U0	BSIM6 uses MOBMOD=3 from BSIM4
	ETAMOB	-	default value of 1 corresponds to BSIM4
	U0L	UP	
	U0LEXP	LPA	
	UA	UA	
	EU	EU	
	UD	UD	
	UCS	UCS	
	UC	UC	
Channel Length Modulation and DITS	PCLM	PCLM	
	PCLMG	PCLMG	
	PSCBE1	PSCBE1	
	PSCBE2	PSCBE2	
	PDITS	PDITS	

	PDITSL PDITSD	PDITSL PDITSD	
Velocity Saturation	VSAT PTWG PSAT PSATX PSATB	VSAT - - - -	
Rs, Rd parameter	XJ VFBSDOFF NRS/NRD MINZ NSD RSH PRWG PRWB WR RDSWMIN RSWMIN RDWMIN RDSW RSW RDW DMCG DMCI DMDG DMCGT	XJ VFBSDOFF NRS/NRD MINZ NSD RSH PRWG PRWB WR RDSWMIN RSWMIN RDWMIN RDSW RSW RDW DMCG DMCI DMDG DMCGT	BSIM6 uses RDSMOD=1 from BSIM4
Impact Ionization	ALPHA0, ALPHA0L, ALPHA0LEXP BETA0	ALPHA0, ALPHA1 BETA0	
GIDL/GISL	AGIDL BGIDL CGIDL EGIDL	AGIDL BGIDL CGIDL EGIDL	

	AGISL BGISL CGISL EGISL	AGISL BGISL CGISL EGISL	
C-V Model	CF CFRCOEFF CFI CGSO CGDO CGBO CGSL CGDL CKAPPAS CKAPPAD ADOS, BDOS, QM0, ETAQM	CF - - CGSO CGDO CGBO CGSL CGDL CKAPPAS CKAPPAD ADOS, BDOS	Taken from BSIMSOI

21 Appendix A : Smoothing Function

21.1 Polynomial Smoothing

The polynomial smoothing is used for a smooth transition between boundaries, maintaining exact values at all the corner points. Consider the function

$$f(x) = \quad x \quad if\ x > \frac{\Delta x}{2} \tag{21.1}$$

$$= \quad k \quad if\ x < \frac{-\Delta x}{2} \tag{21.2}$$

where k is some constant. The function is undefined for the region $\frac{-\Delta x}{2} < x < \frac{\Delta x}{2}$. If this region is approximated by a polynomial function, the complete function and even derivatives can be made continuous. Now consider the more generalized case

$$f(x) = \quad x \quad if\ x > x_1 \tag{21.3}$$

$$= \quad k \quad if\ x < x_2 \tag{21.4}$$

To express (21.4) in the form of (21.2), x is linearly transformed into z. Defining

$$x_0 = \frac{x_1 + x_2}{2} \tag{21.5}$$

$$\Delta x = x_1 - x_2 \tag{21.6}$$

then the boundary points becomes

$$x_1 = x_0 + \frac{\Delta x}{2} \tag{21.7}$$

$$x_2 = x_0 - \frac{\Delta x}{2} \tag{21.8}$$

Let $z = \frac{x - x_0}{\Delta x}$. Thus the above boundary points in z domain becomes,

$$z_1 = \frac{x_1 - x_0}{\Delta x} = \frac{1}{2} \tag{21.9}$$

$$z_2 = \frac{x_2 - x_0}{\Delta x} = -\frac{1}{2} \tag{21.10}$$

so that the function becomes

$$f(z) = \quad z.\Delta x - x_0 \quad if\ z > \frac{1}{2} \tag{21.11}$$

$$= \quad k \quad if\ z < -\frac{1}{2} \tag{21.12}$$

the region $-\frac{1}{2} \leq \ z \leq \ \frac{1}{2}$ is modeled by the polynomial function whose order depends on the number of boundary conditions. For example, to have continuous derivatives upto third order, we need seventh order polynomial as there are 8 boundary conditions.

$$f(z) = a.z^7 + b.z^6 + c.z^5 + d.z^4 + e.z^3 + f.z^2 + g.z + 1 \tag{21.13}$$

Then boundary conditions can be applied to derivatives to determine the polynomial coefficients. For the case of continuous third order derivatives, we found that

$$f(x) = x_0 + \Delta x.\left[\frac{5}{64} + \frac{z}{2} + z^2.\left[\frac{15}{16} - z^2.\left(\frac{5}{4} - z^2\right)\right]\right] \tag{21.14}$$

while for continuous second order derivative

$$f(x) = x_0 + \Delta x.\left[\frac{3}{32} + \frac{z}{2} + z^2.\left[\frac{3}{4} - z^2.\left(\frac{3}{4} - \frac{z^2}{2}\right)\right]\right] \tag{21.15}$$

with $z = \frac{x - x_0}{\Delta x}$. Figure 11 illustrate the concept of polynomial smoothing.

An Example : Let the function be given as

$$f(x) = \quad x \quad if\ x > -90 \tag{21.16}$$

$$= \quad -100 \quad if\ x < -110 \tag{21.17}$$

with the condition that third derivative to exist. From (21.6)

$$x_0 = -100 \tag{21.18}$$

$$\Delta x = 20 \tag{21.19}$$

$$z = \frac{x + 100}{20} \tag{21.20}$$

and function becomes,

$$f(z) = \quad 20.z + 100 \quad if\ z > \frac{1}{2} \tag{21.21}$$

$$= \quad -100 \quad if\ z < -\frac{1}{2} \tag{21.22}$$

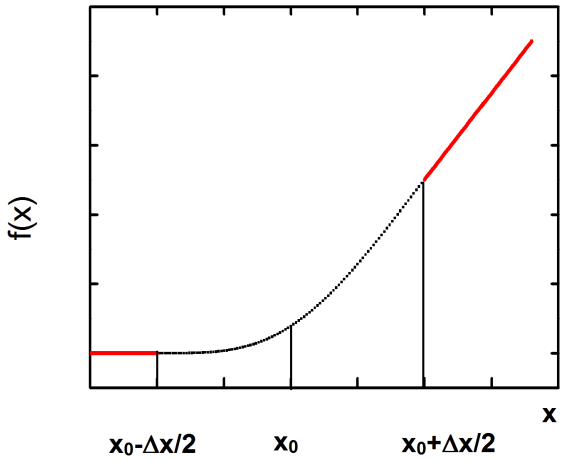

Figure 11: Illustration of Polynomial Smoothing

Boundary Conditions

$$f(\frac{1}{2}) = -90, f(-\frac{1}{2}) = -100 \tag{21.23}$$

$$f^{'}(\frac{1}{2}) = 20, f^{'}(-\frac{1}{2}) = 0 \tag{21.24}$$

$$f^{''}(\frac{1}{2}) = 0, f^{''}(-\frac{1}{2}) = 0 \tag{21.25}$$

$$f^{'''}(\frac{1}{2}) = 0, f^{'''}(-\frac{1}{2}) = 0 \tag{21.26}$$

We have 8 boundary conditions. So let

$$f(z) = a.z^7 + b.z^6 + c.z^5 + d.z^4 + e.z^3 + f.z^2 + g.z + 1 \tag{21.27}$$

Now we have 8 equations and 8 unknowns and hence all the coefficients can be derived. By substituting (21.23-21.26) in (21.27) we get

$$a = 0,\ b = 20,\ c = 0$$

$$d = -25,\ e = 0,\ f = \frac{75}{4} \tag{21.28}$$

$$g = 10,\ h = -\frac{6300}{64} \tag{21.29}$$

Thus

$$f(z) = 20.z^6 - 25.z^4 + \frac{75}{4}.z^2 + 10.z - \frac{6300}{64} \tag{21.30}$$

Figure:12 shows the above function. As can be seen that due to polynomial nature, the

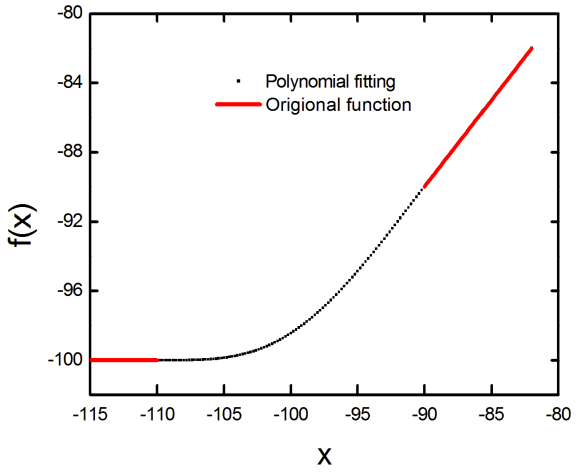

Figure 12: Polynomial Smoothing Function

approximated function undergoes smooth transitions around the boundary points.

References

[1] *BSIM4 user manual*. [Online]. Available: http://www-device.eecs.berkeley.edu/bsim/

[2] Y. Tsividis, *Operation and Modeling of the MOS Transistor 2nd ed.* Oxford, 1999.

[3] Y. S. Chauhan, M. A. Karim, S. Venugopalan, S. Khandelwal, P. Thakur, N. Paydavosi, A. Sachid, A. B.and Niknejad, and C. Hu, "Bsim6:symmetric bulk mosfet model," *Workshop on Compact Modeling, Santa Clara, USA*, June 2012.

[4] J.-M. Sallese, M. Bucher, F. Krummenacher, and P. Fazan, "Inversion charge linearization in mosfet modeling and rigorous derivation of the ekv compact model," *Solid-State Electronics*, vol. 47, no. 4, pp. 677–683, April 2003.

[5] C. C. Enz and E. Vittoz, *Charge-based MOS Transistor Modeling*. John Wiley and Sons, Inc., 2006.

[6] F. Pregaldiny, F. Krummenacher, B. Diagne, F. Pecheux, J.-M. Sallese, and C. Lallement, "Explicit modeling of the double-gate mosfet with vhdl-ams," *International Journal of Numerical Modelling: Electronic Networks, Devices and Fields*, vol. 19, no. 3, pp. 239–256, May 2006.

[7] C. C. Hu, *Modern Semiconductor Devices for Integrated Circuits*. Pearson Education, 2010.

[8] *MOS Model 11 manual*. [Online]. Available: http://www.nxp.com/models/simkit/mos-models/model-11.html

[9] K. K. Hung, P. Ko, and Y. C. Cheng, "A physics-based mosfet noise model for circuit simulator," *IEEE Transaction on Electron Devices*, vol. 37, no. 5, pp. 1323–1333, 1990.

[10] A. J. Scholten, R. Langevelde, L. F. Tiemeijer, and D. B. M. Klaassen, "Compact modeling of noise in cmos," in *CICC*, 2006.

[11] R. A. Bianchi, G. Bouche, and O. Roux-ditBuisson, "Accurate modeling of trench isolation induced mechanical stress effect on mosfet electrical performance," in *2007 Symposium on VLSI Technology*, 2007.

[12] T. Hook, J. Brown, P. Cottrell, E. Adler, D. Hoyniak, J. Johnson, and R. Mann, "Lateral ion implant straggle and mask proximity effect," *IEEE Transaction on Electron Devices*, vol. 50, no. 9, pp. 1946–1951, 2003.

[13] *Compact Model Council*. [Online]. Available: http://www.geia.org/index.asp?bid=597

22 Ackowledgements

We deeply appreciate the feedback we received from (in alphabetical order):

Shantanu Agnihotri(IIT Kanpur)

Maria Anna Chalkiadaki(EPFL)

Kaiman Chan (TI)

Brian Chen (Accelicon)

Sergey Cherepko (ADI)

Geoffrey Coram (ADI)

Krishnanshu Dandu (TI)

Anupam Dutta (IBM)

Christian Eng (EPFL)

Keith Green (TI)

Andre Juge (ST)

Tracey Krakowski (TI)

Francois Krummenacher (EPFL)

Pragya Kushwaha (IIT Kanpur)

Saurabh Sirohi (IBM)

Jing Wang (IBM)

Joddy Wang (Synopsys)

Wenli Wang (Cadence)

Josef Watts (IBM)

Richard Williams (IBM)

Weimin Wu (TI)

Jane Xi (Synopsys)

Jushan Xie (Cadence)

Chandan Yadav(IIT Kanpur)

Fang Yu (Synopsys)

Fulong Zaho (Cadence)

Manual created: May 4, 2013